

ABSTRACT

Title of Document: A COMPARATIVE PROTEOMIC ANALYSIS
OF MITOCHONDRIAL PROTEINS FROM
DRUG SUSCEPTIBLE AND DRUG
RESISTANT HUMAN MCF-7 BREAST
CANCER CELLS

Rachael Strong, Doctor of Philosophy, 2005

Directed By: Professor Catherine Fenselau
Department of Chemistry and Biochemistry

Cancer is a leading cause of death in the United States. Chemotherapy is often used in treatment of the disease; however, it often fails as a result of the development of drug resistance. To improve patient outcome and develop more effective chemotherapeutic agents, it is necessary to better understand the mechanisms responsible for the development of drug resistance. In order to identify mitochondrial proteins that may contribute to drug resistance a comparative proteomic analysis has been performed. Specifically, mitochondria were isolated from a drug susceptible and two drug resistant human MCF-7 breast cancer cell lines. The soluble proteins were extracted and separated by two-dimensional gel electrophoresis. Proteins were identified by mass spectrometry combined with bioinformatics. Comparative densitometry of the gel images was used to determine the relative quantitation of each protein.

One hundred and fifty three unique proteins have been identified in this analysis. Of these, fifteen proteins were found to be significantly more or less abundant between the drug susceptible MCF-7 cell line and the MCF-7 cell lines selected for resistance to adriamycin in the presence of verapamil and to mitoxantrone. In both resistant cell lines, proteins involved in oxidative phosphorylation were shown to have altered abundances. Additional proteins whose abundances changed were detected in the adriamycin resistant cell line. These proteins play a role in several mitochondrial pathways including fatty acid oxidation, heme biosynthesis and apoptosis. Based on our analysis, we conclude that mechanisms responsible for drug resistance are different for adriamycin and mitoxantrone. In addition, we have proposed novel mechanisms of resistance for some of these proteins.

A COMPARATIVE PROTEOMIC ANALYSIS OF MITOCHONDRIAL
PROTEINS FROM DRUG SUSCEPTIBLE AND DRUG RESISTANT HUMAN
MCF-7 BREAST CANCER CELLS

By

Rachael F. Strong

Dissertation submitted to the Faculty of the Graduate School of the
University of Maryland, College Park, in partial fulfillment
of the requirements for the degree of
Doctor of Philosophy
2005

Advisory Committee:
Professor Catherine Fenselau, Chair
Professor Eric Baehrecke
Professor Cheng Lee
Professor George Lorimer
Professor Vikram Vakharia

© Copyright by
Rachael F Strong
2005

Acknowledgements

I would like to take this opportunity to thank Dr. Catherine Fenselau for allowing me to pursue a graduate career in her lab. Working with her has been an invaluable experience and one that I will appreciate for years to come.

In working with Dr. Fenselau, I was fortunate enough to be a member of an extraordinary lab group. It was a pleasure to work with and learn from everyone in her lab.

Many thanks are also due to my advisory committee members, Dr. Eric Baehrecke, Dr. Cheng Lee, Dr. George Lorimer and Dr. Vikram Vakharia. The wealth of information, ideas and time they have shared with me has been tremendous.

Finally, I would like to thank those whose support over the years has meant so much to me. To the girls, I will never forget our laughs, late night gatherings and mall excursions. Without these I would not have kept my sanity. To my family, especially my parents, words cannot express how much you mean to me. For everything you have done, and for all that I know you will continue to do, thank you. To Chris, you are the rock in my life. It is your love, encouragement and support that have made this possible. Thank you for always believing in me.

Table of Contents

Acknowledgements.....	ii
Table of Contents.....	iii
List of Tables.....	iv
List of Figures.....	v
Chapter 1: Introduction.....	1
Breast cancer and chemotherapy.....	1
Drug resistance and its known mechanisms.....	2
Mitochondria.....	7
MCF-7 cells as a model system.....	10
Proteomics and comparative proteomics.....	16
Two-dimensional gel electrophoresis.....	17
Mass spectrometry.....	18
Protein identification and bioinformatics.....	24
Hypothesis and objectives.....	29
Chapter 2: Materials and Methods.....	30
Materials.....	30
MCF-7 cell culture and harvest.....	31
Isolation and purification of mitochondria.....	31
Preparation of soluble proteins.....	32
2-D gel electrophoresis and comparative gel analysis.....	35
In-gel tryptic digestion and preparation of proteins.....	36
Mass spectrometry and protein identification.....	40
Chapter 3: Results.....	45
Preparation of mitochondrial proteins.....	45
Protein identification and evaluation of purification method.....	45
Protein abundance profile of the adriamycin/verapamil resistant MCF-7 cell line.....	61
Protein abundance profiles in the MCF-7 cell line resistant to mitoxantrone.....	74
Chapter 4: Discussion.....	84
Characterization of MCF-7 mitochondria.....	84
Proteomic annotation of the genome.....	85
Annotation of hypothetical proteins.....	88
Biological implications of abundance changes.....	91
Fatty acid oxidation.....	91
Oxidative phosphorylation.....	94
Biosynthesis of heme.....	101
Apoptosis.....	103
Mitochondrial homeostasis.....	106
Proteins not known to be located in mitochondria.....	109
Summary and prospectus.....	113
References.....	115

List of Tables

	Page
Table 1. Proteins identified in the crude mitochondrial fraction.....	48
Table 2. Proteins identified in the purified mitochondrial fraction.....	53
Table 3. Relative abundance of proteins from adriamycin resistant cells.....	64
Table 4. Proteins with altered abundance in adriamycin resistant cells.....	70
Table 5. Relative abundance of proteins from mitoxantrone resistant cells.....	77
Table 6. Proteins with altered abundances in mitoxantrone resistant cells.....	83
Table 7. Comparison of mitochondrial protein catalogs.....	87
Table 8. Predicted subcellular location of hypothetical proteins.....	90
Table 9. Summary of abundance changes.....	92
Table 10. Relative abundance of ATP synthase subunits.....	99
Table 11. Relative abundance of proteins involved in translation machinery....	108

List of Figures

	Page
Figure 1. Known mechanisms of drug resistance.....	4
Figure 2. Extrinsic and intrinsic pathways of apoptosis.....	9
Figure 3. Chemical structure of adriamycin.....	11
Figure 4. Chemical structure of verapamil.....	13
Figure 5. Chemical structure of mitoxantrone.....	15
Figure 6. Schematic of comparative analysis.....	19
Figure 7. Schematic of matrix-assisted laser desorption ionization.....	21
Figure 8. Schematic of electrospray ionization.....	23
Figure 9. Schematic of a quadrupole time-of-flight mass spectrometer.....	26
Figure 10. Fragmentation of a peptide to generate b and y-ions.....	28
Figure 11. Density gradient purification of mitochondria.....	33
Figure 12. Schematic of comparative image analysis.....	37
Figure 13. Identification of prohibitin by peptide mass fingerprinting.....	42
Figure 14. Protein identification by peptide microsequencing.....	44
Figure 15. Annotated 2D-gel map of the crude mitochondrial fraction.....	47
Figure 16. Annotated 2D-gel map of the purified mitochondrial fraction.....	52
Figure 17. 2D-gel map of proteins from adriamycin resistant cells.....	62
Figure 18. Comparative image analysis of the adriamycin resistant cell lines.....	63
Figure 19. Equal abundance of a mitochondrial protein.....	71
Figure 20. Increase in abundance of a mitochondrial protein.....	72
Figure 21. Decrease in abundance of a mitochondrial protein.....	73
Figure 22. 2D-gel map of proteins from mitoxantrone resistant cells.....	75
Figure 23. Comparative image analysis of the mitoxantrone resistant lines.....	76
Figure 24. Altered abundance of ATP synthase alpha subunit.....	98

Chapter 1: Introduction

Breast cancer and chemotherapy

Cancer is the second leading cause of death in the United States, with breast cancer accounting for seven percent of the total. The most common type of cancer in women, more than 217,000 new cases of breast cancer were diagnosed in 2004 and over 40,000 individuals died from the disease.¹ Based on these statistics it is clear that early detection methods and proper treatment must be improved upon.

Breast cancer is typically treated with a combination of surgery, radiation, hormone therapy, and chemotherapy. Chemotherapeutic agents are typically administered intravenously and travel throughout the body allowing them to reach the cancerous mass, whether it is in-situ or invasive. This trademark of antineoplastic agents is a great advantage as it allows for the destruction of early metastases that, if using other forms of treatment would not be targeted. Because cancer cells have gained the ability to proliferate uncontrollably, it follows that the drugs have been designed to target rapidly dividing cells. Unfortunately, this is also a weakness of chemotherapy as it targets otherwise healthy cells in the reproductive system and hair follicles, which must divide rapidly for normal function

Presently, more than sixty chemotherapy drugs are being used in the clinical setting, while the number of those undergoing clinical trials increases daily.² In general, the drugs are designated as cell-cycle specific, meaning they kill cells only in a specific phase of the cell cycle, and non cell-cycle specific, allowing them to kill cells at any stage of the cycle. The drugs are further divided into separate classes depending on their

specific mechanism of action. All chemotherapy drugs work to slow and/or inhibit the growth and development of neoplastic cells, but exactly how they do so differs between the classes. The antimetabolites and mitotic inhibitors, such as 5-fluorouracil and etoposide, are both cell cycle specific and work to impede nucleic acid synthesis to prohibit DNA replication in the S phase and to prevent cell division during mitosis, respectively. On the other hand, alkylating agents, antitumor antibiotics and nitrosureas are all non cell-cycle specific. Alkylating agents, such as melphalan bind DNA to prevent its replication and transcription, while the nitrosureas, which include the drug carmustine, block enzymes that function in DNA repair. The antitumor antibiotics work in several ways including inhibition of nucleic acid synthesis, blocking of enzymes required for cell division and by changing cell membranes. Drugs that fall into this class are either natural products, such as adriamycin, or are synthetic, like mitoxantrone. Improved cancer treatment results when the drugs are used in a combination that is often tailor designed on a case-by-case basis. In this way, chemotherapy can be advantageous for some time. Unfortunately however, chemotherapy often fails as a result of multi-drug resistance.

Drug resistance and its known mechanisms

Multi-drug resistance is the most challenging problem in the successful treatment of cancer and is the main reason why chemotherapy fails.³ When a tumor does not respond to treatment, namely chemotherapy, it is said to be drug-resistant. Drug resistance is classified as either intrinsic or acquired.⁴ Intrinsic resistance results when cancerous cells are unresponsive to the first round of chemotherapeutic(s) they are exposed to. Acquired resistance results when small populations of cells were not killed

after initial exposure to chemotherapy and thus proliferate with genetic alterations conferring this resistance to later populations.⁵ Multi-drug resistance is observed in both intrinsic and acquired resistance. In this phenomenon, if a tumor metastasizes or comes back after remission, the cancerous cells are not only resistant to the drugs used originally, but are also resistant to a wide array of drugs that are not necessarily similar in their chemical structure, mechanism or cellular target.⁶ As a result of multi-drug resistance, chemotherapy is often unsuccessful.

Although multi drug resistance has been studied for nearly four decades it has yet to be fully understood. To date, a handful of mechanisms responsible for drug resistance have been determined, including changes in drug accumulation and detoxification, DNA repair mechanisms and alterations along the apoptotic pathway.⁷ These mechanisms, which are illustrated in Figure 1, can be separated into three general classes; those that act upstream of the molecular target, those that act at the molecular target and those that act downstream of the target. While some of these mechanisms have been studied extensively, others are still not well understood. Furthermore, not all resistance can be explained by the known mechanisms, thus it stands that additional mechanisms of resistance have yet to be determined. In order to improve current clinical treatment and to develop more effective chemotherapeutic agents, it is imperative that more insight be gained into the mechanisms of drug resistance.

The efflux of chemotherapy drugs out of cancer cells through adenosine triphosphate (ATP)-dependent pumps is the most well characterized model of drug resistance. The ATP binding cassette family comprises 48 proteins, ten of which have

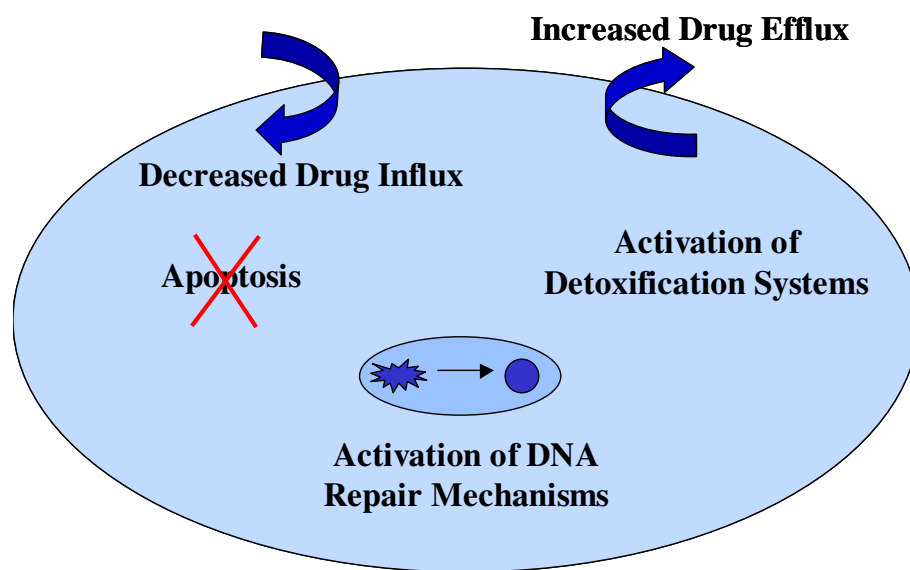


Figure 1. Known mechanisms of drug resistance.

been shown to confer drug resistance in cancer cells.⁸ In this family, the energy released from ATP hydrolysis at one of two ATP binding domains drives the efflux of drugs from the cytosol inside a cell to the outer extracellular matrix.^{6,8,9} In this way, drugs do not accumulate in cancer cells and cannot produce their typical chemotherapeutic effects. P-glycoprotein (Pgp) was the first member of this family shown to confer drug resistance. A product of the MDR1 gene, Pgp is a 170-kDa protein that can detect and expel a variety of drugs, including antitumor antibiotics and mitotic inhibitors. When a drug binds Pgp it activates the first ATP binding cassette to hydrolyze ATP, which in turn causes a conformational change in the protein forcing it to release the drug. ATP hydrolysis at the second binding domain allows Pgp to return to its natural conformation so that it can bind another drug molecule.⁴ Resistance caused by Pgp is detrimental; cells with intrinsic resistance to anticancer drugs conferred upon them by Pgp will induce the expression of high numbers of Pgp pumps once exposed to that same drug. In turn, induction of Pgp then works to reduce the intracellular accumulation of the drug, which can encourage other mechanisms of drug resistance to develop.⁸

Besides Pgp, nine other ATP binding cassette family members that confer drug resistance on cancer cells have been identified, including the breast cancer resistance protein, which has been shown to be over expressed in cells treated with anthracycline antibiotics.^{9,10} A second mechanism of resistance, decrease of drug influx into a cell is not understood nearly as well. It has been shown that cells can gain resistance to drugs that enter the cytosol either through receptor-mediated transport or through endocytosis. Resistance in the former case occurs when mutations cause failure of the receptors to function properly, while in the latter, endocytosis is somehow defective.⁴ Drug resistance

can also be gained through an increase in drug-detoxification.^{11,12} In this way, enzymes such as Cytochrome p450 reductase and glutathione-S-transferase are responsible for the inactivation and excretion of drugs so that they cannot reach their cellular target.

Deoxyribonucleic acid (DNA) is the cellular target for most chemotherapeutic drugs, with the premise that damage to this molecule should prevent cells from dividing uncontrollably. Drug resistance at the DNA level has developed, however, as cancer cells can increase the expression of certain proteins to repair damage and decrease the expression of others to tolerate the damage that drugs impart on them.^{13,14} An increase in DNA repair allows the cancer cells to survive, while tolerance of the damage leads to acquired resistance at a later stage in treatment as it increases the mutation rate throughout the genome. Drug-resistance arising at this point represents a key failure in traditional chemotherapy agents; they work indirectly by targeting DNA rather than the apoptotic pathway.

Current understanding is that chemotherapeutic agents kill cells via apoptosis not by DNA damage.^{15,16} Because traditional drugs have not been designed to target the apoptotic pathway, they work to kill cells indirectly, which has several drawbacks. First, cancer cells that survive after the drug has reached its “target,” or DNA, do so because they have developed alterations in their apoptotic pathway, including the modified expression of many proteins that both promote and prevent programmed cell death.¹⁷ This in turn ensures that the next generation of cells will be resistant to that particular drug. It also guarantees multi-drug resistance as it has been determined that most drugs kill cells by activating the apoptotic pathway, which was disabled after treatment with the original drug.

Although it is clear that drug resistance is a major problem in cancer and other long-term therapy, the mechanisms behind it are not clear. What is known is that drug-resistance is multifactorial; there is likely more than one type of mechanism working in a single tumor at any given time.¹⁸ This reflects the fact that within a tumor, the individual cells themselves are heterogeneous in their genome and proteome.⁹ The goal of drug resistance research is to improve patient outcomes by developing multiple strategies to overcome and prevent drug resistance.^{19,20} In order to achieve this goal it is necessary to better understand the underlying mechanisms of resistance.

Drug resistance is multi-factorial; therefore no single protein will be responsible for all resistance. Furthermore, proteins work in tandem to confer and promote resistance.^{21,22} Because many proteins are involved in drug resistance, it is advantageous to use experimental strategies that observe changes in the protein abundance profiles of a large number of proteins at once. A proteomic analysis provides the most direct and robust approach.

Mitochondria

Together, rough human genome sequence information contained in public databases and advances in mass spectrometry have facilitated the emergence of proteomics as a tool for large-scale protein analysis. Due to the complexity of human cells, it is advantageous to study only a particular cell subset, such as an organelle.²³ In this study, a mitochondrial fraction has been used for a proteomic analysis to interrogate differences in the protein profiles between a drug susceptible and drug resistant human MCF-7 breast cancer cell lines.

Mitochondria are dynamic organelles that play key roles in many cellular

processes, including apoptosis. A cell can undergo apoptosis by means of the extrinsic or intrinsic pathway, both of which can converge at the mitochondria, as seen in Figure 2.²⁴ The extrinsic pathway is initiated when death activators such as tumor necrosis factor and the fas ligand bind transmembrane receptors to recruit FADD and activate the caspase cascade. The intrinsic pathway is stimulated by stress factors including DNA damage that results from chemotherapy. A hallmark of the intrinsic pathway is permeabilization of the inner and outer mitochondrial membranes by members of the Bcl-2 family of proteins.^{25,26,27} This permeabilization is critical, as it leads to the release of proteins such as cytochrome c and apoptosis inducing factor from the inner membrane space into the cytosol.^{28,29} Once in the cytosol, these proteins activate caspases, the family of proteins responsible for the morphological changes exhibited by apoptotic cells.^{30,31}

As a result of the central role that mitochondria play in mediating apoptosis, the organelle is now the direct target of several experimental anticancer treatments designed to overcome apoptosis related resistance. The experimental drug Lonidamine, currently in phase III clinical trials for breast cancer targets the permeability transition pore, a complex that spans the mitochondrial membranes and has been shown to be directly involved in apoptosis.^{32,33} In addition, mitochondrial DNA, which encodes thirteen proteins, has potential therapeutic implications as mutations in the genome are reported in most cancers, including breast, and are believed to be another mechanism of chemoresistance.^{34,35} Finally, the nuclear gene transcript, Mm-trag, which localizes to mitochondria is associated with taxol and adriamycin resistance in various cancer cell lines.³⁶ Collectively, these observations provide evidence that mitochondria are intimately involved in drug resistance and support the rationale that the identification of

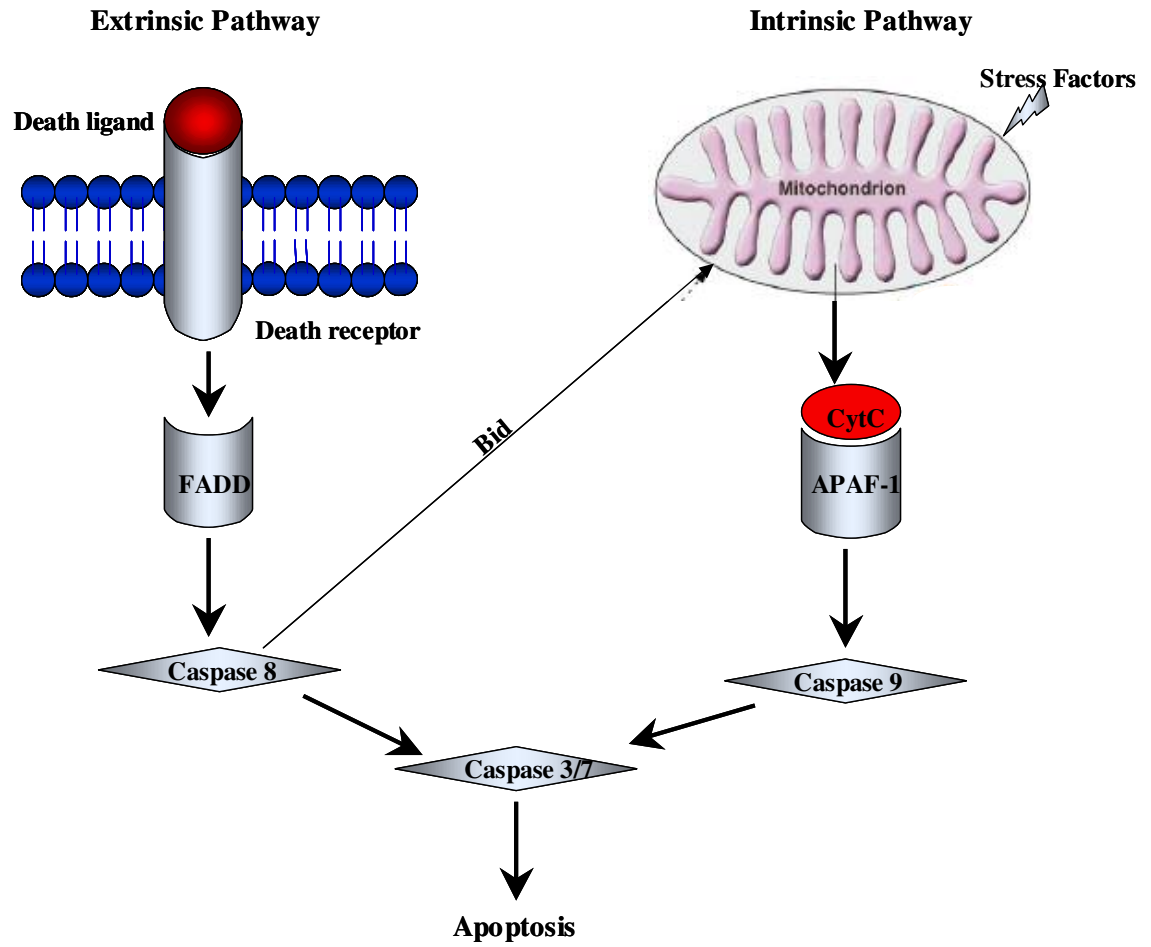


Figure 2. Extrinsic and intrinsic pathways of apoptosis

proteins with altered abundances and structures in this organelle is vital to overcoming the problem.

MCF-7 cells as a model system

A comparative proteomic analysis has been performed between a parental, drug-susceptible MCF-7 breast cancer cell line and the MCF-7 cell lines that have been selected for resistance to adriamycin in the presence of verapamil and for mitoxantrone. The MCF-7 breast cancer cell line was established in 1970 from the pleural effusion of a patient with metastatic breast cancer.³⁷ This cell line is a prominent model for studying estrogen-receptor positive breast cancer, as it has retained qualities of mammary epithelial cells and has also proven to be very stable.³⁸ Because of this stability, multiple resistant lines have been derived from the original MCF-7 cell line, making it the most the most widely used breast cancer model to study drug resistance in-vitro.³⁹

Professor Douglas Ross at the University of Maryland Medical School established the first MCF-7 cell line resistant to adriamycin in the presence of verapamil. The parental MCF-7 cells were subjected to increasing step-wise concentrations of adriamycin and verapamil resulting in a line that is 900-fold resistant to adriamycin.¹⁰ Drug-resistance in this line cannot be attributed to over expression of P-glycoprotein.⁴⁰ It has been shown that the breast cancer resistance protein is over expressed in this line, however further mechanisms of resistance are hypothesized.^{41,42,43}

Adriamycin is a natural anthracycline antibiotic that is used to treat a variety of cancers. Shown in Figure 3, adriamycin is a cell cycle specific inhibitor that targets the S phase. The cytotoxicity of adriamycin is two-fold. At complex I of the electron transport chain in mitochondria, adriamycin is reduced by one electron to its semi-quinone form.⁴⁴

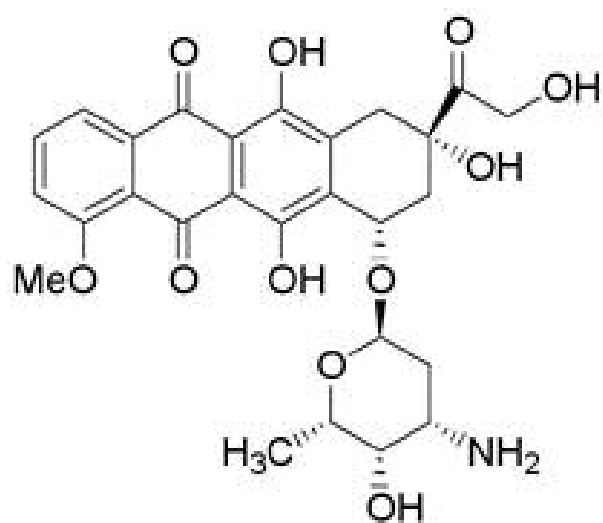


Figure 3. Chemical structure of adriamycin.

The semi-quinone can then react with oxygen or hydrogen peroxide to produce reactive oxygen species.⁴⁵ In turn, production of these free radicals generates oxidative damage to the cells so that apoptosis is initiated.⁴⁶ In its second mechanism of action, adriamycin intercalates along the DNA helix where it interacts with topoisomerase II and causes double strand breaks in the nucleic acid so that DNA synthesis is prevented.^{44,47}

The chemical structure of verapamil is shown in Figure 4. Verapamil is a small hydrophobic calcium channel blocker that works as competitive inhibitor of Pgp to compete with all of its possible substrates, including adriamycin.⁹ It has been determined that an MCF-7 cell line selected for resistance to adriamycin alone produced a cell line with genetic and proteomic phenotypes distinct from those of the parental MCF-7 cell line.^{48,49} Furthermore, that cell line is now categorized as the ovarian cancer cell line, OVCAR-8. Thus, in the MCF-7 cell line selected for resistance to adriamycin in the presence of verapamil, the Pgp inhibitor does not serve to overcome drug-resistance. Rather, the presence of verapamil during selection of this line ensures that it is a direct sub line of the MCF-7 cell line established in 1970.

As previously described, adriamycin localizes to mitochondria where it is reduced to a semi-quinone that can lead to the production of free radicals. This largely contributes to the widespread use of adriamycin as an anticancer agent but also limits dosage, as the generation of reactive oxygen species results in irreversible cardiac damage.⁵⁰ It has been shown that the increased expression of the mitochondrial protein, peroxiredoxin 3, can protect cancer cells against anthracycline induced apoptosis, however this has yet to be demonstrated with adriamycin.⁵¹ In addition to its localization at the electron transport chain, it has been shown that adriamycin interacts with

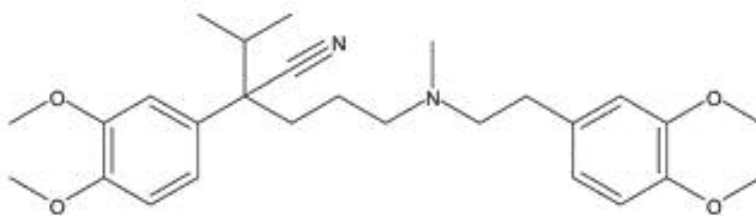


Figure 4. Chemical structure of verapamil.

cardiolipin, a lipid of the inner mitochondrial membrane.⁵² Adriamycin can also inhibit mitochondrial enzymes such as succinate dehydrogenase.⁵³ Finally, in leukemia cells resistant to adriamycin, mitochondrial modifications have been reported.⁵⁴ Whether such actions play a role in drug resistance is not yet clear, but together the data clearly support the use of the MCF-7 cell line selected for resistance to adriamycin in the presence of verapamil for the comparative analysis.

The second cell line that has been used to study the role of mitochondria is that resistant to mitoxantrone. This cell line was selected at the National Institutes of Health in the laboratory of Dr. Ken Cowan by increasing the concentration of mitoxantrone to which the MCF-7 cells were exposed. The resultant cell line is 4000-fold resistant to mitoxantrone.⁵⁵ A known mechanism that contributes to resistance is enhanced drug efflux due to the increased expression of the breast cancer resistance protein located in the plasma membrane.^{56,57}

Mitoxantrone is a synthetic anthracenedione antibiotic. The structure of the drug is shown in Figure 5. It was designed to intercalate and bind DNA to cause single and/or double strand breaks and inter/intra-strand cross-linking, respectively.⁵⁸ Also, mitoxantrone inhibits the activity of topoisomerase II to result in double strand breaks in DNA. Collectively, the mechanisms result in the inhibition of DNA synthesis and repair. Drug resistance in this cell line is due in part to increased drug efflux but other mechanisms are likely. It is worth studying the potential role that mitochondria may play in resistance for several reasons. First, mitoxantrone toxicity is dependent on a fully functional electron transport chain.⁵⁹ Second, mitoxantrone damages mitochondria, including disruption of the semi-permeability of the inner mitochondrial membrane and

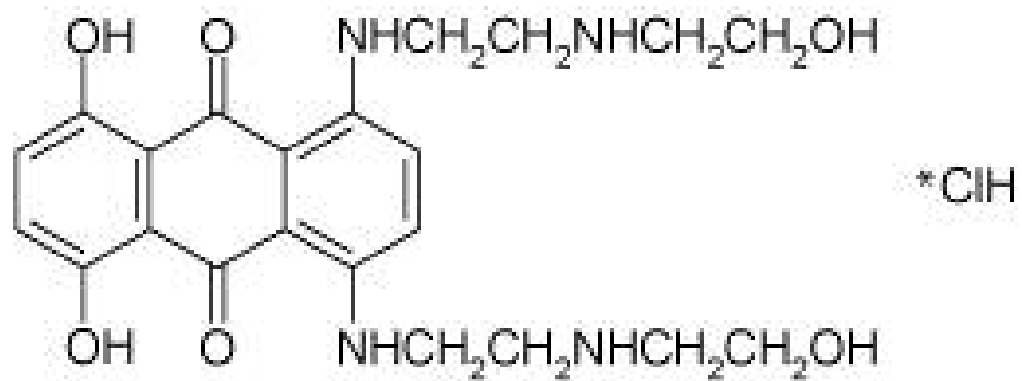


Figure 5. Chemical structure of mitoxantrone.

the uncoupling of oxidative phosphorylation.⁶⁰ Although this does not necessarily indicate a direct link between mitochondria and chemoresistance to mitoxantrone, the association between the drug and proteins within this organelle is apparent and should be explored. This study will allow for the comparison of protein changes in cells resistant to adriamycin and mitoxantrone, both of which are used clinically against breast cancer.

Proteomics and comparative proteomics

Proteomics is the study of the proteome, or protein complement of the genome. After the human genome project was completed in 2000 it became apparent that genetic information is not sufficient to predict the biological function of proteins. There are over 20,000 human genes, but the number of estimated proteins is much greater than 100,000 as a result of alternative splicing and post-translational modifications, the latter of which often determines the function of a protein and its expression status.⁶¹ Also, there is unreliable correlation between the levels of messenger RNA transcripts and the predicted amount of protein.⁶² Thus, from the gene sequence alone it is impossible to predict if a protein will be expressed, which isform, and when at a given time in a particular cell state.

The development of proteomics as a tool for the large-scale analysis of proteins in a single study was facilitated by the availability of rough human gene sequences publicly available and by advances in mass spectrometry that have allowed for rapid analyses with increased sensitivity.⁶³ Initially the main focus of proteomics was to identify every protein in a given cell type. More recently however, it has become apparent that proteomics has widespread applications including comparison of disease states and

characterization of protein-protein interactions to elucidate the components of protein complexes, signaling pathways and metabolic networks.⁶⁴

A comparative proteomic analysis provides a quantitative comparison of abundances of proteins in two different states, such as disease versus normal or responses to the presence and absence of environmental stimuli. The value of comparative proteomics cannot be underestimated. Determination of protein changes in a cell in response to disease may decipher how disease occurs at the molecular level.⁶⁵ In addition, the identification of biomarkers will allow for early detection and progression of diseases like cancer and allow for the development of novel therapies directed at those proteins.^{66,67}

Two-dimensional gel electrophoresis

The first stage of most proteomic analyses is to reduce sample complexity by isolating a cell fraction of interest, such as an organelle. Proteins are then solubilized and separated, usually by 2-dimensional gel electrophoresis (2D-GE) and identified by mass spectrometry combined with bioinformatics. Using 2D-GE one can separate complex mixtures and successfully resolve up to 1000 proteins on a single gel.⁶¹ The resultant gel map of intact proteins can be used to determine changes in protein abundances and the existence of post-translational modifications.⁶⁸ These changes can be observed through manual inspection and quantified with the assistance of computer software.

Two-dimensional gel electrophoresis separates proteins by isoelectric point on an immobilized pH gradient gel (IPG) strip in the first dimension and according to molecular weight by sodium dodecyl sulfate electrophoresis in the second.⁶⁹ Since its conception in the 1970's, 2D-GE has been improved upon in many ways, including the

development of immobilized IPG strips. This innovation, whereby the pH gradient is fixed within the acrylamide matrix of the gel, has markedly increased the reproducibility and resolution of conventional 2-D gels and has simplified the procedure, making it a robust method for proteomics work.^{62,68} Following protein separation, the gels are stained to reveal the proteins, which can be visualized as individual spots. To identify the proteins, spots of interest are excised from the gel and subjected to an in-gel proteolytic digestion to produce peptides that can be recovered from the gel and analyzed by mass spectrometry. Upon recovery, the peptides are identified by peptide mass fingerprinting or microsequencing, and the parent protein is identified from various databases. An overview of the analysis is presented in Figure 6.

Mass spectrometry

Mass spectrometry is a powerful analytical technique that determines the mass of an ion based on its mass to charge (m/z) ratio. A mass spectrometer consists of three parts; the ionization source, a mass analyzer and a detector. For analysis, sample molecules must be charged and must be airborne. The ionization source generates ions. The ions are then directed to the mass analyzer where they are separated by their m/z ratio. Finally, the ions are sent to the detector, which detects the arrival of ions at each m/z value and converts them into an electric signal. Mass spectrometers vary in their type of ion source and mass analyzer, which ultimately dictate the instrument of choice for a particular need.

Although mass spectrometry has been around for nearly a century, its application to biological macromolecules was limited until nearly fifteen years ago when two ionization sources, matrix-assisted laser desorption ionization (MALDI) and electrospray

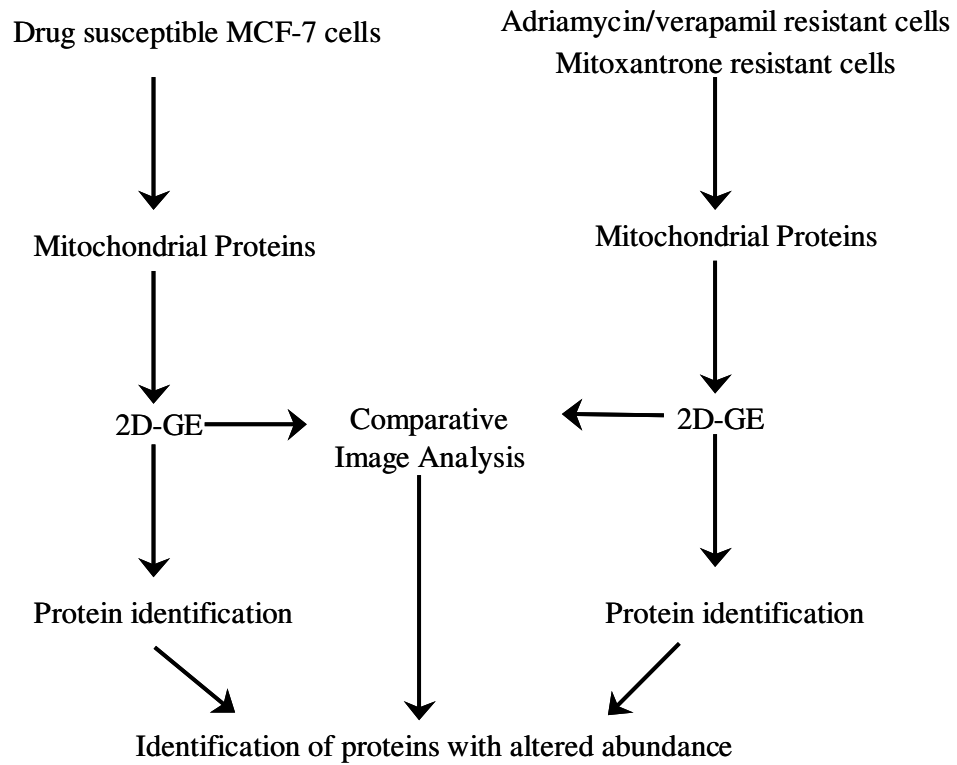


Figure 6. Schematic of comparative analysis.

ionization (ESI) were introduced. Prior to the development of MALDI and ESI, it was difficult to generate ions from nonvolatile molecules, such as proteins and peptides. The advent of these methods allowed for “soft” ionization, meaning fragmentation is minimized, a characteristic that is necessary for protein identification. These methods revolutionized biological research and are often regarded as the most significant breakthrough in proteomics.⁶¹

Two separate groups introduced MALDI almost simultaneously in 1988.^{70,71} A schematic of MALDI is shown in Figure 7. As the name implies, ionization requires co-crystallization of the sample analyte with an organic, aromatic matrix. Both vaporization and ionization occur when a laser strikes the matrix, causing its crystals to absorb the energy from the laser.^{72,73} Absorption of the laser's energy causes the matrix crystals to heat and expand so that sample analyte becomes airborne in a plume. Ions are generated from a gas-phase proton transfer between the excited matrix and analyte molecules. Fragmentation of the sample is minimized because the matrix absorbs most of the energy from the laser itself, thereby protecting the sample. Once formed, the ions, which are typically singly charged, enter a vacuum and are directed to the mass analyzer.

A time-of-flight (TOF) analyzer determines the m/z ratio of ions by measuring the time it takes for the ions to move to the detector. In a mixture of peptides generated by trypsin digestion, each ion will have a different mass. Once in the analyzer, the same amount of energy will be applied to the group of ions, which are then accelerated towards the detector. Each ion will reach the detector at a different time; the lighter the ion, the more quickly it will reach the detector and vice versa. The time it takes each ion to reach the detector is directly proportional to the m/z ratio of an individual ion and can be used

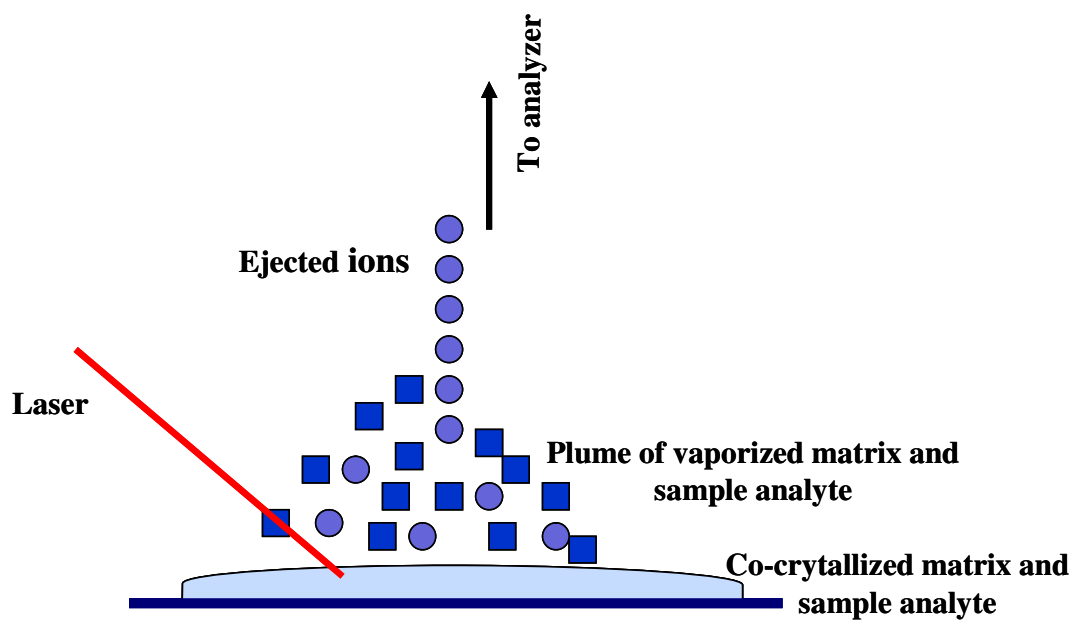


Figure 7. Schematic of matrix-assisted laser desorption ionization (MALDI).

to determine the mass of the ion following the formula, $m/z = 2eEl_s(t/l_d)^2$, where e is the electronic charge, E is the extraction field, l_s is the length of the source, l_d is the length of the field drift region, and t is the time of flight of the ion.

John Fenn combined electrospray ionization with mass spectrometry in the 1980's.^{74,75} In this method, which is illustrated in Figure 8, samples are volatilized and ionized directly from a liquid solution of sample analyte and solvent. The liquid mixture is sprayed from the tip of a needle towards the orifice of the mass spectrometer across a strong electric field. This serves to generate a fine mist of charged droplets.⁷⁶ Dry gas and/or heat is applied to the droplets at atmospheric pressure to evaporate the solvent, which produces gaseous charged ions. Unlike MALDI, where the ions are most often singly charged, ESI produces multiply charged ions usually as a result of multiple protonations or deprotonations.⁷⁴ This characteristic of ESI is advantageous as it allows for the masses of large molecules to be determined even if the mass range of the analyzer is small. Another advantage of ESI is that it can be readily interfaced to liquid separation techniques such as HPLC. ESI was improved upon through the advent of nanoelectrospray, which utilizes a smaller needle that is positioned closer to the orifice, to result in higher sensitivity.⁷⁷

It is commonplace that ESI is combined with a triple quadrupole mass analyzer or quadrupole TOF (ESI-qTOF) analyzer to perform tandem mass spectrometry (MS/MS). In the former, three quadrupoles are aligned in a row while in the latter, a TOF analyzer replaces the last quadrupole. One use of MS/MS is to sequence peptides. To do so, the ions must first be generated and then selected for activation and fragmentation. In the first quadrupole, precursor ions are selected. The second quadrupole houses gas for

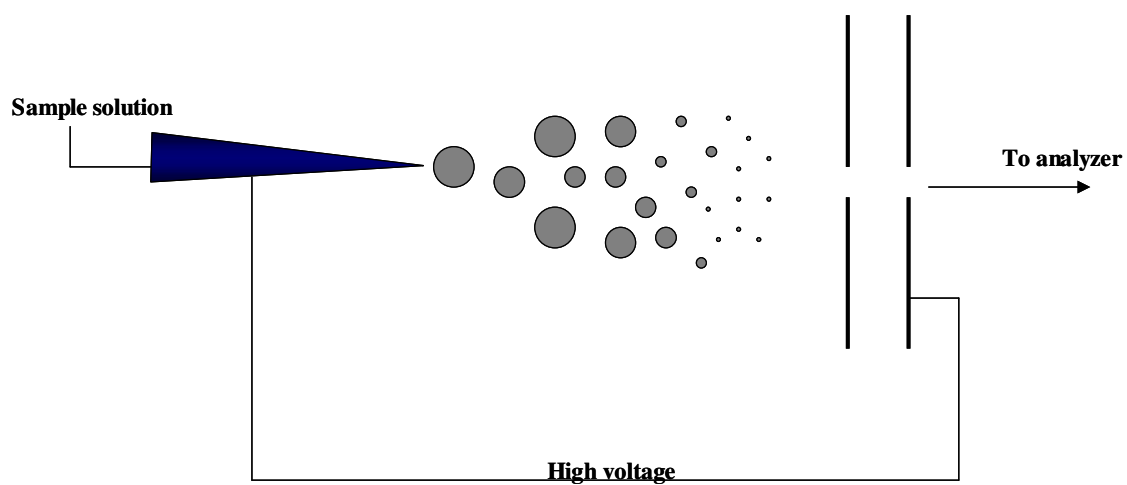


Figure 8. Schematic of electrospray ionization (ESI).

collisional activation, while the third analyzes product ions from the selected precursors.

Protein identification and bioinformatics

Protein identification using mass spectrometry combined with bioinformatics is achieved by either peptide mass fingerprinting or peptide microsequencing. To identify a protein by peptide mass fingerprinting, a peptide mixture is generated from the proteolytic digestion of a purified protein. A mass spectrum is then produced of all the observed molecular masses of the ions, each corresponding to a single peptide. Using a search engine such as Mascot, this list of peptides is compared to the theoretical digest generated in silico from all proteins in a selected database, such as SwissProt.⁷⁸ Search engines allow the user to change certain variables that he/she has controlled for, including taxonomy, proteolytic enzyme used and number of allowable missed cleavages. Using its own algorithm, the search engine creates a set of candidate proteins with which the measured peptides correlate, then ranks and scores the proteins based on how closely they meet the users selected criteria. Positive protein identification usually requires that five to eight peptides be matched for a 50 kDa protein and even more for larger proteins.⁷⁹ There are several limitations to peptide mass fingerprinting. First, this method cannot be used to identify mixtures of proteins. Second, small proteins are troublesome to identify, as they do not yield many peptide fragments. Also, occasionally, two peptides with the same mass but different amino acid sequences occur which without sequence information cannot be distinguished.

Peptide fragmentation, or microsequencing, on the other hand, can be used for protein mixtures as it does provide sequence information, thus making it much more specific than peptide mass fingerprinting. In this method, peptides are fragmented by

collision-induced dissociation. An ion of interest is selected and subjected to fragmentation to generate a mass spectrum from which part of its amino acid sequence can be interpreted. Like peptide mass fingerprinting, protein identification based on microsequencing is facilitated through bioinformatics. Usually, the partial sequence information is combined with mass information and submitted to a search engine.^{78,80} The search engine then returns the ranked and scored proteins from which that peptide may have originated. Using sequence tags from more than one peptide decreases the likelihood that the protein identification is erroneous. It is also possible to submit entire MS/MS spectra combined with mass information to a search engine.⁷³ In this case, the engine generates theoretical spectra from peptides of that mass and determines the best match.

Collision induced dissociation can be done on a variety of instruments including ESI-qTOF mass spectrometers. In this instrument, which is illustrated in Figure 9, there are two quadrupole cells, Q0 and Q1, a collision cell, Q2 and a TOF-reflectron analyzer. A single mass spectrometric analysis is done to determine what ions are present in the sample mixture. In this precursor ion scan, Q0 and Q1 serve as an ion guide whereby all ions are pulsed into the TOF analyzer. To fragment the ions of interest, a product ion scan or MS/MS analysis is run. In this mode, Q0 serves as the ion guide while Q1 serves as a mass filter; it only accelerates the ion of interest into the collision cell. Here, nitrogen gas is transmitted into the cell where it repeatedly collides with the ion to produce fragment ions that are then accelerated to the analyzer and fragment ion spectra recorded. This analysis usually produces two types of product ions by cleavages at the peptide bonds, designated as b and y ions. If the charge from the parent ion is retained on

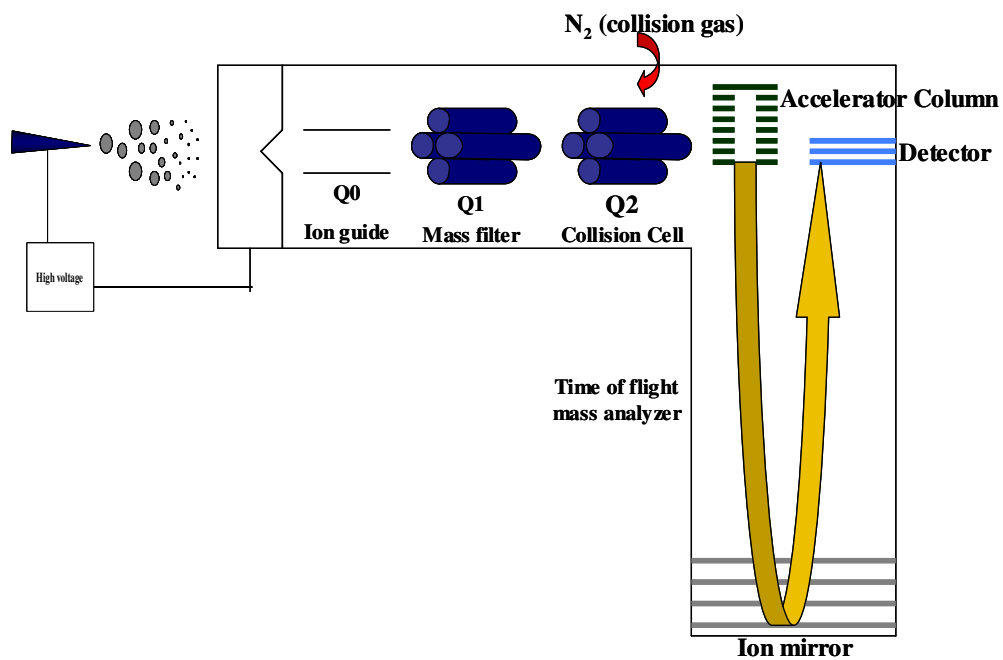


Figure 9. Schematic of a quadrupole time of flight mass spectrometer

the amino terminus of the fragment ion, a 'b' ion is produced. Conversely, if the charge is retained at the carboxy terminus, the detectable fragment is a 'y'. This is illustrated in Figure 10. Amino acid sequences generated from collision induced dissociation are relatively simple to interpret, as the mass difference between two consecutive b or y-ions is equal to the mass of an amino acid.

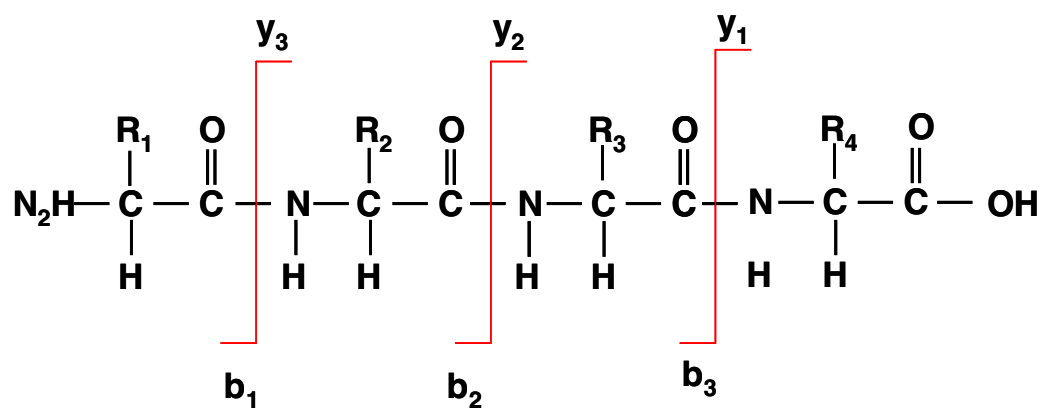


Figure 10. Fragmentation of a peptide to generate b and y-ions.

Hypothesis and objectives

Drug-resistance due to chemotherapy is the most common cause of treatment failure in cancer. It is important to understand the mechanisms of drug resistance in order to improve patient outcome and develop enhanced therapies. The ability of cancer cells to evade apoptosis is one way in which drug-resistance develops. Mitochondria play a central role in mediating apoptosis; many proteins associated with the organelle can promote or inhibit apoptosis. Also, many chemotherapy drugs associate intimately with mitochondria. Mitochondrial proteins may play an important role in the development of drug resistance. We hypothesize that the identification and characterization of mitochondrial proteins with altered abundances in drug resistant cancer cells will help decipher the mechanisms drug resistance.

The primary objective of this research is to contribute to the understanding of mechanisms of drug-resistance conferred by mitochondrial proteins. To do so I have:

1. Developed a reproducible method to isolate, purify and obtain the soluble proteins from MCF-7 cancer cell mitochondria
2. Created a proteomic gel map of the soluble mitochondrial proteins from MCF-7 cancer cells
3. Identified proteins with altered abundances between a drug-susceptible MCF-7 cancer cell line and MCF-7 cell lines selected for resistance to adriamycin in the presence of verapamil and for mitoxantrone
4. Considered mechanisms of drug resistance based on the function of altered mitochondrial proteins

Chapter 2: Materials and Methods

Materials

Dr. Ken Cowan at the National Institutes of Health generously provided the parent and mitoxantrone resistant MCF-7 human breast cancer cell lines.^{12,81} Dr. Douglas Ross at the University of Maryland medical school graciously provided the MCF-7 breast cancer cell line selected for resistance to adriamycin in the presence of verapamil.¹⁰ The two-dimensional quantitation kit, two-dimensional clean up kit and Percoll were obtained from Amersham Biosciences, which is now part of GE Healthcare (Piscataway, New Jersey). The protein isoelectric focusing cell, immobilized pH gradient (IPG) strips (17 cm, pH 3-10), IPG buffer, Protean II ready gels (8-16% Tris-HCl precast gel 193x183x1.0mm IPG comb) and BioSafe Coomassie blue stain were obtained from Bio-Rad (Hercules, California). Sequence grade, modified porcine trypsin was obtained from Promega Corporation (Madison, Wisconsin). Phosphate buffered saline (PBS), urea, thiourea, 3-[(3-cholamidopropyl) dimethylammonio]-1-propanesulfonate (CHAPS), dithiothreitol (DTT), iodoacetamide, ethylene glycol-bis (β -aminoethyl ether)-tetraacetic acid (EGTA), mannitol, sucrose, 4-morpholinepropanesulfonic acid (MOPS), calcium chloride, ammonium bicarbonate, sodium chloride, trifluoroacetic acid (TFA), Eagle's minimal media (MEM), fetal bovine serum (FBS), cell culture grade trypsin, penicillin streptomycin antibiotic solution, Trizma base, sodium dodecylsulfate (SDS) and glycerol were obtained from Sigma Aldrich (St. Louis, Missouri).

MCF-7 cell culture and harvest

The drug susceptible MCF-7, adriamycin resistant and mitoxantrone resistant MCF-7 cell lines were cultured in house. The cells were grown on 150 cm² flasks (Corning Incorporated, Corning, New York) in MEM supplemented with 10% fetal bovine serum and 1% penicillin streptomycin antibiotic solution. The cells were sustained in an incubator at a temperature of 37°C with 5% carbon dioxide. Once they reached confluence, the cells were harvested. First, cells were washed with 25 mL of 10 mM PBS. Then, 5 mL of cell culture grade trypsin was added and the flasks returned to the incubator in order to dislodge the cells. After several minutes (5 minutes for parent and mitoxantrone resistant cells, 10 minutes for the adriamycin resistant cells), 15 ml of MEM was added to hinder the trypsin. Cells were washed from the flask and pelleted in a centrifuge at 500g for 5 minutes. The cell pellet was washed two times with PBS, weighed and subjected to subcellular fractionation.

Isolation and purification of mitochondria

Mitochondria were isolated through a combination of homogenization, differential centrifugation and density gradient purification. All work was done on ice unless specified otherwise. The cell pellet was suspended in mitochondria isolation buffer (MIB; 220 mM mannitol, 70 mM sucrose, 5 mM MOPS, pH 7.4 plus 2 mM EGTA) at a ratio of 1 g cell pellet to 10 mL MIB.⁸² The suspension was manually homogenized using 70 strokes in 4 mL aliquots in a 7 mL Tenbroeck tissue grinder (VWR International Incorporated, Bridgeport, New Jersey). The homogenate was spun at 400g for 10 minutes to pellet the unbroken cells and nuclei. The supernatant was transferred to a pre-weighed 50 mL centrifuge tube (Fisher Scientific, Pittsburgh,

Pennsylvania) and kept on ice. The procedure was repeated but the pellet suspended in half the quantity of MIB used originally, and homogenized with only 50 manual strokes. After a second spin at 400g for 10 minutes, the supernatant was combined with that obtained previously and spun at 7000g for 10 minutes to pellet the crude mitochondrial fraction.

The crude mitochondria were weighed and suspended in a ratio 800 μ l mitochondria purification buffer (MPB; 220 mM mannitol, 70 mM sucrose, 5 mM MOPS, pH 7.4) to 0.8 g crude mitochondria. One milliliter of the suspension was layered over 14 ml of MPB and 6 mL of Percoll in a 50 mL thickwall polycarbonate centrifuge tube (Beckman Coulter, Palo Alto, California). The sample was spun in a fixed angle rotor (Ti 70, Beckman Coulter) at 38,900 rotations per minute (rpm) in a preparative ultra-centrifuge (Beckman Coulter). As seen in Figure 11, upon removal from the centrifuge, three layers could be distinguished, the bottom two of which contain mitochondria. The top layer was removed to waste with a 1 mL pipette. The bottom, dark yellow layers were collected into 4 separate centrifuge tubes in 5 mL aliquots, diluted 10 fold with MPB buffer and centrifuged at 7000g for 10 minutes to pellet the mitochondria.⁸³ The purified mitochondria from each tube were combined into one pre-weighed tube, washed twice with MPB buffer and weighed.

Preparation of soluble proteins

Purified mitochondria were suspended in protein extraction buffer (PEB; 7M Urea, 2M thiourea, 4% Chaps, 65 mM DTT, and 2% IPG buffer) at a ratio of 0.1g mitochondria to 600 μ l PEB.⁸⁴ To rupture the mitochondria, the suspension was placed in a beaker of ice and subjected to six, five second bursts of probe sonication (Sigma

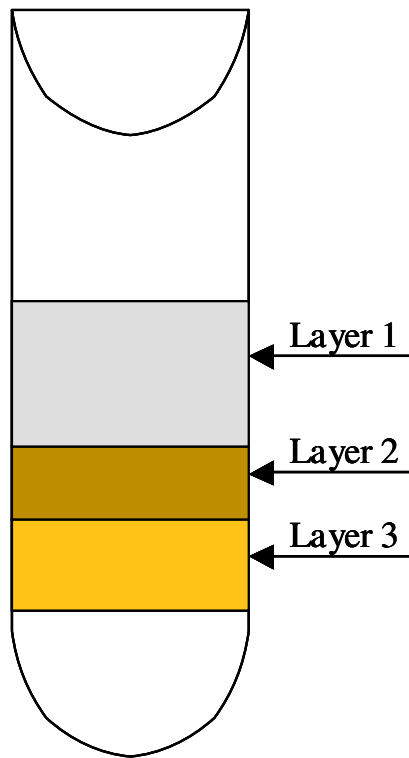


Figure 11. Schematic of density gradient purification of mitochondria. Layer 1 contains cellular debris and peroxisomes. Layers 2 and 3 contain purified mitochondria.

Aldrich) with a one-minute rest in between. Equal volumes of the sample were placed in 15 mL ultra-clear centrifuge tubes (Beckman Coulter) and centrifuged in a swinging bucket rotor (SW 60, Beckman Coulter) at 28,000 rpm for one hour to separate the soluble and insoluble proteins. The supernatant, or soluble protein fraction was collected and portioned into 1 ml aliquots so that protein concentration could be determined.

The two-dimensional quantitation kit was used to measure protein concentration, as it is compatible with the high concentrations of chemicals in the PEB. Two sample dilutions were made in triplicate for accuracy and reproducibility. A series of bovine serum albumin dilutions; 0, 10, 20, 30, 40 and 50 $\mu\text{g}/50\mu\text{L}$ were used to generate the standard curve. Absorbance was read at 480 nm on a DU 530 life science UV/Vis spectrometer (Beckman Coulter). Protein concentration was calculated based on absorbance and dilution fold. The volume of mitochondrial protein extract required to run a single 2-D gel experiment, 300 μg , was placed in individual Eppendorf tubes, flash frozen with liquid nitrogen and stored in a -80°C freezer.

Prior to 2-D gel electrophoresis the mitochondrial proteins were precipitated using the two-dimensional clean-up kit. The mitochondrial extract contains salts and buffers that can interfere with protein separation in the first dimension of 2-D gel electrophoresis. Thus, the proteins must be separated from the contaminants for a successful gel experiment. To do so, the two-dimensional clean-up kit was used to precipitate the mitochondrial proteins. Generally, recovery was about 90%, which was compensated for by increasing the volume of sample that was used. Following precipitation, the mitochondrial protein pellet was solubilized in 320 μl of rehydration buffer (7M urea, 2M

thiourea, 2% Chaps, 50mM DTT and 1% IPG buffer) and incubated on the bench top for 1 hr at room temperature.

2-D gel electrophoresis and comparative gel analysis

For a single 2-D gel experiment, we required that 300 µg of mitochondrial proteins be used. To begin the first dimension separation, the rehydration solution was pipetted onto the isoelectric focusing tray. An electrode wick saturated with 6 µL of distilled water was placed over the electrode at the anode, while a second wick saturated with 6 µL of 15 mM DTT was placed at the cathode to facilitate focusing of basic proteins.⁸⁵ A 17 cm IPG strip, pH 3-10 was placed gel side down and covered with 1.5 mL of mineral oil to prevent it from burning. The strip was rehydrated for 12 hours, after which proteins were focused for 60,000 V-hr.

After completion of isoelectric focusing, the IPG strip was placed in 3.5 mL of equilibration buffer (0.375 M tris-HCl, pH 8.8, 6M urea, 20% glycerol, and 2% sodium dodecylsulfate (SDS)) containing 2% DTT followed by 2.5% iodoacetamide to reduce and alkylate the proteins, respectively. Because it contained SDS, the equilibration buffer served to denature the proteins and also coated them with a negative charge. Thus, the inherent shape and charge of each protein had no effect and the proteins were separated in the second dimension based only on their molecular weight. The strip was placed on top of an 8-16% Tris-HCl precast gel and covered with agarose solution. The gel was developed at 16 mA for 30 minutes followed by 24 mA for approximately 5hr. Once the second dimension was complete, the gel was removed from between two glass plates and rocked gently for 1 hour in 500 ml of, 45% methanol, 5% acetic acid and 50% distilled water, to fix the proteins. After it was fixed, the gel was washed in water for 15

minutes and then stained overnight in Bio-safe colloidal Coomassie blue. Lastly, the gels were destained with gentle rocking in several washes of water so that densitometric image analysis could be performed with little background interference.

Two-dimensional gel images were visualized using a GS-800 calibrated densitometer (Bio-Rad) and its associated software. The gel images were scanned into the computer and saved as TIFF files. Image analysis was performed using Compugen Z3 software (Compugen Limited, Tel Aviv, Israel). Each gel image was registered and the software measured the relative expression of each spot in the gel. For comparative analysis, two gel images of choice were registered, layered on top of one another and the spots were matched after local adjustments had been made. The difference in abundance between the same spot on two gels was calculated based on the quotient of their relative expression on each gel, and was displayed by the computer program. For verification of the results, manual calculations were performed on each pair of spots. In order to ensure that the changes in abundance were not a result of biological or manual variation, each cell line was harvested four separate times and at least two gels were run from each of the harvest. As a minimum, the exemplary gel from each harvest, for each MCF-7 cell line, was used to complete the comparative analysis. Figure 12 is a schematic representation of comparative image analysis using Compugen Z3 software.

In-gel tryptic digestion and preparation of proteins

Peptides were analyzed to identify proteins of interest. An in-gel trypsin digestion was performed on protein spots with some modifications on the method of Mann.⁸⁶ All steps were done at room temperature except as noted otherwise. Using a plastic pipette, the protein spot of interest was carefully excised from the gel. The spot

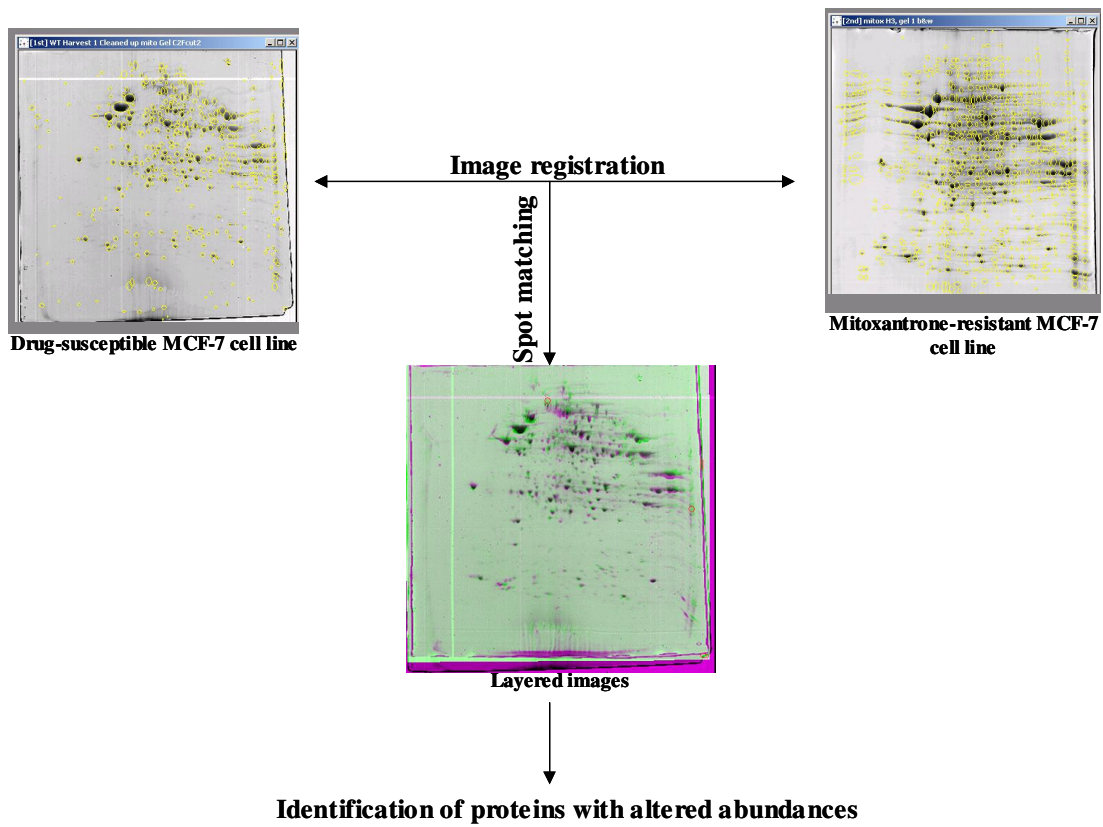


Figure 12. Schematic of comparative image analysis using Compugen Z3 software.

was placed in a 1.5 mL Eppendorf tube (Brinkmann Instruments, Westbury, New York) and using a scalpel, cut into cubes approximately 1-mm³ in size. Gel pieces were washed for 15 minutes in 50 µL of distilled water followed by 15 minutes in 50 µL of 50% acetonitrile. The liquid was removed and replaced with 50 µL of acetonitrile for 3 minutes to shrink the gel particles. Once they shrank, the acetonitrile was removed and 50 µL of 0.1 M ammonium bicarbonate (NH₄HCO₃) solution was added to the tube. After 5 minutes, 50 µL of acetonitrile was added and the gel pieces were incubated for 15 minutes at room temperature. All liquid was then removed and the gel pieces were completely dried down in a vacuum centrifuge for 15 minutes. Once dry, 50 µL of 10mM DTT in 0.1M NH₄HCO₃ was added and the tubes were incubated at 56°C in a water bath for 45 minutes to reduce the proteins. Upon removal from the water bath, the tubes were placed on the bench top for 10 minutes so that they could cool to room temperature. The liquid was removed, replaced with 50 µL of 55 mM iodoacetamide in 0.1 M NH₄HCO₃ and placed in the dark for 30 minutes to alkylate the proteins. Next, the liquid was removed and an additional wash step was done to ensure that no Coomassie blue remained in the gel pieces, as its presence would not be conducive to mass spectrometry analysis. To begin the wash, 50 µL of 0.1 M NH₄HCO₃ was added to the gel for 5 minutes, followed by the addition of 50 µL of acetonitrile. The liquid was removed and the gel pieces were completely dried down in a vacuum centrifuge for 15 minutes. To digest the proteins, 20 µL of digestion buffer (50 mM NH₄HCO₃, 5 mM CaCl₂ and 12.5 ng/µL of sequence grade trypsin) was added to each tube, which was immediately placed on ice and incubated for 45 minutes. Incubation at this stage ensured that the trypsin was taken up by the gel pieces. After 45 minutes, the digestion solution

was removed and replaced with 20 μL of, 50 mM NH_4HCO_3 and 5 mM CaCl_2 solution and placed in a 37°C water bath overnight for digestion to take place. After digestion had finished the peptides needed to be eluted from the gel pieces. To begin, 25 μL of 25 mM NH_4HCO_3 was added to each tube for 15 minutes to swell the gel pieces. Next, 25 μL of acetonitrile was added for 15 minutes to shrink the gel pieces. This cycle of swelling and shrinking served to push the peptides out of the gel pieces and into the supernatant, which was subsequently collected in a new Eppendorf tube. The extraction process was repeated two times with 5% formic acid in place of ammonium bicarbonate and the combined supernatants were completely dried down in a vacuum centrifuge for approximately 45 to 60 minutes.

Once the peptides had dried down, they were desalted. This step was imperative as salt hinders ionization, produces noise in spectra and can damage a mass spectrometer. To desalt peptides that originated from proteins that were more basic, of high molecular weight and/or were in high abundance, ZipTipC18 columns (Millipore, Billerica, Massachusetts) were used, while proteins that were smaller or less abundant were desalted on Omix Tip C18 columns (Varian, Lake Forest, California). Both are reverse phase columns that utilized the same procedure. To begin, the dried peptides were dissolved in 10 μL of 0.1% TFA in water. The column was then equilibrated; it was attached to a pipette and 10 μL of wetting solution (50% acetonitrile) was drawn into the tip, two times, followed by two rounds of aspiration of equilibration solution (10 μL of 0.1% TFA in water). To bind peptides to the column, 10 μL of peptide extract was drawn into and dispensed from the tip ten times. Bound peptides were then washed twice with equilibration solution. Finally, desalted peptides were recovered from the column

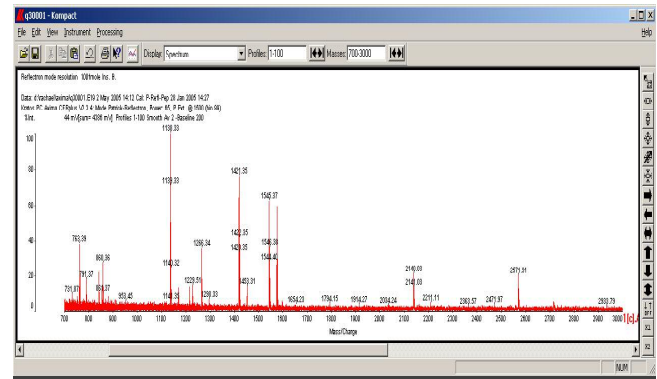
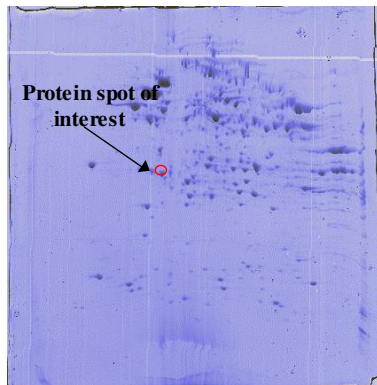
when 4 μ L of elution solution (0.1% TFA in 50% acetonitrile) was aspirated and dispensed from the tip ten times. For MALDI-TOF mass spectrometry, one microliter of the peptide extract was placed in a separate tube to be used directly for analysis. For electrospray, the extract was dried down in a vacuum centrifuge for 10 minutes and dissolved in 5 μ L of electrospray solution (49% water, 49% methanol, 2% acetic acid).

Mass spectrometry and protein identification

MALDI-TOF analyses were performed on an AXIMA-CFR instrument (Kratos Analytical, Chestnut Ridge, New York) on protein spots that were high in abundance. A half microliter of peptide extract was placed on the sample plate, over which the same volume of matrix (50 mM alpha-hydroxycinnamic acid in 0.1% TFA/ 70% acetonitrile) solution was placed. The analyte and matrix co-crystallized when dried at room temperature for approximately 20 minutes, after which time the plate was introduced into the mass spectrometer. Following the manufacturer's recommendation for protein identification by peptide mass fingerprinting, the instrument was set in reflectron mode, with laser power between 45 and 55, and a scan range of 1-4000 m/z units. Spectra were generated by averaging 100 profiles, each of which was taken from a different area as the sample was advanced across the lasers focal point. Those spectra, whose peak height to background noise ratio was greater than 2 to 1, were recorded in the Mascot search engine available at www.matrixscience.com, and submitted to the protein database SwissProt. Mascot generates a list of tryptic peptide masses for each protein in the SwissProt database and compares the experimental list of masses with each theoretical list. Mascot then ranks the proteins and returns a positive identification when the chance of a false-positive identification is less than one in twenty. The identification was then

checked to see if the pI and molecular weight of the protein correspond to that of the 2D-gel spot from which it was obtained. Figure 13 illustrates the use of peptide mass fingerprinting to obtain an identification of the mitochondrial protein, prohibitin.

Proteins that could not be identified by peptide mass fingerprinting and those that were less abundant, as determined by intensity of that spot on the 2-D gel map were examined by generating peptide sequence tags with tandem mass spectrometry. In this study all MS/MS work was done by collision induced dissociation on an API QSTAR Pulsar Qq-TOF electrospray ionization instrument (Applied Biosystems, Foster City, California). To introduce the sample, 1.5 μ L of electrospray buffer solution containing the peptide mixture was loaded into a capillary tip (Protana Incorporated, Odense, Denmark) and placed in the nanospray source. In order to determine what peptide molecular ions were present in the sample mixture, it was necessary to first run a precursor scan. To do so, the spray voltage was set to 900 V and the MS scan range was set between 350-1000 m/z; only peptides whose m/z ratio fell within that range were allowed to pass through the Q1, or mass filter quadrupole cell. Once the MS spectrum had been produced, doubly charged peptides were manually chosen for fragmentation. In the product ion scan, only the peptide of interest was isolated in Q1 and allowed to pass into the collision cell, Q2. To induce fragmentation, a controlled amount of nitrogen gas was transmitted into the collision cell. Typically ions whose m/z value was less than 600 required collision energy in the range of 20 to 32, while the collision energy needed to fragment ions of a larger m/z value ranged between 32 and 45. The fragmented ions were pulsed to the detector and an MS/MS spectrum was recorded. Because CID spectra generally produce b and y-ions, a partial peptide sequence could be easily deduced,



1 MAAKFESIGK FGLALA VAGGVNSALYNVDA GHRA VIEDFRGVQDIVV
 51 GEGTHFLIPWVQKPIIFDCRSRPRNVPVITGSKDLQNVNITLRILFRPVA
 101 SQLPRIFTSIGEDYDERVLPSTTEILKSVVARFDAGELITQRELVSRQV
 151 SDDLTERAA TFGLILDDVSLTHLTFGKEFTEAVEAKQVAQQAERARFVV
 201 EKAEQQKKAIIISAEGDSKAAELIANSLATAGDGLIELRKLAAEDIA YQ
 251 LSRNRNITYLPAGQSVLLQLPQ

Mass List
 1149.4
 1185.4
 1213.4
 1396.5
 1444.3
 1606.3
 1997.2
 2118.2

Protein identified as prohibitin with 40 % sequence coverage

Figure 13. Identification of the mitochondrial protein prohibitin by peptide mass fingerprinting.

most usually by calculating the mass differences between consecutive peaks. Usually, sequence tags from two to five peptides were used for protein identification. The sequence tags, masses of the peptides and masses on each side of the tag were submitted through Mascot using the BioExplore software program associated with the mass spectrometer, which interrogates the protein databases, SwissProt and NCBI (National Center for Biotechnology Information). Again, the search engine (Mascot) returned a list of candidate proteins from which the sequence tags could have originated. Mascot ranked the proteins and determined the identity to a 95% confidence level. It follows that the identification was more reliable when an increased number of peptide sequence tags were matched to a single protein. As with proteins identified by peptide mass fingerprinting, the pI and molecular weight of the candidate protein were checked against the location of that spot on the 2-D gel. Figure 14 shows the identification of delta3,5-delta2,4-dienoyl CoA isomerase, a mitochondrial matrix protein, using tandem mass spectrometry.

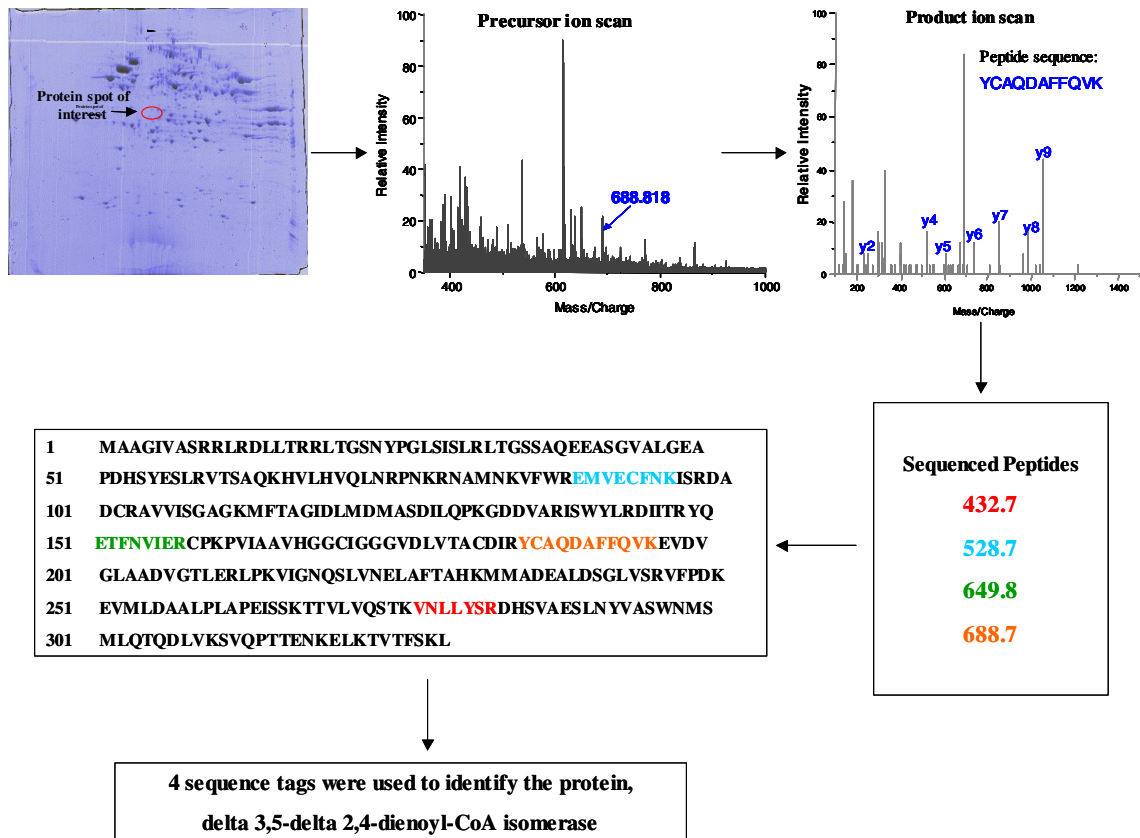


Figure 14. Identification of the mitochondrial protein, delta3,5-delta2,4-dienoyl-CoA isomerase by peptide microsequencing.

Chapter 3: Results

Preparation of mitochondrial proteins

A reproducible method to isolate, purify and extract the soluble proteins from MCF-7 cancer cell mitochondria has been optimized. At confluence, approximately $6-8 \times 10^6$ cells were harvested from each of twenty 150 cm^2 flasks. Typically, between three and four grams of cell pellet was obtained. From this, we were able to isolate a crude mitochondrial pellet and purified mitochondrial pellet that weighed one-half and one-tenth of the weight of the original cell pellet, respectively. Following purification of the organelle, we were able to extract one milligram of soluble mitochondrial proteins.

Protein identification and evaluation of purification method

The soluble mitochondrial proteins were separated by 2D-GE. After the gel images were recorded, protein spots of interest were excised and subjected to in-gel digestion with trypsin. The resultant peptides were analyzed by mass spectrometry and proteins were identified based on peptide mass fingerprinting or microsequencing combined with bioinformatics.

Proteins that were identified by peptide mass fingerprinting matched five or more peptides. For microsequencing, at least two sequence tags were typically used for protein identification. For some proteins however, a positive identification was obtained with only one sequence tag. In these cases, a theoretical digest of the protein was performed and the experimental mass spectra were manually interpreted to determine if the identification could be accepted. All of the proteins identified in this analysis have a

Mascot score that exceeds the 95% confidence level set by the software. Also, the pI and molecular weight of each protein were verified on the 2D-gel image.

Most mitochondrial proteins are encoded by the nuclear genome and synthesized as precursors in the cytosol. From here, the precursor proteins are imported into the organelle based on targeting sequences that are cleaved once they reach the mitochondria. The targeting sequence is not part of a functional mitochondrial protein. Thus, that part of the amino acid sequence does not influence the pI and molecular weight of a given protein. Unfortunately, for some mitochondrial proteins, the amino acid portion of the targeting sequence has not yet been determined. Thus, the pI and molecular weight of some proteins, as reported in databases such as SwissProt does not correspond to the position of the protein on the 2D-gel map.

Sample purity was evaluated based on protein identification. An annotated 2D-gel image of the crude mitochondrial fraction is shown in Figure 15. Table 1 lists the proteins identified in the crude fraction. Of the 93 spots that were identified, 48, or 52% are currently known to be associated with a cellular compartment other than mitochondria. Thus, only 48% of the proteins identified in the crude fraction are known to localize to mitochondria. Figure 16 shows the annotated proteomic gel map of the purified mitochondrial fraction. Table 2 lists the proteins identified in the purified mitochondrial fraction. In this fraction, we have identified 184 spots, corresponding to 156 unique protein identifications. Of these 156 proteins, 132, or 80% are reported to belong to the mitochondria, while only 24 of the proteins are not known to be associated with the organelle. Based on these results, we have optimized a method to isolate purified mitochondria.

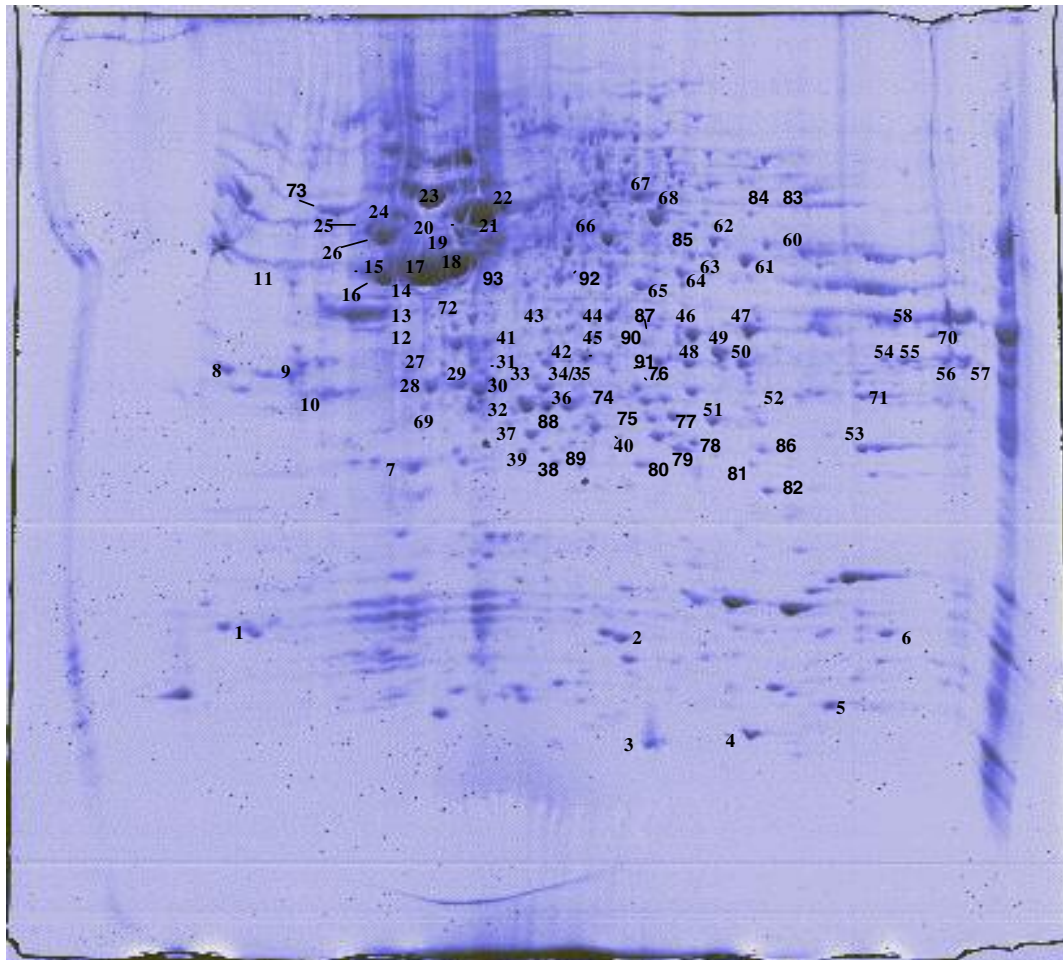


Figure 15. Annotated 2D-gel map of the soluble proteins extracted from the crude mitochondrial fraction.

Spot	Accession Number	Protein	Location
1	P30049	ATP synthase delta chain	M
2	P10606	Cytochrome c oxidase polypeptide Vb	M
3	P02248	Ubiquitin	C
4	P02249	Ubiquitin	C
5	P14179	Macrophage migration inhibitory factor	M
6	Q04837	Single-stranded DNA binding protein	M
7	O75947	ATP synthase D chain	M
8	Q07021	Complement component 1	M
9	P42655	Mitochondrial import stimulation factor	M
10	P35214	14-3-3 protein gamma	C
11	P08865	40S ribosomal protein SA	R
12	P29692	Elongation factor 1-delta	C
13	O60812	Heterogenous nuclear protein c-like	N
14	P07910	Heterogenous nuclear protein C1/C2	N
15	P08727	Cytokeratin 19	C
16	P19012	Cytokeratin 15	C
17	P02570	Beta-actin	C
18	P05783	Cytokeratin 18	C
19	P04765	Eukaryotic initiation factor 4A-1	C
20	P05787	Cytokeratin 8	C
21	P31930	Ubiquinol-cyt. C reductase protein 1	M
22	P30101	Disulfide isomerase, ER-60	ER
23	P10809	HSP-60	M
24	Q9BQE3	Tubulin, alpha-6 chain	C
25	P05218	Tubulin, beta-5 chain	C
26	P06756	ATP synthase beta chain	M
27	P05388	60S acidic ribosomal protein P0	R

Table 1. Proteins identified in the crude mitochondrial fraction. SwissProt accession numbers are provided. Subcellular location abbreviations: M-mitochondria, C-cytosol, ER-endoplasmic reticulum, N-nucleus, L-lysosome, R-ribosome.

Spot	Accession Number	Protein	Location
28	P07339	Cathepsin D	L
29	P35232	Prohibition	C
30	P07339	Cathepsin D	L
31	P47756	F-actin capping protein beta subunit	C
32	Q13162	Peroxiredoxin 4	C
33	P30084	Enoyl-CoA hydratase	M
34	P42126	3,2-trans-enoyl CoA isomerase	M
35	P30040	ER protein 29	ER
36	P45880	VDAC-2	M
37	P04792	HSP-27	C
38	P30048	Peroxiredoxin 3	M
39	Q9HAV7	GrpE protein homolog 1	M
40	P47985	Ubiquinol-cyt C reductase iron-sulfur	M
41	P49411	Elongation factor Tu	M
42	P50897	Palmitoyl-protein thioesterase 1	L
43	O43464	Serine protease HTRA2	M
44	P43897	Elongation factor Tu	M
45	Q13011	Delta3,5-delta2,4-dienoyl-CoA isomerase	M
46	P04406	Glyceraldehyde 3-phosphate dehydrogenase	C
47	P07355	Annexin-2	PM
48	P13804	Electron transfer flavoprotein alpha-subunit, precursor	M
49	P45880	VDAC-2	M
50	P25388	Receptor of activated protein kinase C1	C
51	Q99714	3-hydroxyacyl-CoA dehydrogenaseII	ER
52	Q9BSE5	Agmatinase, precursor	M
53	Q06830	Peroxiredoxin-1	C
54	Q16836	Short chain 3-hydroxyacyl-CoA dehydrogenase	M

Table 1. Proteins identified in the crude mitochondrial fraction. SwissProt accession numbers are provided. Subcellular location abbreviations: M-mitochondria, C-cytosol, ER-endoplasmic reticulum, N-nucleus, L-lysosome, R-ribosome.

Spot	Accession Number	Protein	Location
55	Q16836	Short chain 3-hydroxyacyl-CoA dehydrogenase	M
56	P21796	VDAC-1	M
57	P21796	VDAC-1	M
58	P22695	Ubiquinol-cyt C reductase protein 2	M
59	P22695	Ubiquinol-cyt C reductase protein 2	M
60	O75390	Citrate synthase	M
61	P12532	Creatine kinase	M
62	P07954	Fumarate hydratase	M
63	P26440	Isovaleryl-CoA dehydrogenase	M
64	O96008	TOM-40 homolog	M
65	Q15365	Poly(rC)-binding protein 1	N/C
66	P06733	Alpha enolase	C
67	P25705	ATP synthase alpha chain	M
68	P00367	Glutamate dehydrogenase 1	M
69	O75489	NADH-ubiquinone oxidoreductase 30 kDa subunit	M
70	P40926	Malate dehydrogenase	M
71	P38117	Electron transfer flavoprotein beta-subunit	M
72	P11016	Guanine nucleotide binding protein	C
73	P05218	Tubulin beta-5 chain	C
74	P30041	Peroxisredoxin 6	C
75	P60174	Trioesphosphate isomerase	C
76	P18669	Phosphoglycerate mutase 1	C
77	P55795	Heterogenous nuclear protein H	N
78	P30043	Flavin reductase	C
79	P17080	GTP-binding nuclear protein RAN	N
80	P25705	ATP synthase alpha chain	M
81	P30043	Flavin reductase	C

Table 1. Proteins identified in the crude mitochondrial fraction. SwissProt accession numbers are provided. Subcellular location abbreviations: M-mitochondria, C-cytosol, ER-endoplasmic reticulum, N-nucleus, L-lysosome, R-ribosome.

Spot	Accession Number	Protein	Location
82	P30086	Phosphatidylethanolamine-binding protein	C
83	P25705	ATP synthase alpha chain	M
84	P49821	NADH-ubiquinone oxidoreductase 51 kDa subunit	M
85	P19474	52-kD SS-A/Ro autoantigen	C
87	P45880	Voltage dependent selective anion channel protien 2	M
88	P31943	Heterogenous nuclear protein H	N
89	O75608	Acyl-protein thioesterase 1	C
90	Q8TDO2	Hepatocarcinoma high-expression protein	C
91	Q8WUFO	Nit protein 2	M
92	P13639	Elongation factor 2	C
93	Q9P129	Calcium binding transporter	M

Table 1. Proteins identified in the crude mitochondrial fraction. SwissProt accession numbers are provided. Subcellular location abbreviations: M-mitochondria, C-cytosol, ER-enodplasmic reticulum, N-nucleus, L-lysosome, R-ribosome.

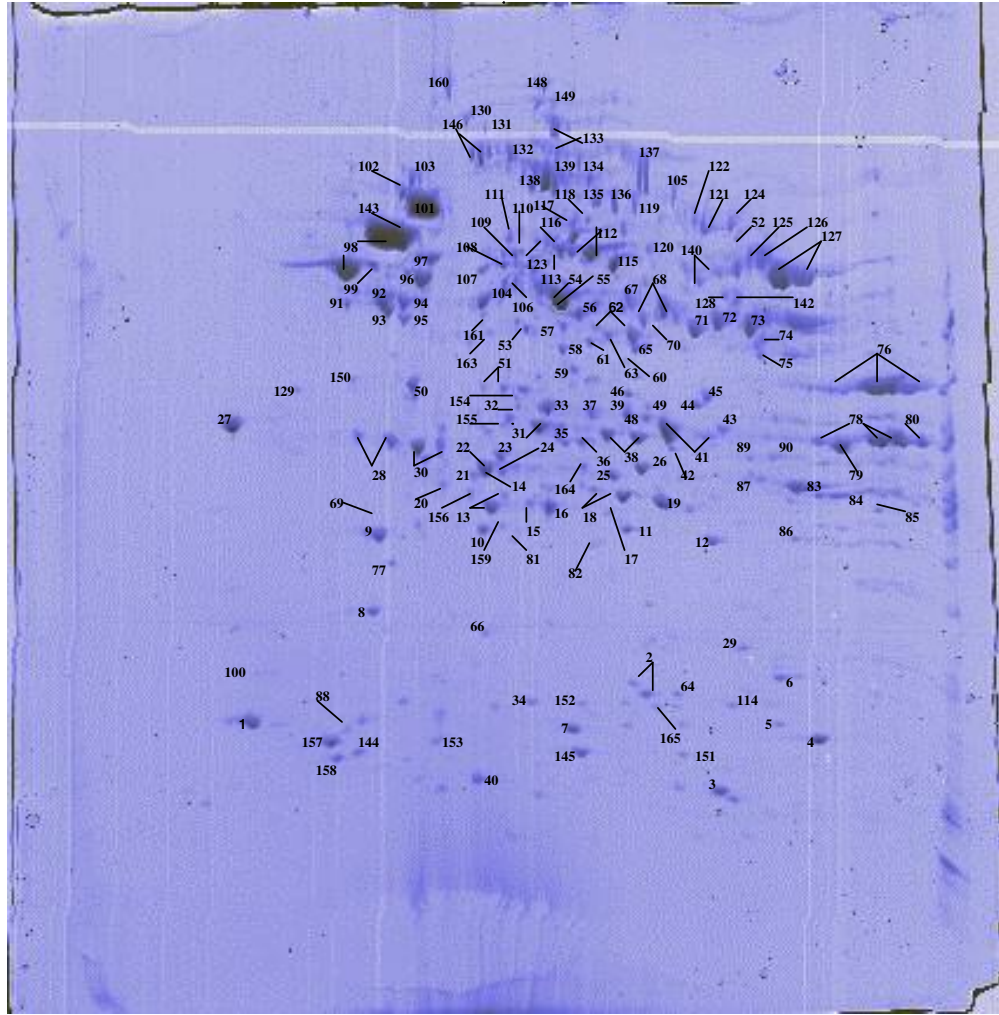


Figure 16. Annotated 2D-gel map of the soluble proteins extracted from the purified mitochondrial fraction.

Spot	Accession Number	Protein	Location	pI	MW	Sequence Tags
1	P30049	ATP synthase, delta chain	M	4.53	15019	2
2	P30044	Peroxisredoxin 5	M	6.96	16899	4
3	P82644	28S ribosomal protein S10	M	7.78	22985	2
4	Q04837	Single-stranded DNA binding protein	M	8.24	15195	3
5	Q9P0J0	NADH-ubiquinone oxiooreductase B16.6	M	8.23	16557	2
6	P23528	Cofilin	C/N/M	8.22	18491	2
7	P10606	Cytochrome c oxidase, polypeptide Vb	M	6.33	10613	1
8	P52815	60S ribosomal protein L12	M	5.37	16394	3
9	O75947	ATP synthase, D chain	M	5.22	18348	4
10	Q9HAV7	GrpE protein homolog 1	M	6.03	21336	3
11	P04179	Superoxide dismutase	M	6.86	22204	2
12	Q9H5G0	Hypothetical protein FLJ23469	C	7.66	24082	5
13	P30048	Peroxisredoxin 3	M	5.77	21468	4
14	P04792	Heat shock protein 27	C	5.95	22768	2
15	O75608	Acyl-protein thioesterase 1	C	6.29	24653	2
16	P47985	Ubiquinol-cytochrome c reductase iron-sulfur	M	6.3	21616	2
17	P25705	ATP synthase alpha chain	M	8.28	55209	2
18	P30042	ES1 protein homolog	M	6.63	24016	3
19	Q99714	3-hydroxyacyl-CoA dehydrogenase type II	ER	7.66	26906	5
20	O75489	NADH-ubiquinone oxidoreductase 30	M	5.48	26414	2
21	O75431	Metaxin 2	M	5.9	29744	1
22	P30084	Enoyl-CoA hydratase	M	5.88	28354	2
23	P42126	3,2 trans-enoyl CoA isomerase	M	6	28736	3
24	Q9Y398	CGI-90 protein	M	8.57	35693	3
25	O43819	SCO2 protein homolog	M	6.41	25138	11
26	Q8N723	Epoxide hydrolase	M	9.29	33842	4

Table 2. Proteins identified in the purified mitochondrial fraction. SwissProt accession numbers are provided. Subcellular location abbreviations: M-mitochondria, C-cytosol, ER-enodoplasmic reticulum, N-nucleus, L-lysosome, P-peroxisome, U-unknown, R-ribosome. The isoelectric point and molecular weight is provided. The number of microsequences used for protein identification is provided as sequence tags.

Spot	Accession Number	Protein	Location	pI	MW	Sequence Tags
27	Q07021	Complement component 1	M	4.32	23783	1
28	P07339	Cathepsin D	L	5.6	37852	3
29	P51970	NADH-ubiquinone oxoreductase 19	M	7.93	19961	3
30	P35232	Prohibitin	M	5.57	29786	6
31	Q13011	Delta3,5-delta2,4-dienoyl CoA isomerase	M	6.61	35971	4
32	P53701	Cytochrome c-type heme lyase	M	6.25	30582	2
33	P43897	Elongation factor Ts	M	6.26	30503	4
34	Q9BX68	Histidine triad nucleotide binding protein	C	9.2	17151	2
35	Q8WUF0	Nit protein 2	M	6.82	30561	3
36	Q9BSH4	Hypothetical protein UPF0082	U	8.37	32457	3
37	P45880	Voltage anion dependent selective channel protein 2	M	6.32	38069	5
38	P13804	Electron transfer flavoprotein, alpha subunit	M	8.62	35058	3
39	Q16762	Thisulfate sulfurtransferase	M	6.83	33277	5
40	P14854	Cytochrome c oxidase, polypeptide VIb	M	6.78	10005	3
41	P45880	Voltage anion dependent selective channel protein 2	M	6.32	38069	5
42	Q9H7Z7	Hypothetical protein FLJ14038	M	9.22	41917	3
43	P32322	Pyroline-5-carboxylate reductase	C	7.18	33354	2
44	P07355	Annexin A2	C	7.56	38449	2
45	P13995	NAD-dependent methylenetetrahydrofolate dehydrogenase	M	7.34	34137	4
46	Q9NX40	Hypothetical protein FLJ20455	C	7.02	27609	3
48	Q9BYD6	Ribosomal protein L1	M	8.19	34431	3
49	Q9H9J2	39S ribosomal protein L44	M	8.64	37512	4

Table 2. Proteins identified in the purified mitochondrial fraction. SwissProt accession numbers are provided. Subcellular location abbreviations: M-mitochondria, C-cytosol, ER-endoplasmic reticulum, N-nucleus, L-lysosome, P-peroxisome, U-unknown, R-ribosome. The isoelectric point and molecular weight is provided. The number of microsequences used for protein identification is provided as sequence tags.

Spot	Accession Number	Protein	Location	pI	MW	Sequence Tags
50	P11177	Pyruvate dehydrogenase E1 component, beta subunit	M	5.38	35890	5
51	Q9H2U2	Inorganic pyrophosphatase	M	5.97	34707	3
52	P14618	Pyruvate kinase, isozymes M1/M2	C	7.95	57769	3
53	P82650	28S ribosomal protein S22	M	7.7	41254	7
54	P49411	Elongation factor Tu	M	6.31	45045	4
56	P08559	Pyruvate dehydrogenase E1 component, alpha subunit	M	6.51	40228	2
57	Q9UKU7	Acyl-CoA dehydrogenase family member 8	M	8.12	45040	1
58	Q9H370	PRO1512	M	5.81	34101	3
59	Q9NYK5	39S ribosomal protein L39	M	6.47	34204	2
60	P36551	Coproporphyrinogen III oxidase	M	7.31	36865	2
61	Q96DV4	Ribosomal protein L38	M	6.2	40731	3
62	O96008	Probable mitochondrial import receptor TOM40	M	6.79	37869	2
63	Q9BS94	Similar to 3-hydroxisobutyryl-CoA hydrolase	M	8.76	37356	2
64	P62937	Peptidyl-prolyl cis-trans isomerase	C	8.37	17128	2
65	O95299	NADH-ubiquinone oxidoreductase 42	M	6.87	37147	2
66	P82663	28S ribosomal protein S10	M	7.78	22985	4
67	P11310	Acyl-CoA dehydrogenase, medium chain	M	7.02	43642	4
68	P07954	Fumarate hydratase	M	6.99	50081	4
69	O00217	NADH-ubiquinone oxidoreductase 23	M	5.1	20290	2
70	P40939	Trifunctional enzyme, alpha subunit	M	8.98	79009	2

Table 2. Proteins identified in the purified mitochondrial fraction. SwissProt accession numbers are provided. Subcellular location abbreviations: M-mitochondria, C-cytosol, ER-endoplasmic reticulum, N-nucleus, L-lysosome, P-peroxisome, U-unknown, R-ribosome. The isoelectric point and molecular weight is provided. The number of microsequences used for protein identification is provided as sequence tags.

Spot	Accession Number	Protein	Location	pI	MW	Sequence Tags
71	P12532	Creatine kinase	M	7.31	43080	4
72	O75390	Citrate synthase	M	6.98	49000	3
73	P22695	Ubiquinol-cytochrome c reductase protein 2	M	7.74	46784	4
74	P24752	Acetyl-CoA acetyltransferase	M	8.16	41386	3
76	P40926	Malate dehydrogenase	M	8.54	33000	3
77	P32119	Peroxiredoxin 2	C	5.66	21878	2
78	P21796	Voltage anion dependent selective channel protein 1	M	8.63	30623	4
79	Q16836	Short chain 3-hydroxyacyl-CoA dehydrogenase	M	8.38	32822	3
80	Q9Y277	Voltage anion dependent selective channel protein 3	M	8.85	30639	3
81	P25705	ATP synthase, alpha subunit	M	8.28	55209	2
82	P25705	ATP synthase, alpha subunit	M	8.28	55209	3
83	P38117	Electron transfer flavoprotein beta-subunit	M	8.24	27826	3
84	Q9NX63	Coiled-coil-helix-coiled-coil helix domain containing protein 3	M	8.48	26136	3
85	Q9UFN0	NipSnap3A protein	C	9.21	28449	1
86	Q06830	Peroxiredoxin 1	C	8.27	22096	3
87	P54819	Adenylate kinase isoenzyme 2	M	7.85	26330	3
88	Q16595	Frataxin	M	5.59	17235	2
89	Q9BTZ2	Dehydrogenase/reductase SDR member 4	P	7.66	27554	2
90	Q02338	D-beta-hydroxybutyrate dehydrogenase	M	8.16	33075	3
91	P08727	Cytoskeletal keratin 19	C	5.04	44079	4
92	P02571	Actin	C	5.31	41766	2

Table 2. Proteins identified in the purified mitochondrial fraction. SwissProt accession numbers are provided. Subcellular location abbreviations: M-mitochondria, C-cytosol, ER-endoplasmic reticulum, N-nucleus, L-lysosome, P-peroxisome, U-unknown, R-ribosome. The isoelectric point and molecular weight is provided. The number of microsequences used for protein identification is provided as sequence tags.

Spot	Accession Number	Protein	Location	pI	MW	Sequence Tags
93	Q96I99	Succinyl-CoA ligase [GDP-forming] beta-chain	M	5.17	42564	4
94	P05783	Cytoskeletal keratin 18	C	5.34	47897	2
95	Q9UJZ1	Membrane associated protein SLP-2	N	6.88	38510	4
96	P31930	Ubiquinol-cytochrome-c reductase protein I	M	5.43	49101	4
97	P05787	Cytoskeletal keratin 8	C	5.52	53510	4
98	P06756	ATP synthase, beta chain	M	5	51769	5
99	Q12849	G-rich sequence factor-1	C	5.51	47969	1
100	P07919	Ubiquinol-cytochrome c reductase 11	M	4.46	9246	2
101	P38646	Stress-70 protein	M	5.44	68759	4
102	Q96IS6	HSP A8 protein fragment	M	5.36	64562	2
103	P28331	NADH-ubiquinone oxidoreductase 75	M	5.36	77053	2
104	Q9P129	Calcium binding transporter, fragment	M	5.31	45790	5
105	P43304	Glycerol-3-phosphate dehydrogenase	M	6.17	76323	4
106	P04181	Ornithine aminotransferase	M	5.72	44808	4
107	P36957	Dihydrolipoamide succinyltransferase	M	5.89	41349	2
108	P28838	Cytosol aminopeptidase	C	6.29	52607	2
109	Q10713	Mitochondrial processing peptidase alpha subunit	M	5.88	54646	2
110	O00330	Pyruvate dehydrogenase protein X component	M	6.01	48024	3
111	P30837	Aldehyde dehydrogenase X	M	6.01	55292	2
112	P09622	Dihydrolipoyl dehydrogenase	M	6.35	50147	2
113	P49419	Aldehyde dehydrogenase family 7 member A1	M	6.24	55200	2

Table 2. Proteins identified in the purified mitochondrial fraction. SwissProt accession numbers are provided. Subcellular location abbreviations: M-mitochondria, C-cytosol, ER-endoplasmic reticulum, N-nucleus, L-lysosome, P-peroxisome, U-unknown, R-ribosome. The isoelectric point and molecular weight is provided. The number of microsequences used for protein identification is provided as sequence tags.

Spot	Accession Number	Protein	Location	pI	MW	Sequence Tags
114	P62937	Peptidyl-prolyl cis-trans isomerase A	C	8.37	17128	2
115	P00367	Glutamate dehydrogenase 1	M	6.71	56008	4
116	Q9HCC0	Methylcrotonoyl-CoA carboxylase beta chain	M	7.57	61294	3
117	Q9H7G2	Hypothetical protein FLJ20920	M	7.5	68081	3
118	Q16134	Electron transfer flavoprotein-ubiquinone oxidoreductase	M	6.52	64675	3
119	P30038	Delta-1-pyrroline-5-carboxylate dehydrogenase	M	6.96	59034	3
120	P51649	Succinate semialdehyde dehydrogenase	M	7.17	52302	2
121	O95831	Apoptosis-inducing factor	M	6.86	55699	4
122	P23786	Carnitine O-palmitoyltransferase II	M	7.27	71129	4
123	P11413	Glucose-6-phosphate 1-dehydrogenase	C	6.76	59096	7
124	P49748	Acyl-CoA dehydrogenase, very-long-chain	M	7.74	66175	4
125	Q02252	Methylmalonate-semialdehyde dehydrogenase	M	8.01	54388	4
126	P34897	Serine hydroxymethyltransferase	M	8.11	52559	3
127	P25705	ATP synthase, alpha subunit	M	8.28	55209	6
128	P80404	4-aminobutyrate aminotransferase	M	7.19	53270	2
129	O00165	HS1-binding protein	M	4.99	31621	3
130	P36776	Lon protease homolog	M	6.01	106422	3
131	P04264	Cytoskeletal keratin 2	C	8.16	65847	2
132	Q96RP9	Elongation factor G1	M	6.58	83452	2
133	P54886	Delta 1-pyrroline-5-carboxylate synthetase	M	6.66	87248	3

Table 2. Proteins identified in the purified mitochondrial fraction. SwissProt accession numbers are provided. Subcellular location abbreviations: M-mitochondria, C-cytosol, ER-endoplasmic reticulum, N-nucleus, L-lysosome, P-peroxisome, U-unknown, R-ribosome. The isoelectric point and molecular weight is provided. The number of microsequences used for protein identification is provided as sequence tags.

Spot	Accession Number	Protein	Location	pI	MW	Sequence Tags
134	Q96RQ3	Methylcrotonoyl-CoA carboxylase alpha chain	M	6.44	75030	2
135	Q9H455	Hypothetical protein FLJ12692	M	8.16	75432	2
136	Q16822	Phosphoenolpyruvate carboxykinase	M	6.58	67004	5
137	Q99798	Aconitate hydratase	M	6.85	82452	2
138	Q12931	Heat shock protein 75	M	8.05	79961	4
139	P43304	Glycerol-3-phosphate dehydrogenase	M	6.17	76323	2
140	P49821	NADH-ubiquinone oxidoreductase 51	M	7.53	48505	3
142	P22570	NADPH:adrenodoxin oxidoreductase	M	7.11	49967	2
143	P10809	60 kDa heat shock protein	M	5.24	57962	5
144	Q86SX6	Glutaredoxin-related protein C14orf87	M	6.28	16618	2
145	gi 4099125	Cytochrome c oxidase subunit Via	M	6.43	9744	1
146	Q16891	Mitofilin	M	6.08	83626	7
148	P11498	Pyruvate carboxylase	M	6.14	127339	3
149	Q02218	2-oxoglutarate dehydrogenase E1 component	M	6.24	108880	4
150	gi 56078960	Hypothetical protein DKFZp434K046	U	5.61	35847	3
151	O75380	NADH-ubiquinone oxidoreductase 13	M	7.13	10698	1
152	gi 55957569	OTTHUMO00000016217	N	7.82	11902	1
153	Q16718	NADH-ubiquinone oxidoreductase 13 kDa-B	M	5.76	13319	3
154	Q9Y375	Complex I intermediate-associated protein 30	M	5.88	35003	2
155	Q92506	Estradiol 17-beta-dehydrogenase 8	M	6.09	26957	4

Table 2. Proteins identified in the purified mitochondrial fraction. SwissProt accession numbers are provided. Subcellular location abbreviations: M-mitochondria, C-cytosol, ER-endoplasmic reticulum, N-nucleus, L-lysosome, P-peroxisome, U-unknown, R-ribosome. The isoelectric point and molecular weight is provided. The number of microsequences used for protein identification is provided as sequence tags.

Spot	Accession Number	Protein	Location	pI	MW	Sequence Tags
156	P19404	NADH-ubiquinone oxidoreductase 24	M	5.71	23760	3
157	gi 18999392	Cytochrome c oxidase subunit Va	M	6.3	16752	1
158	Q99757	Thioredoxin	M	4.88	11867	1
159	Q9Y6N1	Cytochrome c oxidase assembly protein COX11	M	9.21	31438	2
160	P42707	130 kDa leucine-rich protein	C	5.5	145109	3
161	P45954	Acyl-CoA dehydrogenase, short/branched chain	M	5.72	43695	3
163	P50213	Isocitrate dehydrogenase, alpha subunit	M	5.71	36640	3
164	gi 8923001	Hypothetical protein FLJ11342	M	5.84	25886	3
165	Q13405	39S ribosomal protein L49	M	9.47	19186	1

Table 2. Proteins identified in the purified mitochondrial fraction. SwissProt accession numbers are provided. Subcellular location abbreviations: M-mitochondria, C-cytosol, ER-endoplasmic reticulum, N-nucleus, L-lysosome, P-peroxisome, U-unknown, R-ribosome. The isoelectric point and molecular weight is provided. The number of microsequences used for protein identification is provided as sequence tags.

Protein abundance profile of the adriamycin/verapamil resistant MCF-7 cell line

Comparative densitometry was used to compare the protein abundance profiles between the drug-susceptible MCF-7 cell line and the cell line selected for resistance to adriamycin in the presence of verapamil. Figure 17 shows a 2D-gel map of the soluble proteins extracted from the resistant cell line. Figure 18 shows the results of the comparative analysis and Table 3 lists the relative abundance of each protein that has been identified. In Figure 18, proteins that are circled in red show an increase in abundance in the resistant cell line, while proteins circled in yellow show a decreased abundance. In the cell line resistant to adriamycin, eleven proteins show an altered abundance. These proteins are listed in Table 4. Figure 19 shows the 60S ribosomal protein L12 as an example of a protein whose abundance does not change. Conversely, Figures 20 and 21 illustrate the appearance of proteins that have altered abundances as they show the increased abundance of 3,2 trans-enoyl CoA isomerase and the decrease in abundance of GrpE protein, homolog 1, respectively.

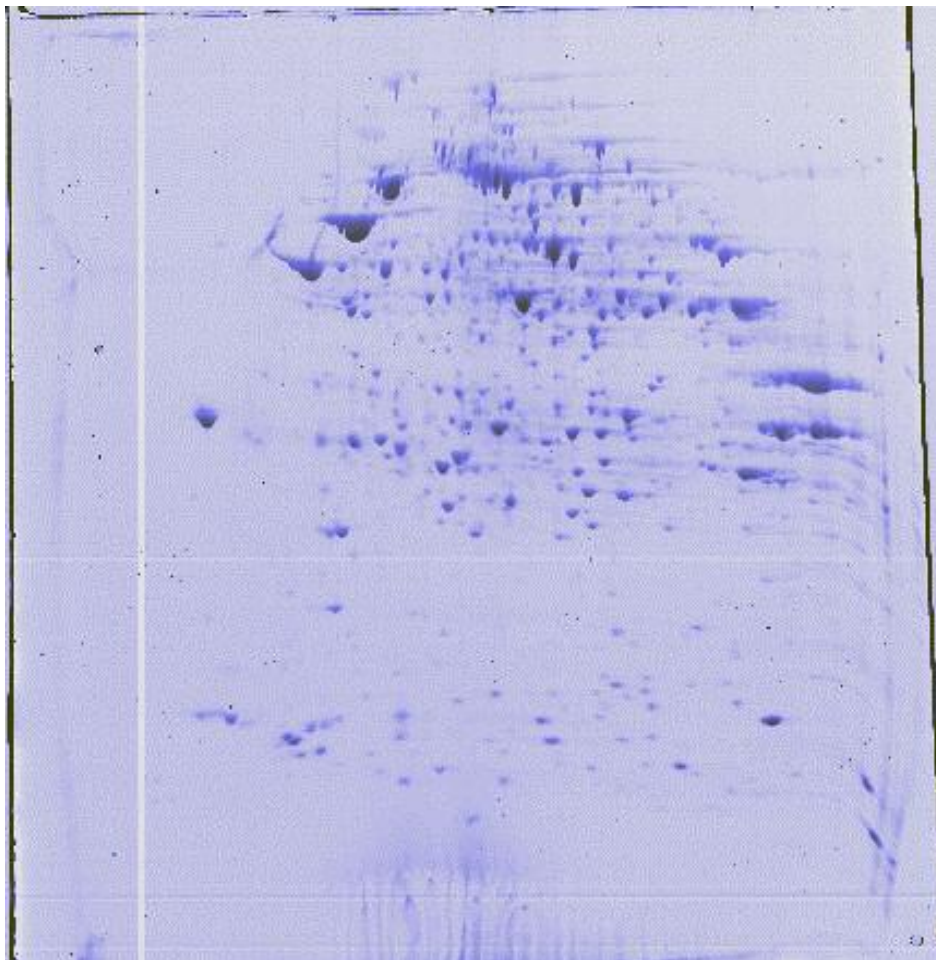


Figure 17. 2D-gel map of the mitochondrial proteins from the adriamycin resistant MCF-7 cell line.

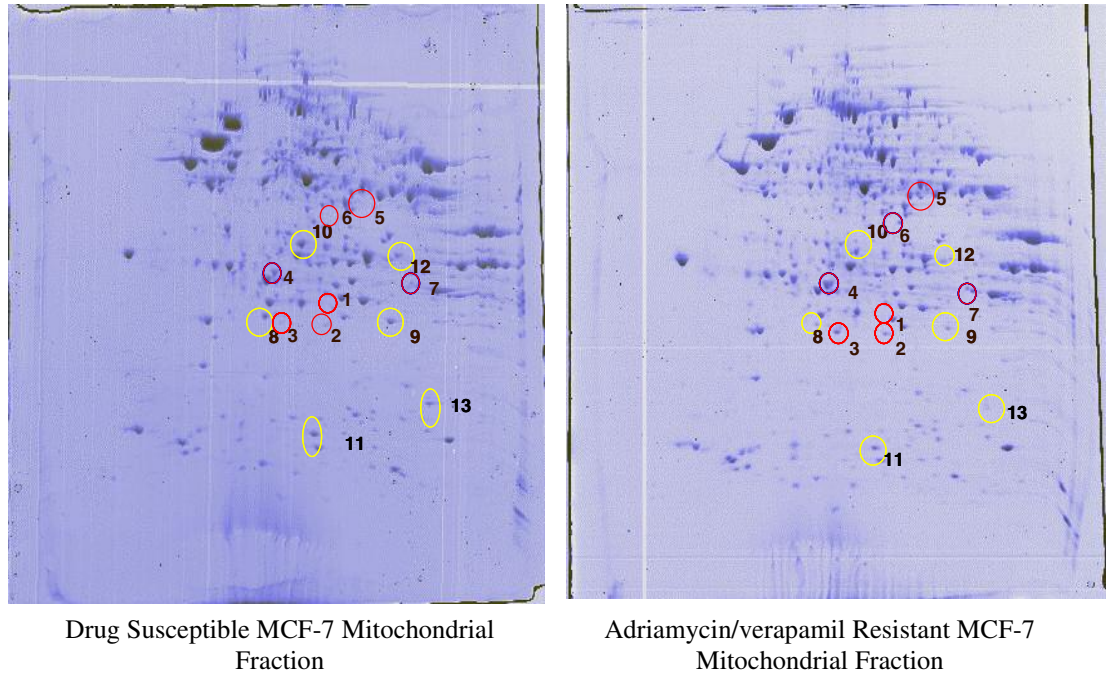


Figure 18. Comparative 2D-gel image analysis of the mitochondrial fraction from drug-susceptible and adriamycin resistant MCF-7 cells. Protein spots circled in red show an increased abundance in the resistant cell line. Protein spots circled in yellow show a decrease in abundance in the resistant cell line.

Spot	Protein	Abundance Level
1	ATP synthase, delta chain	0.58± 0.02
2	Peroxiredoxin 5	0.63±0.06
3	28S ribosomal protein S10	0.77±0.08
4	Single-stranded DNA binding protein	1.07±0.15
5	NADH-ubiquinone oxioeductase B16.6 subunit	0.89±0.07
6	Cofilin	0.69±0.18
7	Cytochrome c oxidase, polypeptide Vb	0.71±0.14
8	60S ribosomal protein L12	1.02±0.03
9	ATP synthase, D chain	0.82±0.09
10	GrpE protein homolog 1	0.41±0.05
11	Superoxide dismutase	1.24±0.04
12	Hypothetical protein FLJ23469	0.39± 0.02
13	Peroxiredoxin 3	0.98±0.12
14	Heat shock protein 27	0.87±0.05
15	Acyl-protein thioesterase 1	1.10±0.02
16	Ubiquinol-cytochrome c reductase iron-sulfur protein	1.05±0.13
17	ATP synthase alpha chain	8.74± 1.17
18	ES1 protein homolog	0.65±0.01
19	3-hydroxyacyl-CoA dehydrogenase type II	0.62±0.11
20	NADH-ubiquinone oxidoreductase 30 kDa subunit	1.23±0.10
21	Metaxin 2	0.89±0.16
22	Enoyl-CoA hydratase	1.03±0.11
23	3,2 trans-enoyl CoA isomerase	2.91± 0.11
24	CGI-90 protein	0.55±0.17
25	SCO2 protein homolog	0.99±0.04
26	Epoxide hydrolase	0.90±0.07
27	Complement component 1	1.10±0.09
28	Cathepsin D	1.63±0.04
29	NADH-ubiquinone oxioeductase 19 kDa subunit	1.07±0.12
30	Prohibitin	0.66±0.29

Table 3. Relative abundance of proteins from the drug susceptible and adriamycin resistant cell lines. Abundances are based on four cell harvests, two gels each.

Spot	Protein	Abundance Level
31	Delta3,5-delta2,4-dienoyl-CoA isomerase	1.57±0.03
32	Cytochrome c-type heme lyase	1.50±0.24
33	Elongation factor Ts	0.41± 0.02
34	Histidine triad nucleotide binding protein	1.37± 0.03
35	Nit protein 2	0.88±0.02
36	Hypothetical protein UPF0082	1.12±0.16
37	Voltage anion dependent selective channel protein 2	1.15±0.01
38	Electron transfer flavoprotein, alpha subunit	1.57±0.03
39	Thisulfate sulfurtransferase	0.78±0.08
40	Cytochrome c oxidase, polypeptide VIb	0.65±0.04
41	Voltage anion dependent selective channel protein 2	0.58±0.07
42	Hypothetical protein FLJ14038	1.47±0.10
43	Pyrroline-5-carboxylate reductase	0.36±0.05
44	Annexin A2	1.24±0.01
45	NAD-dependent methylenetetrahydrofolate dehydrogenase	0.73±0.05
46	Hypothetical protein FLJ20455	1.04±0.22
48	Ribosomal protein L1	0.77±0.11
49	39S ribosomal protein L44	0.79±0.06
50	Pyruvate dehydrogenase E1component, beta subunit	0.55±0.03
51	Inorganic pyrophosphatase	1.25±0.05
52	Pyruvate kinase, isozymes M1/M2	1.11±0.10
53	28S ribosomal protein S22	1.21±0.12
54	Elongation factor Tu	0.86±0.09
56	Pyruvate dehydrogenase E1component, alpha subunit	1.00±0.07
57	Acyl-CoA dehydrogenase family member 8	0.88±0.04
58	PRO1512	1.03±0.07
59	39S ribosomal protein L39	0.54±0.02
60	Coproporphyrinogen III oxidase	3.04±0.19
61	Ribosomal protein L38	1.34±0.03
62	Probable mitochondrial import receptor subunit TOM40 homolog	1.45±0.01

Table 3. Relative abundance of proteins from the drug susceptible and adriamycin resistant cell lines. Abundances are based on four cell harvests, two gels each.

Spot	Protein	Abundance Level
63	Similar to 3-hydroxisobutyryl-CoA hydrolase	1.35±0.04
64	Peptidyl-prolyl cis trans isomerase A	0.87±0.02
65	NADH-ubiquinone oxio reductase 42 kDa subunit	1.23±0.07
66	28S ribosomal protein S10	1.02±0.08
67	Acyl-CoA dehydrogenase, medium chain specific	1.14±0.11
68	Fumarate hydratase	1.12±0.09
69	NADH-ubiquinone oxidoreductase 23 kDa subunit	1.00±0.01
70	Trifunctional enzyme, alpha subunit	3.27±0.07
71	Creatine kinase	0.81±0.04
72	Citrate synthase	0.97±0.04
73	Ubiquinol-cytochrome c reductase complex core protein 2	0.85±0.05
74	Acetyl-CoA acetyltransferase	0.90±0.11
76	Malate dehydrogenase	1.50±0.10
77	Peroxiredoxin 2	1.50±0.11
78	Voltage anion dependent selective channel protein 1	1.71±0.28
79	Short chain 3-hydroxyacyl-CoA dehydrogenase	1.28±0.24
80	Voltage anion dependent selective channel protein 3	1.06±0.03
81	ATP synthase, alpha subunit	18.68±3.60
82	ATP synthase, alpha subunit	2.31±0.01
83	Electron transfer flavoprotein beta-subunit	1.26±0.03
84	Coiled-coil helix-coiled-coil helix domain containing protein 3	1.03±0.18
85	NipSnap3A protein	0.72±0.01
86	Peroxiredoxin 1	1.54±0.02
87	Adenylate kinase isoenzyme 2	2.40±0.08
88	Frataxin	1.73±0.10
89	Dehydrogenase/reductase SDR family member 4	0.72±0.12
90	D-beta-hydroxybutyrate dehydrogenase	1.16±0.21
91	Cytoskeletal keratin 19	0.90±0.08
92	Actin	0.70±0.09
93	Succinyl-CoA ligase [GDP-forming] beta-chain	1.19±0.10

Table 3. Relative abundance of proteins from the drug susceptible and adriamycin resistant cell lines. Abundances are based on four cell harvests, two gels each.

Spot	Protein	Abundance Level
94	Cytoskeletal keratin 18	0.66±0.12
95	Membrane associated protein SLP-2	0.74±0.08
96	Ubiquinol-cytochrome-c reductase complex core protein I	0.98±0.10
97	Cytoskeletal keratin 8	0.96±0.01
98	ATP synthase, beta chain	1.56±0.10
99	G-rich sequence factor-1	1.23±0.02
100	Ubiquinol-cytochrome c reductase complex 11 kDa protein	1.00±0.01
101	Stress-70 protein	0.84±0.14
102	HSP A8 protein fragment	0.52±0.03
103	NADH-ubiquinone oxoreductase 75 kDa subunit	1.22±0.44
104	Calcium binding transporter, fragment	0.96±0.06
105	Glycerol-3-phosphate dehydrogenase	1.23±0.07
106	Ornithine aminotransferase	1.52±0.64
107	Dihydrolipoamide succinyltransferase component of 2-oxoglutarate dehydrogenase complex	1.15±0.07
108	Cytosol aminopeptidase	1.29±0.41
109	Mitochondrial processing peptidase alpha subunit	1.01±0.03
110	Pyruvate dehydrogenase protein X component	1.39±0.11
111	Aldehyde dehydrogenase X	0.79±0.26
112	Dihydrolipoyl dehydrogenase	1.07±0.08
113	Aldehyde dehydrogenase family 7 member A1	0.80±0.15
114	Peptidyl-prolyl cis trans isomerase A	0.99±0.10
115	Glutamate dehydrogenase 1	0.96±0.05
116	Methylcrotonoyl-CoA carboxylase beta chain	1.11±0.13
117	Hypothetical protein FLJ20920	1.46±0.07
118	Electron transfer flavoprotein-ubiquinone oxidoreductase	1.22±0.12
119	Delta-1-pyrroline-5-carboxylate dehydrogenase	1.14±0.19
120	Succinate semialdehyde dehydrogenase	1.99±0.07
121	Apoptosis-inducing factor	1.12±0.04
122	Carnitine O-palmitoyltransferase II	0.97±0.05

Table 3. Relative abundance of proteins from the drug susceptible and adriamycin resistant cell lines. Abundances are based on four cell harvests, two gels each.

Spot	Protein	Abundance Level
123	Glucose-6-phosphate 1-dehydrogenase	1.06±0.06
124	Acyl-CoA dehydrogenase, very-long-chain specific	0.66±0.01
125	Methylmalonate-semialdehyde dehydrogenase	1.48±0.37
126	Serine hydroxymethyltransferase	1.02±0.06
127	ATP synthase, alpha subunit	0.75±0.04
128	4-aminobutyrate aminotransferase	1.46±0.13
129	HS1-binding protein	0.63±0.02
130	Lon protease homolog	1.04±0.08
131	Cytoskeletal keratin 2	1.22±0.09
132	Elongation factor G1	0.92±0.05
133	Delta 1-pyrroline-5-carboxylate synthetase	0.88±0.04
134	Methylcrotonoyl-CoA carboxylase alpha chain	0.83±0.18
135	Hypothetical protein FLJ12692	1.05±0.14
136	Phosphoenolpyruvate carboxykinase	1.45±0.35
137	Aconitate hydratase	0.58±0.05
138	Heat shock protein 75 kDa	1.08±0.09
139	Glycerol-3-phosphate dehydrogenase	1.06±0.08
140	NADH-ubiquinone oxidoreductase 51 kDa subunit	0.95±0.06
142	NADPH:adrenodoxin oxidoreductase	0.64±0.01
143	60 kDa heat shock protein	1.21±0.20
144	Glutaredoxin-related protein C14orf87	1.36±0.26
145	Cytochrome c oxidase subunit VIa	0.99±0.13
146	Mitofilin	1.00±0.08
148	Pyruvate carboxylase	0.93±0.07
149	2-oxoglutarate dehydrogenase E1 component	0.94±0.16
150	Hypothetical protein DKFZp434K046	0.74±0.02
151	NADH-ubiquinone oxidoreductase 13 kDa-A subunit	1.14±0.11
152	OTTHUMO00000016217	0.60±0.28
153	NADH-ubiquinone oxidoreductase 13 kDa-B subunit	1.50±0.19
154	Complex I intermediate-associated protein 30	0.96±0.04

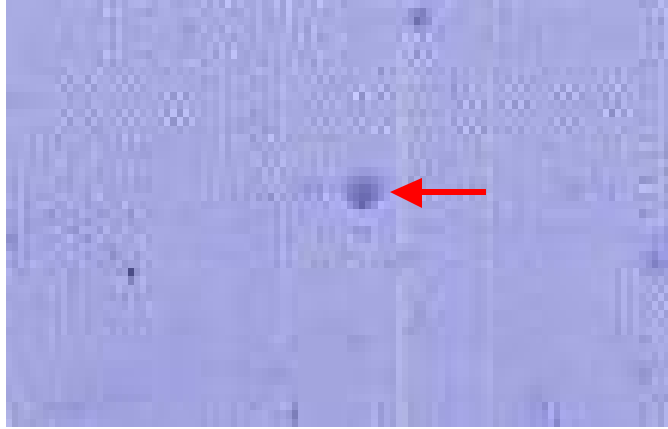
Table 3. Relative abundance of proteins from the drug susceptible and adriamycin resistant cell lines. Abundances are based on four cell harvests, two gels each.

Spot	Protein	Abundance Level
155	Estradiol 17-beta-dehydrogenase 8	1.08±0.11
156	NADH-ubiquinone oxidoreductase 24 kDa subunit	0.74±0.15
157	Cytochrome c oxidase subunit Va	1.31±0.29
158	Thioredoxin 2	1.10±0.04
159	Cytochrome c oxidase assembly protein COX11	1.80±0.63
160	130 kDa leucine-rich protein	0.74±0.01
161	Acyl-CoA dehydrogenase, short/branched chain specific	0.77±0.13
163	Isocitrate dehydrogenase, alpha subunit	1.52±0.06
164	Hypothetical protein FLJ11342	1.37±0.17
165	39S ribosomal protein L49	0.85±0.17

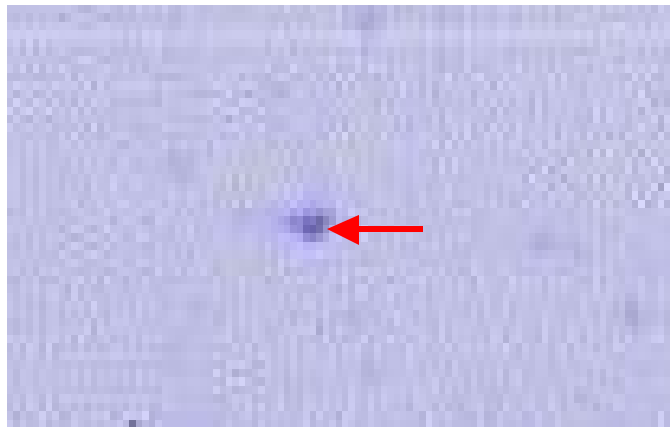
Table 3. Relative abundance of proteins from the drug susceptible and adriamycin resistant cell lines. Abundances are based on four cell harvests, two gels each.

Spot Number	Protein	Relative Abundance
1	Similar to ATP synthase alpha chain	8.74±1.17
2	ATP synthase alpha chain	18.68±3.6
3	ATP synthase alpha chain	2.31±0.01
4	3,2 trans-enoyl CoA isomerase	2.91±0.11
5	Trifunctional enzyme alpha subunit	3.27±0.07
6	Coproporphyrinogen III oxidase	3.04±0.19
7	Adenylate kinase isoenzyme 2	2.4±0.08
8	GrpE protein homolog 1	0.41±0.05
9	Hypothetical protein FLJ23496	0.39±0.02
10	Elongation factor Ts	0.41±0.02
11	Cytochrome c oxidase Vb subunit	0.39±0.02
12	Pyrroline-5-carboxylate reductase	0.36±0.05
13	Cofilin	0.29±0.08

Table 4. Proteins with altered abundances in the adriamycin/verapamil resistant MCF-7 cell line. Only changes ≥ 2 are considered significant.

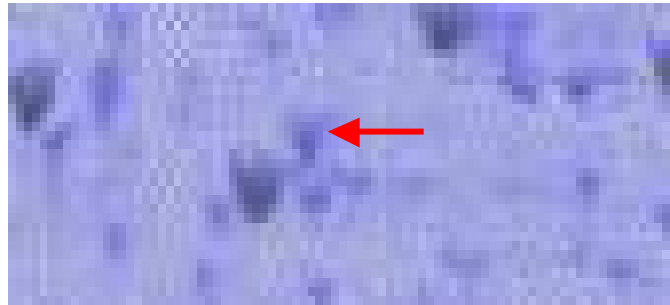


Drug-susceptible

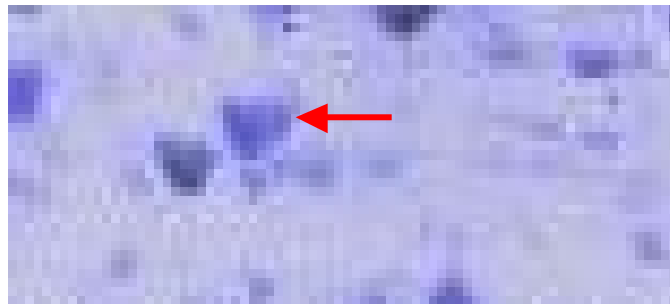


Adriamycin/verapamil-resistant

Figure 19. Equal abundance of the 60S ribosomal protein L12 between the drug susceptible and adriamycin/verapamil resistant MCF-7 cell line.

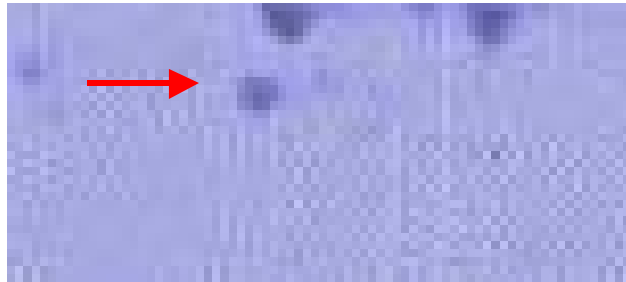


Drug-susceptible

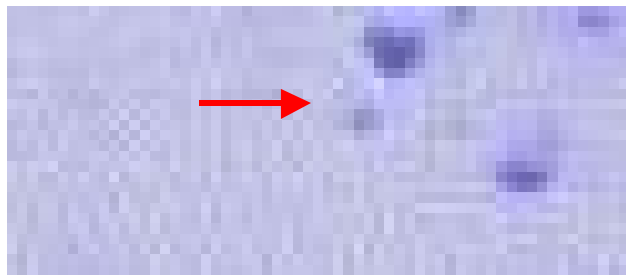


Adriamycin/verapamil-resistant

Figure 20. Increase in abundance of 3,2 trans-enoyl CoA isomerase between the drug susceptible and adriamycin resistant MCF-7 cell line.



Drug-susceptible



Adriamycin/verapamil-resistant

Figure 21. Decrease in abundance of the GrpE protein homolog 1 between the drug susceptible and adriamycin/verapamil resistant MCF-7 cell line.

Protein abundance profiles in the MCF-7 cell line resistant to mitoxantrone

Using comparative densitometry, we have identified four proteins that have altered abundances in the cell line selected for resistance to mitoxantrone. Figure 22 shows a representative 2D-gel image of the soluble proteins extracted from the mitoxantrone-resistant cell line. Figure 23 shows the results of the comparative analysis, where proteins that have an increased abundance are circled in red and proteins with a decrease in abundance are circled in yellow. The relative abundance of each protein is presented in Table 6. Table 7 lists the proteins that show alterations in their abundance profiles between the drug-susceptible and mitoxantrone resistant cell lines. Two proteins involved in the oxidative phosphorylation, Cytochrome c oxidase subunit Va, and the ATP synthase, alpha subunit show an increase in their abundance. Conversely, two proteins not known to be associated with the mitochondria, Annexin A2 and the hypothetical protein FLJ20455 show a decrease in their abundance.

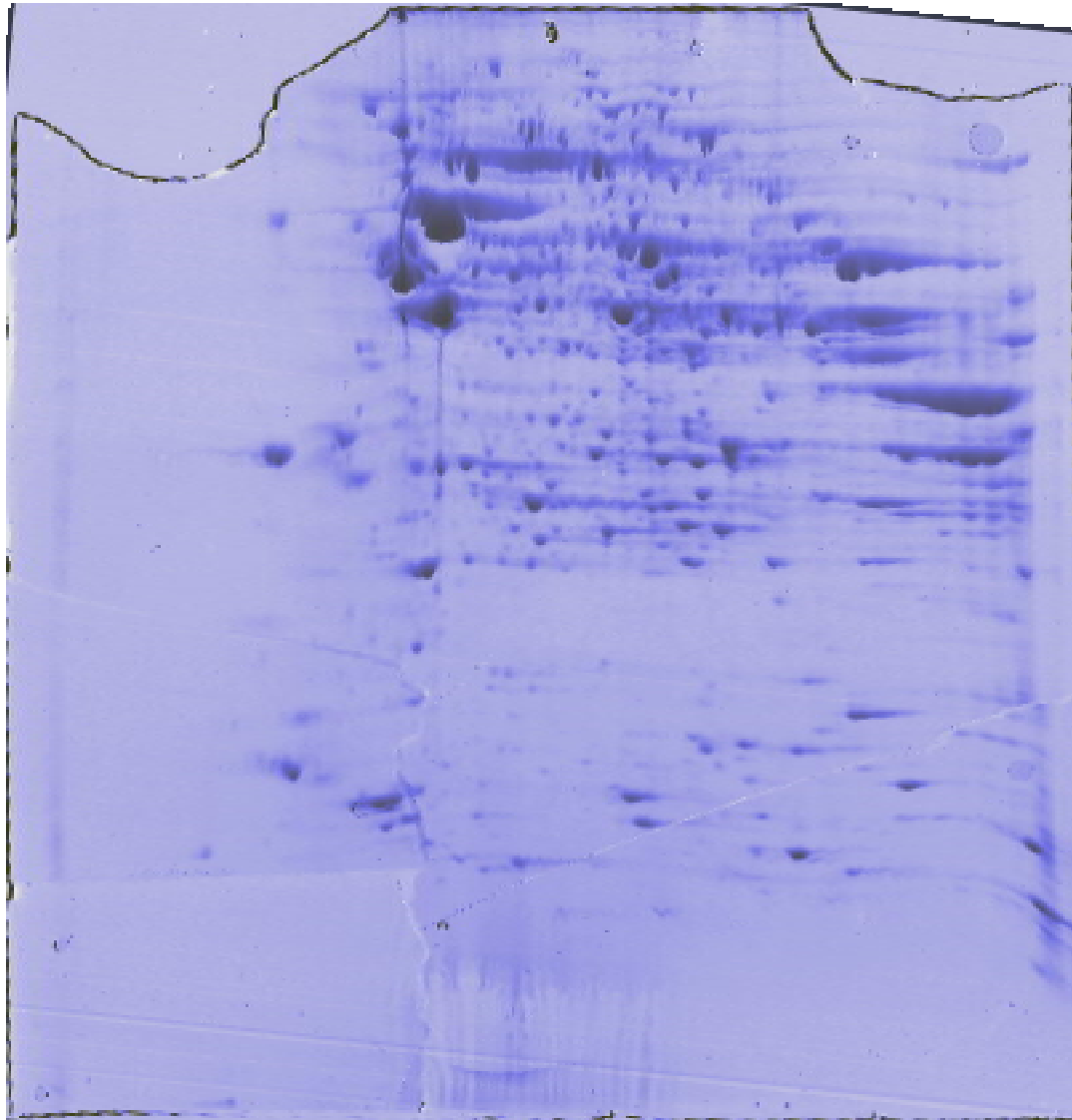
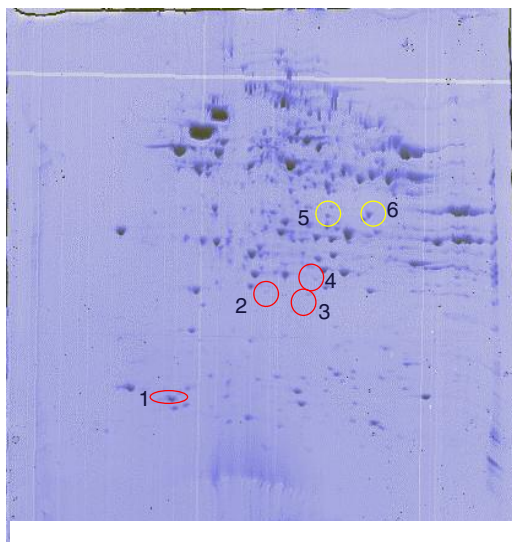
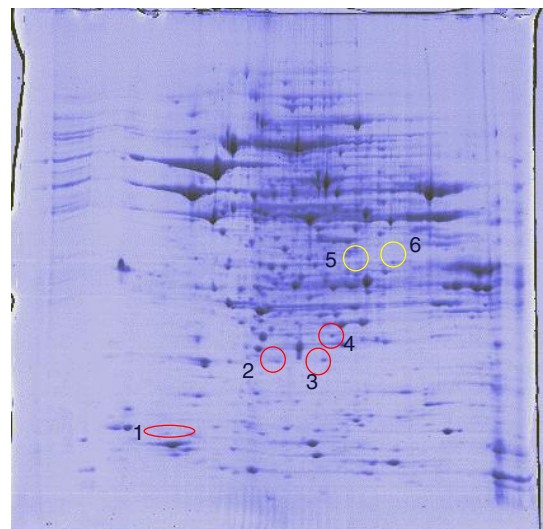


Figure 22. 2D-gel map of the mitochondrial proteins from the mitoxantrone resistant MCF-7 cell line.



Drug Susceptible MCF-7
Mitochondrial Fraction



Mitoxantrone Resistant MCF-7
Mitochondrial Fraction

Figure 23. Comparative 2D-gel image analysis of the mitochondrial fraction from drug-susceptible and mitoxantrone-resistant MCF-7 cells. Protein spots circled in red show an increased abundance in the resistant cell line. Protein spots circled in yellow show a decrease in abundance in the resistant cell line.

Spot	Protein	Relative Abundance
1	ATP synthase, delta chain	1.55± 0.11
2	Peroxiredoxin 5	1.19±0.04
3	28S ribosomal protein S10	1.99±0.15
4	Single-stranded DNA binding protein	1.09±0.18
5	NADH-ubiquinone oxio reductase B16.6 subunit	1.00±0.02
6	Cofilin	1.21±0.16
7	Cytochrome c oxidase, polypeptide Vb	1.89±0.09
8	60S ribosomal protein L12	1.11±0.09
9	ATP synthase, D chain	1.93±0.10
10	GrpE protein homolog 1	1.41±0.15
11	Superoxide dismutase	1.42±0.12
12	Hypothetical protein FLJ23469	0.71± 0.25
13	Peroxiredoxin 3	1.38±0.12
14	Heat shock protein 27	1.16±0.17
15	Acyl-protein thioesterase 1	0.70±0.02
16	Ubiquinol-cytochrome c reductase iron-sulfur protein	1.44±0.19
17	ATP synthase alpha chain	4.48± 0.55
18	ES1 protein homolog	1.22±0.19
19	3-hydroxyacyl-CoA dehydrogenase type II	1.28±0.18
20	NADH-ubiquinone oxidoreductase 30 kDa subunit	1.09±0.17
21	Metaxin 2	1.07±0.14
22	Enoyl-CoA hydratase	1.45±0.09
23	3,2 trans-enoyl CoA isomerase	1.14± 0.03
24	CGI-90 protein	1.40±0.23
25	SCO2 protein homolog	0.79±0.03
26	Epoxide hydrolase	1.19±0.18
27	Complement component 1	1.23±0.15
28	Cathepsin D	1.05±0.05
29	NADH-ubiquinone oxio reductase 19 kDa subunit	1.38±0.35
30	Prohibitin	1.96±0.20

Table 5. Relative abundance of proteins from the drug susceptible and mitoxantrone resistant cell lines. Abundances are based on four cell harvests, two gels each.

Spot	Protein	Relative Abundance
31	Delta3,5-delta2,4-dienoyl-CoA isomerase	1.27±0.21
32	Cytochrome c-type heme lyase	0.86±0.05
33	Elongation factor Ts	0.58± 0.14
34	Histidine triad nucleotide binding protein	1.52± 0.11
35	Nit protein 2	0.95±0.09
36	Hypothetical protein UPF0082	1.21±0.23
37	Voltage anion dependent selective channel protein 2	1.09±0.27
38	Electron transfer flavoprotein, alpha subunit	0.96±0.12
39	Thisulfate sulfurtransferase	1.33±0.07
40	Cytochrome c oxidase, polypeptide VIb	1.52±0.33
41	Voltage anion dependent selective channel protein 2	1.08±0.09
42	Hypothetical protein FLJ14038	1.72±0.12
43	Pyrroline-5-carboxylate reductase	0.92±0.11
44	Annexin A2	0.33±0.21
45	NAD-dependent methylenetetrahydrofolate dehydrogenase	1.03±0.11
46	Hypothetical protein FLJ20455	0.25±0.05
48	Ribosomal protein L1	1.54±0.29
49	39S ribosomal protein L44	0.57±0.14
50	Pyruvate dehydrogenase E1component, beta subunit	1.17±0.15
51	Inorganic pyrophosphatase	1.64±0.05
52	Pyruvate kinase, isozymes M1/M2	1.24±0.05
53	28S ribosomal protein S22	1.71±0.67
54	Elongation factor Tu	1.04±0.22
56	Pyruvate dehydrogenase E1component, alpha subunit	0.89±0.22
57	Acyl-CoA dehydrogenase family member 8	0.85±0.03
58	PRO1512	1.42±0.16
59	39S ribosomal protein L39	0.61±0.10
60	Coproporphyrinogen III oxidase	N/A
61	Ribosomal protein L38	1.45±0.16
62	Probable mitochondrial import receptor subunit TOM40 homolog	0.81±0.19

Table 5. Relative abundance of proteins from the drug susceptible and mitoxantrone resistant cell lines. Abundances are based on four cell harvests, two gels each.

Spot	Protein	Relative Abundance
63	Similar to 3-hydroxisobutyryl-CoA hydrolase	1.18±0.09
64	Peptidyl-prolyl cis-trans isomerase A	1.81±0.10
65	NADH-ubiquinone oxidoreductase 42 kDa subunit	0.74±0.17
66	28S ribosomal protein S10	1.31±0.15
67	Acyl-CoA dehydrogenase, medium chain specific	1.30±0.29
68	Fumarate hydratase	1.17±0.22
69	NADH-ubiquinone oxidoreductase 23 kDa subunit	1.62±0.04
70	Trifunctional enzyme, alpha subunit	1.24±0.18
71	Creatine kinase	0.59±0.07
72	Citrate synthase	0.77±0.08
73	Ubiquinol-cytochrome c reductase complex core protein 2	0.93±0.32
74	Acetyl-CoA acetyltransferase	0.70±0.04
76	Malate dehydrogenase	1.57±0.33
77	Peroxiredoxin 2	1.16±0.14
78	Voltage anion dependent selective channel protein 1	1.10±0.31
79	Short chain 3-hydroxyacyl-CoA dehydrogenase	0.97±0.29
80	Voltage anion dependent selective channel protein 3	1.19±0.21
81	ATP synthase, alpha subunit	2.86±0.51
82	ATP synthase, alpha subunit	5.30±0.77
83	Electron transfer flavoprotein beta-subunit	1.14±0.10
84	Coiled-coil helix-coiled-coil-helix domain containing protein 3	1.13±0.27
85	NipSnap3A protein	1.15±0.45
86	Peroxiredoxin 1	1.58±0.16
87	Adenylate kinase isoenzyme 2	1.59±0.01
88	Frataxin	1.13±0.21
89	Dehydrogenase/reductase SDR family member 4	1.26±0.13
90	D-beta-hydroxybutyrate dehydrogenase	1.06±0.19
91	Cytoskeletal keratin 19	1.45±0.03
92	Actin	0.89±0.09
93	Succinyl-CoA ligase [GDP-forming] beta-chain	1.07±0.10

Table 5. Relative abundance of proteins from the drug susceptible and mitoxantrone resistant cell lines. Abundances are based on four cell harvests, two gels each.

Spot	Protein	Relative Abundance
94	Cytoskeletal keratin 18	1.32±0.13
95	Membrane associated protein SLP-2	1.08±0.04
96	Ubiquinol-cytochrome-c reductase complex core protein I	1.65±0.06
97	Cytoskeletal keratin 8	0.56±0.06
98	ATP synthase, beta chain	0.99±0.11
99	G-rich sequence factor-1	1.58±0.21
100	Ubiquinol-cytochrome c reductase complex 11 kDa protein	0.97±0.05
101	Stress-70 protein	0.86±0.13
102	HSP A8 protein fragment	1.57±0.15
103	NADH-ubiquinone oxidoreductase 75 kDa subunit	1.06±0.23
104	Calcium binding transporter, fragment	0.96±0.11
105	Glycerol-3-phosphate dehydrogenase	0.95±0.07
106	Ornithine aminotransferase	1.04±0.22
107	Dihydrolipoamide succinyltransferase component of 2-oxoglutarate dehydrogenase complex	1.15±0.01
108	Cytosol aminopeptidase	0.99±0.02
109	Mitochondrial processing peptidase alpha subunit	1.37±0.09
110	Pyruvate dehydrogenase protein X component	0.78±0.10
111	Aldehyde dehydrogenase X	1.24±0.08
112	Dihydrolipoyl dehydrogenase	0.67±0.49
113	Aldehyde dehydrogenase family 7 member A1	1.74±0.12
114	Peptidyl-prolyl cis-trans isomerase A	1.89±0.13
115	Glutamate dehydrogenase 1	1.49±0.22
116	Methylcrotonoyl-CoA carboxylase beta chain	0.98±0.16
117	Hypothetical protein FLJ20920	1.30±0.08
118	Electron transfer flavoprotein-ubiquinone oxidoreductase	0.95±0.07
119	Delta-1-pyrroline-5-carboxylate dehydrogenase	1.29±0.01
120	Succinate semialdehyde dehydrogenase	1.70±0.34
121	Apoptosis-inducing factor	1.58±0.42
122	Carnitine O-palmitoyltransferase II	1.04±0.07

Table 5. Relative abundance of proteins from the drug susceptible and mitoxantrone resistant cell lines. Abundances are based on four cell harvests, two gels each.

Spot	Protein	Relative Abundance
123	Glucose-6-phosphate 1-dehydrogenase	1.29±0.25
124	Acyl-CoA dehydrogenase, very-long-chain specific	1.15±0.16
125	Methylmalonate-semialdehyde dehydrogenase	0.86±0.07
126	Serine hydroxymethyltransferase	0.93±0.10
127	ATP synthase, alpha subunit	0.65±0.13
128	4-aminobutyrate aminotransferase	1.33±0.05
129	HS1-binding protein	1.41±0.05
130	Lon protease homolog	0.75±0.09
131	Cytoskeletal keratin 2	0.61±0.14
132	Elongation factor G1	1.05±0.06
133	Delta 1-pyrroline-5-carboxylate synthetase	1.02±0.13
134	Methylcrotonoyl-CoA carboxylase alpha chain	1.42±0.48
135	Hypothetical protein FLJ12692	1.34±0.42
136	Phosphoenolpyruvate carboxykinase	1.09±0.11
137	Aconitate hydratase	1.39±0.06
138	Heat shock protein 75 kDa	1.20±0.29
139	Glycerol-3-phosphate dehydrogenase	1.56±0.44
140	NADH-ubiquinone oxidoreductase 51 kDa subunit	1.76±0.19
142	NADPH:adrenodoxin oxidoreductase	0.97±0.08
143	60 kDa heat shock protein	1.08±0.09
144	Glutaredoxin-related protein C14orf87	1.67±0.42
145	Cytochrome c oxidase subunit Via	1.80±0.09
146	Mitofilin	1.08±0.28
148	Pyruvate carboxylase	0.86±0.12
149	2-oxoglutarate dehydrogenase E1 component	1.44±0.27
150	Hypothetical protein DKFZp434K046	1.28±0.26
151	NADH-ubiquinone oxidoreductase 13 kDa-A subunit	1.55±0.29
152	OTTHUMO00000016217	0.58±0.12
153	NADH-ubiquinone oxidoreductase 13 kDa-B subunit	1.03±0.43
154	Complex I intermediate-associated protein 30	115±0.09

Table 5. Relative abundance of proteins from the drug susceptible and mitoxantrone resistant cell lines. Abundances are based on four cell harvests, two gels each.

Spot	Protein	Relative Abundance
156	NADH-ubiquinone oxidoreductase 24 kDa subunit	1.75±0.13
157	Cytochrome c oxidase subunit Va	3.57±1.24
158	Thioredoxin	1.25±0.14
159	Cytochrome c oxidase assembly protein COX11	1.04±0.06
160	130 kDa leucine-rich protein	1.50±0.16
161	Acyl-CoA dehydrogenase, short/branched chain specific	1.40±0.09
163	Isocitrate dehydrogenase, alpha subunit	0.80±0.11
164	Hypothetical protein FLJ11342	1.32±0.03
165	39S ribosomal protein L49	0.88±0.08

Table 5. Relative abundance of proteins from the drug susceptible and mitoxantrone resistant cell lines. Abundances are based on four cell harvests, two gels each.

Spot Number	Protein	Abundance
1	Cytochrome c oxidase subunit Va	3.57±1.24
2	Similar to ATP synthase alpha chain	2.86±0.51
3	ATP synthase alpha chain	4.48±0.55
4	ATP synthase alpha chain	5.30±0.77
5	Annexin A2	0.33±0.21
6	Hypothetical protein FLJ20455	0.25±0.05

Table 6. Proteins with altered abundances between the mitoxantrone resistant MCF-7 cell line. Only changes ≥ 2 are considered significant.

Chapter 4: Discussion

Characterization of MCF-7 mitochondria

Mitochondria are not static organelles. Electron microscopy reveals that the appearance of mitochondria differs between cell and tissue types. Likewise, it has been shown that the number of mitochondria in a given cell type can range from a few hundred to thousands, and that the copy number of mitochondrial DNA can also vary.⁸⁷ Furthermore, depending on the energy requirements of a tissue, mitochondria can also exhibit alterations in their patterns of substrate utilization and biosynthetic pathways.⁸⁸ Although these observations show that mitochondria are altered between cell types, little information exists on the extent to which mitochondria differ, how the organelle changes in response to stress or disease, or the molecular basis for these differences.

In an attempt to gain more insight into these differences, a recent proteomic study was undertaken to compare the mitochondrial profiles between the brain, heart, liver and kidney proteins from a mouse.⁸⁹ From this work it was shown that fifteen to twenty percent of mitochondrial proteins differ between the tissue types. Based on this conclusion and the previously mentioned observations, it is apparent that mitochondria differ between cell types at the molecular level. Thus, it is important to characterize the MCF-7 mitochondrial proteome. To do so, a method to extract the soluble protein fraction from purified mitochondria has been optimized. A 2D-gel map has been produced, from which protein spots were identified by mass spectrometry. Following

identification, the mitochondrial proteins have been cataloged for use as a reference in future work that utilizes mitochondria from MCF-7 cell lines.

Proteomic annotation of the genome

Several important pieces of information can be deduced when the subcellular location of a protein is determined. First, it aids in the understanding of how an organelle functions. Second, when a novel or uncharacterized protein is identified, its subcellular location can provide clues as to the function of that protein.⁹⁰ Historically, the compartmental location of a protein has been proposed by computational or direct experimental methods. These methods can be somewhat limited however. More recently, proteomic strategies that employ subcellular fractionation have allowed for the determination of protein locations on a large-scale. This is not only the most direct approach to elucidate location, but it has also allowed for in-depth investigations of proteins that previously were not known to be associated with a particular organelle. One exemplary analysis was conducted on the proteome of the nucleolus. In this study, thirty percent of the identified proteins, including heterochromatin protein 1 γ isoform, were not previously known to belong to the nucleolus.⁹¹ Similarly, a mitochondrial proteomic study was undertaken, in which, of 599 proteins identified, 163 had not been known to be associated with the mitochondria.⁸⁹ After employing several tests and experimental analyses, including analysis of targeting sequences and the formation of GST fusions to detect protein location, the authors confirmed that 133 or eighty-five percent of the 163 proteins are located within the mitochondria.

In an effort to classify the proteins identified in our work, and to elucidate whether those proteins that have not been previously associated with the mitochondria,

are actually contaminants from other organelles or in fact could also be mitochondrial, we have sought to compare our catalog to those reported in other mitochondrial proteomic surveys. This data is summarized in Table 7, where column one lists the proteins identified in this study that are classically reported to belong to other organelles, or whose location has yet to be defined. Column two represents the subcellular location to which the proteins are currently reported in the SwissProt database. In columns three and four, the proteins were extracted from mitochondria isolated from tissue samples, and purified on either a Percoll or metrizamide gradient, respectively. The proteins in column five were obtained from mitochondria derived from a neuroblastoma cell line and purified on a metrizamide gradient.^{89,92,93} While additional mitochondrial proteomic analyses have been reported, these papers were chosen to provide a spectrum of experimental conditions, including whether the mitochondria were from tissue sample or cell lines and the manner in which those mitochondria were purified. Although part of our reference catalog, proteins including the cytokeratins and actin are excluded from this table, as they are known to be highly abundant in cells and are accepted as permanent contaminants of most organellar fractions. The results show that several proteins, such as dehydrogenase/reductase SDR family member 4, known to be associated with other organelles are not present in the proteomic studies chosen for comparison and are likely contaminants in our sample. On the other hand, proteins such as cathepsin D may be associated with the mitochondria. This protein, which is present in our sample and in both the study using Percoll and metrizamide purification strategies, is classified as a lysosomal protein. It has been reported however, that cathepsin D is required for Bax insertion into the outer mitochondrial membrane, a process that is required for apoptosis.⁹⁴

Proteins Identified in this Study	Subcellular Location as Reported by SwissProt	From Tissue Isolated on Percoll	From Tissue Isolated with Metrizamide	From Cell Culture Isolated with Metrizamide
Acyl-protein thioesterase 1	Cytosol	Yes	Yes	No
3hydroxyacyl CoA dehydrogenase	Endoplasmic reticulum	No	Yes	Yes
Cathepsin D	Lysosome	Yes	Yes	No
Nit protein 2	None	Yes	No	No
Pyrroline-5-carboxylate reductase	Cytosol	Yes	No	Yes
Annexin A2	Cytosol	Yes	No	Yes
NipSnap3A protein	Cytosol	Yes	No	Yes
Peroxiredoxin 1	Cytosol	Yes	Yes	Yes
Dehydrogenase /reductase SDR family member 4	Peroxisomal	No	No	No
G-rich sequence factor-1	Cytosol	No	No	Yes
Heat shock protein A8	Cytosol Nucleus	No	No	No
130 kDa leucine-rich protein	Cytosol	No	Yes	Yes

Table 7. Comparison of mitochondrial protein catalogs.

More direct experimental evidence has been obtained to show that nit protein 2 is part of the mitochondria. Currently, nit protein 2 does not have an organellar classification in protein databases such as SwissProt. Using confocal microscopy to track a GST-fusion protein however, it has been shown that nit 2 does in fact localize to mitochondria.⁸⁹ Finally, pyrroline-5-carboxylate reductase and peroxiredoxin 1 are present in two of the three and all three proteomic studies, respectively. Because the experimental conditions of analyses chosen for comparison are not the same, and because these proteins are present in most of the studies, it seems possible that these proteins are closely associated with the mitochondria in vivo. It can be speculated that proteomic studies such as these will contribute to the reassignment of proteins to organelles other than those to which they have historically been assigned.

Annotation of hypothetical proteins

Upon sequencing of the human genome, it became apparent that approximately thirty percent of open reading frames could encode for proteins that have yet to be characterized.⁹⁵ Although such hypothetical proteins have only been predicted based on nucleic acid sequence, they account for numerous positive protein identifications in proteomic based work and more recently, such proteins have been postulated to play a role in diseases such as Down syndrome.⁹⁶ Specifically, our work shows an altered abundance of two such proteins. Thus, we have sought to determine the subcellular location of the hypothetical proteins identified in this study using two Internet based programs, Mitopred (<http://mitopred.sdsc.edu/>) and Psort (<http://psort.nibb.ac.jp/>).

Mitopred is used exclusively to determine whether a protein is mitochondrial. Users can submit either the SwissProt accession number of the protein, or its amino acid

sequence. The program predicts whether the protein is mitochondrial or non-mitochondrial based on three factors; occurrence patterns of Pfam domains, amino acid composition and pI value differences between mitochondrial and non-mitochondrial locations.⁹⁷ Unlike Mitopred, Psort is used to predict the subcellular location of all proteins using one criterion, the presence of sorting signals within the amino acid sequence.⁹⁸ Such sorting signals include cleaveable targeting sequences that are often found in mitochondrial proteins, as more than 99% are encoded by the nucleus and must be transported to the mitochondria based on those sequences.⁹⁹

The results of this analysis are shown in Table 8. All proteins identified as hypothetical in this study were first evaluated using MitoPred. If the reported result was non-mitochondrial, those protein locations were then predicted using Psort. As can be seen in rows 2 and 7, hypothetical proteins UPF0082 and DKFZp43k046 were predicted as non-mitochondrial using MitoPred, but predicted to be mitochondrial using Psort. Because Psort uses only one method to calculate location, it is generally accepted that MitoPred can predict mitochondrial proteins more reliably. Thus, we have concluded that at this time, it is not possible to classify the subcellular location of these proteins. Interestingly, when mitofilin, protein number 146 in Table 2, was first identified, it had yet to be characterized and was a hypothetical protein. Using the MitoPred algorithm, it was predicted to be mitochondrial at a confidence level of 69%. Upon characterization, it was demonstrated that mitofilin does localize to mitochondria.¹⁰⁰ Therefore, we feel certain in the prediction that the hypothetical proteins, FLJ12962 and FLJ11342, which have similar confidence levels, are mitochondrial.

Hypothetical Protein	Prediction of Subcellular Location Based on MitoPred	Prediction of Subcellular Location Based on Psort
FLJ23469	Non-mitochondrial	Cytosolic with 76% confidence
UPF0082	Non-mitochondrial	Mitochondrial with 48% confidence
FLJ14038	Mitochondrial with 92% confidence	Not applied
FLJ20920	Mitochondrial with 92% confidence	Not applied
FLJ12692	Mitochondrial with 62% confidence	Not applied
FLJ20455	Non-mitochondrial	Nuclear with 70% confidence
DKFZp43k046	Non-mitochondrial	Mitochondrial with 57% confidence
FLJ11342	Mitochondrial with 74% confidence	Not applied
PRO1512	Mitochondrial with 100% confidence	Not applied
OTTHUMP000000 16217	Non-mitochondrial	Nuclear with 76% confidence
Stomatin like protein 2	Mitochondrial with 92% confidence	Not applied

Table 8. Predicted subcellular location of hypothetical proteins. MitoPred and Psort prediction algorithms are exploited.

Biological implications of abundance changes

In this study, we have detected the altered abundance of 15 proteins from the MCF-7 cell lines resistant to adriamycin and mitoxantrone. These proteins, listed in Table 9, are involved in a number of mitochondrial pathways. In an effort to contribute to the understanding of drug resistance, we have sought to determine the biological implications of these abundance changes.

Fatty acid oxidation

Fatty acid, or β -oxidation is the process whereby fatty acid molecules are broken down. This process is essential for maximum cellular energy yield, as it drives the synthesis of ATP. Short, medium and long chain fatty acids are released from adipose cells to the cytosol, where they are linked to coenzyme A (CoA). The resultant fatty acyl CoA molecules are then transported from the cytosol to the mitochondrial matrix via carnitine palmitoyl transferase. Through a series of four reactions in the matrix, each fatty acyl CoA molecule is oxidized to form one molecule of acetyl CoA and is shortened by 2 carbon atoms. The process continues as all of the carbon atoms are converted to acetyl CoA molecules, which are then fed into the citric acid cycle. In addition to acetyl CoA, each turn of β -oxidation also yields one molecule each of NADH and FADH₂ that, together with the NADH and FADH₂ generated from glycolysis and the oxidation of acetyl CoA in the citric acid cycle, are used to power ATP synthesis via the electron transport chain. In our work with the adriamycin resistant MCF-7 cell line we detect the increased abundance of two key enzymes involved in fatty acid oxidation, 3,2 trans-enoyl CoA isomerase and the trifunctional enzyme α -subunit.

Protein	Adriamycin resistant MCF-7 Cell Line	Mitoxantrone resistant MCF-7 Cell Line
Similar to ATP synthase alpha chain	8.74±1.17	2.86±0.51
ATP synthase alpha chain	18.68±3.6	4.48±0.55
ATP synthase alpha chain	2.31±0.01	5.30±0.77
3,2 trans-enoyl CoA isomerase	2.91±0.11	1.14± 0.03
Trifunctional enzyme alpha subunit	3.27±0.07	1.24±0.18
Coproporphyrinogen III oxidase	3.04±0.19	Not determined
Adenylate kinase isoenzyme 2	2.4±0.08	1.59±0.01
Cytochrome c oxidase subunit Va	1.31±0.29	3.57±1.24
GrpE protein homolog 1	0.41±0.05	1.41±0.15
Hypothetical protein FLJ23496	0.39±0.02	0.71± 0.25
Elongation factor Ts	0.41±0.02	0.58± 0.14
Cytochrome c oxidase Vb subunit	0.39±0.02	1.89±0.09
Pyrroline-5-carboxylate reductase	0.36±0.05	0.92±0.11
Cofilin	0.29±0.08	1.21±0.16
Annexin A2	1.24±0.01	0.33±0.21
Hypothetical protein FLJ20455	1.04±0.22	0.25±0.05

Table 9. Summary of abundance changes in the drug-resistant MCF-7 cell lines.

Three, two-trans-enoyl CoA isomerase functions as a homodimer to isomerize both 3-cis and 3-trans double bonds into the 2-trans configuration. For complete degradation of a fatty acid molecule, its double bonds and those of its intermediates must have a trans-configuration. Unlike the intermediates produced from saturated fatty acids, which always meet this criterion, the double bonds of intermediates from unsaturated fatty acids can be in a cis configuration. Processing of such intermediates requires up to three additional enzymatic steps. The isomerase is fundamental in the conversion of such bonds; mice deficient in the enzyme are incapable of β -oxidation of unsaturated fatty acids.¹⁰¹ An increased abundance of 3,2 trans-enoyl CoA isomerase has been reported in breast and colon cancer but what role it plays in the malignant transformation is not understood.¹⁰²

The trifunctional enzyme contains four α and four β subunits to catalyze three steps in fatty acid oxidation. The α subunit plays a role in steps two and three of the process, as it harbors the 3-hydroxyacyl-CoA dehydrogenase and the enoyl CoA hydratase activities. Individually, the trifunctional enzyme has not been shown to play a role in cancer, although alterations in it are responsible for several other diseases.¹⁰³ Based on the increased abundance of 3,2 trans-enoyl CoA isomerase and the trifunctional enzyme α -subunit, we propose that there is an increase in fatty acid oxidation in the cell line resistant to adriamycin, as compared to the drug -susceptible cell line. It is important to note however, that we have identified additional enzymes involved in fatty acid oxidation that do not have altered abundances.

Since the mid 1900's it has been known that cancer cells have an altered metabolism, including an increase in glycolysis for the production of ATP.¹⁰⁴

Furthermore, it is now accepted that the increased rate of glycolysis is accompanied by a decrease in fatty acid oxidation.³³ Consistent with our suggestion of an increase in fatty acid oxidation in the resistant cell line, is a recent study, which demonstrates that drug-susceptible cancer cells do increase the rate of glycolysis, while drug-resistant cancer cells revert back to fatty acid oxidation for ATP synthesis.¹⁰⁵

Fatty acid oxidation is more efficient than glycolysis for the production of ATP. The former can lead to the production of reactive oxygen species, which can damage the newly synthesized DNA of cancer cells. Such damage can force cells to undergo apoptosis, which may explain the need for a decrease in fatty acid oxidation. Drug-resistant cancer cells, on the other hand, have evolved mechanisms whereby they can repair such damage, or even ignore it, which allows them to use the more efficient fatty acid oxidation to sustain ATP synthesis. It has been suggested that such alterations are a typical quality of most drug-resistant cells. However, we do not see evidence for an increase in fatty acid oxidation in the cell line resistant to mitoxantrone. Taking into consideration our results, and the previous work that demonstrated an increase in fatty acid oxidation in drug-resistant cancer cells, we offer that the alterations observed in 3,2 trans-enoyl CoA isomerase and the trifunctional enzyme α subunit are consistent with the altered metabolic phenotype of drug-resistant cancer cells, which in turn may work to support the drug-resistant phenotype.

Oxidative phosphorylation

Mitochondria are responsible for generating 80-90% of the cell's energy needs through the process of oxidative phosphorylation. In this way, ATP production is coupled to the transfer of electrons to oxygen along protein complexes in the inner

mitochondrial membrane. The electrons are donated from the reduced coenzymes, NADH and FADH₂, generated during fatty acid oxidation, glycolysis and the citric acid cycle. In three protein complexes along the way, the transfer of electrons is coupled to the uphill movement of protons from the mitochondrial matrix across the inner mitochondrial membrane to form a proton concentration gradient. This movement of protons also causes the matrix to become negatively charged with respect to the inner membrane space and results in formation of an electric potential. The proton motive force, or energy equivalent of the proton concentration gradient and electric potential, powers ATP synthesis when protons from the inner membrane space spontaneously travel to the mitochondrial matrix through the ATP synthase complex.

Oxidative phosphorylation, begins at complex I of the electron transport chain, NADH-CoQ reductase. Here, the reduced coenzyme, NADH, donates a pair of electrons to coenzyme Q (CoQ) to form CoQH₂. At complex II, succinate CoQ reductase, FADH₂ also donates two electrons to CoQ to form CoQH₂. Reduced coenzyme Q then donates electrons, a pair at a time, to the third complex, CoQH₂-cytochrome c reductase, where the electrons are transferred to cytochrome c through a series of intermediate protein acceptors. The reduced cytochrome c then travels to complex IV, cytochrome c oxidase, where it transports the electrons, one at a time until they are ultimately transferred to a molecule of oxygen to produce H₂O. At complexes I, III and IV, protons are pumped across the inner membrane. When these protons spontaneously travel back from the innermembrane space to the matrix through the ATP synthase complex, energy is released to power the synthesis of ATP from ADP and inorganic phosphate.

In the cell line resistant to adriamycin, we see a decrease in abundance of cytochrome c oxidase subunit Vb, while in the mitoxantrone resistant cell line we see an increase in the Va subunit of cytochrome c oxidase. As seen in Table 9, we have identified both subunits in each of the cell lines, but their changes in abundance are not consistent. In addition, we have also identified additional subunits of the cytochrome c oxidase complex, however only subunits Va and Vb have altered abundances.

Cytochrome c oxidase is the fourth protein complex of the electron transport chain and is composed of thirteen protein subunits. Subunits I, II and III are encoded by mitochondrial DNA and account for the catalytic activity of the complex. The function of the remaining ten subunits, including Va and Vb, has yet to be elucidated. It has been demonstrated that in breast and prostate cancers, there is an increased abundance of these subunits.^{106,107} In the prostate study, it was also shown that there is an increase in abundance of subunit IV and a decrease in the abundance of subunit I. The authors concluded that these alterations support the metabolic shift, as previously described, of malignant cells to utilize glycolysis for the production of ATP, as opposed to non-transformed cells, which make use of oxidative phosphorylation. As compared to the increased abundance of the Vb subunit in the prostate study, we see a decrease in abundance of the Vb subunit in the adriamycin resistant cell line. We believe that this result supports the hypothesis that drug resistant cancer cells revert back to the use of fatty acid oxidation for ATP synthesis, as compared to glycolysis.

In another study, it was observed that adriamycin resistant leukemia cell lines have a decreased cytochrome c oxidase activity.¹⁰⁸ The same authors later showed that this decrease likely results from the altered expression of several cytochrome c oxidase

subunits.⁵² It was put forward that these alterations may have been generated initially as a result of adriamycin resistance, but once modified, the proteins are likely to confer the drug resistant phenotype to cancer cells. Thus, we suggest that alterations in cytochrome c oxidase subunits Va and Vb support the shift in metabolic strategy used by drug resistant cancer cells and that this alteration can promote drug-resistance.

In both drug resistant cell lines, as seen in Figure 24, we see a decrease in abundance of the full-length ATP synthase α -subunit protein, while we see an increased abundance in truncated isoforms of this protein. In addition to these changes, we have also detected the altered abundance of two additional subunits of the ATP synthase complex, d and δ , as shown in Table 10. Although these proteins do not quite meet our criteria of a 2-fold change, it may be possible that they are also involved in the mechanism of drug-resistance in both the adriamycin and mitoxantrone resistant cell lines.

The ATP synthase complex has two components, F1, which is the catalytic part of the complex made up of subunits; α , β , γ , δ and ϵ and F0, which contains a, b and c and d subunits. Three subunits each, of α and β , alternate to form a ring that sits atop the γ subunit, which fits into the c subunit ring of F0. When protons move from the innermembrane space to the matrix during oxidative phosphorylation, they release their energy and travel down the transmembrane channel of F0, comprised of subunits a and b. This energy powers rotation of the γ subunit within the c ring, to drive conformational changes in the β -subunits so that they can; bind ADP and inorganic phosphate, spontaneously produce ATP and finally release it.

Alterations in the ATP synthase complex have been reported in a number of

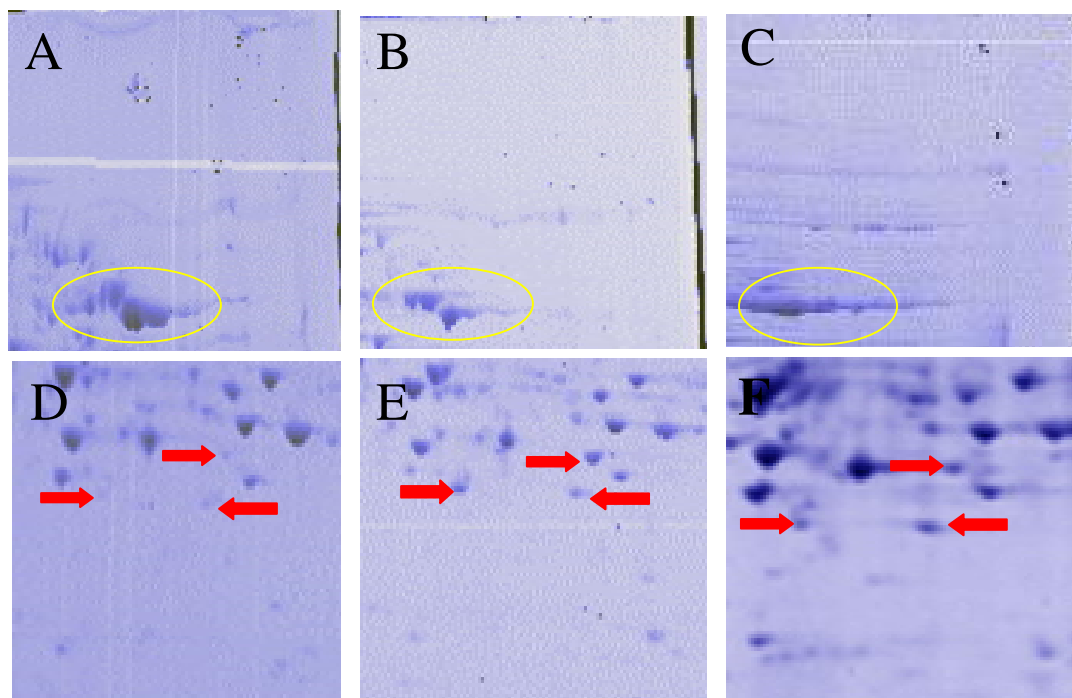


Figure 24. The altered abundance of ATP synthase, α -subunit. Panels A, B and C show the decrease in abundance of the full-length protein, as circled in yellow, in the drug-susceptible, adriamycin/verapamil resistant and mitoxantrone resistant MCF-7 cell lines, respectively. Panels D, E and F show the increase in abundance of the truncated proteins, as highlighted by red arrows in the drug-susceptible, adriamycin/verapamil resistant and mitoxantrone resistant MCF-7 cell lines, respectively.

ATP synthase subunit	Relative Abundance in the Adriamycin Resistant MCF-7 Cell Line	Relative Abundance in the Mitoxantrone Resistant MCF-7 Cell Line
Full-length α	0.75±0.04	0.65±0.13
Truncated α^*	9.91±8.20	4.21±1.24
b	1.56±0.10	0.99±0.11
Δ	0.58± 0.02	1.55± 0.11
d	0.82±0.09	1.93±0.10

Table 10. Relative abundance of ATP synthase subunits in the drug resistant MCF-7 cell lines. * In the comparative analysis, 3 isoforms of the truncated alpha subunit have been identified. The abundance of these isoforms has been averaged.

cancers. In liver cancer, it has been shown that there is an overall reduction of ATP synthase components. Similarly, in other cancers, including breast, lung and oesophageal, it has been shown that a decreased abundance of the β -subunit can be used as a marker of tumor progression.^{109,110} The authors of these studies concluded that the alterations supported the fact that tumor cells decrease oxidative phosphorylation for the production of ATP and suggested that alterations in the complex may also cause drug resistance, as a functional complex is required for apoptosis.^{111,112}

More recently, a proteomic analysis has been conducted to determine if there are alterations in protein abundances between a drug-susceptible colon cancer cell line and a colon cancer line that is resistant to 5-fluorouacil, a commonly used chemotherapeutic. Using 2D-GE and comparative densitometry, it was shown that there is a decrease in abundance of the full-length ATP synthase, α -subunit.¹¹³ Furthermore, the authors found that this decrease led to a reduced activity of the ATP synthase complex and that a functional ATP synthase complex is required for 5-fluorouacil activity. Taken together, the authors concluded that the down-regulation of ATP synthase directly results in drug resistance. Based on the findings in our work, that there is a decrease in abundance of the full length ATP synthase, α -subunit protein and an increase in truncations of this protein in the cell lines resistant to mitoxantrone and adriamycin, in combination with the results described for 5-fluorouacil resistance, we suggest that a decrease in the activity of ATP synthase may be one mechanism by which cancer cells become drug-resistant. Also, we propose that this mechanism may be conserved across different classes of chemotherapeutic agents, as adriamycin and mitoxantrone are antibiotics and 5-fluorouacil is an antimetabolite.

Biosynthesis of heme

The biosynthesis of heme is an important process, as heme is found in a variety of proteins including the cytochromes, hemoglobin, and the anti-oxidants catalase and peroxidase. These proteins are involved in a variety of processes required for cellular homeostasis and their expression can be regulated by reavailability of heme.¹¹⁴ Heme synthesis begins in the mitochondria, where succinyl CoA, generated during the citric acid cycle, is converted to δ -aminolevulinic acid by δ -aminolevulinic acid synthase. Once converted, the metabolite translocates into the cytosol where it undergoes three enzyme-catalyzed reactions to yield coproporphyrinogen III. This product then moves back into the mitochondria where it is converted into protoporphyrinogen IX by the enzyme, coproporphyrinogen III oxidase. The synthesis of heme is finally completed by another two reactions in the mitochondria.

In the cell line resistant to adriamycin, there is an increased abundance of sixth enzyme in the pathway, coproporphyrinogen III oxidase. This enzyme, located in the innermembrane space of mitochondria, has already been shown to influence the heme content in cells. Using yeast as the model system, a deficiency in heme was shown to induce transcription of the gene encoding coproporphyrinogen III oxidase and in erythroid cells, where the need for heme is greatest, transfection of an antisense oligonucleotide to the enzyme resulted in a decrease in heme production.^{115,116} In addition, the coproporphyrinogen III step is the rate-limiting step in the synthetic pathway. Based on these reports and our observation of an increase in abundance of coproporphyrinogen III oxidase, we conclude that there is an increase in the biosynthesis of heme in the cell line

that is resistant to adriamycin. Furthermore, the increase in heme content allows for the conjecture of a novel mechanism of resistance to adriamycin.

One mode of adriamycins' toxicity is its ability to generate reactive oxygen species. Specifically, this was demonstrated when transgenic mice were made to overexpress the anti-oxidant superoxide dismutase. Mice that did not overexpress the enzyme incurred damage from adriamycin, while the transgenic mice were protected from the free radical damage.¹¹⁷ A mitochondrial enzyme, superoxide dismutase, converts superoxide free radicals into hydrogen peroxide, which is further degraded into water and oxygen by another antioxidant, catalase. Several reports have shown that heme transcriptionally activates the genes that encode for both superoxide dismutase and catalase.¹¹⁴

In untreated breast cancer, the capacity for heme biosynthesis is enhanced 20-fold.¹¹⁸ Rodents treated with adriamycin show a decrease in cellular heme content.¹¹⁹ In our MCF-7 cell line selected for resistance to adriamycin in the presence of verapamil, we present evidence for an increase in heme synthesis. Taking these data into consideration we suggest the following mechanism for chemoresistance of adriamycin in the presence of verapamil:

A: In untreated breast cancer cells, there is an increase in heme production. This increase activates production of the anti-oxidants superoxide dismutase and catalase to protect the newly formed cancer cells from damage by reactive oxygen species that can be generated during a number of cellular processes. The cancer cells survive.

B: In breast cancer cells that are treated with and susceptible to adriamycin, the drug targets mitochondria and causes a decrease in heme. Therefore, the anti-oxidants cannot

be activated and the cancer cells are susceptible to damage by reactive oxygen species. The cancer cells undergo apoptosis.

C: In breast cancer cells that are treated with, but resistant to adriamycin, the drug stimulates expression of coproporphyrinogen III oxidase which in turn stimulates production of heme. Heme activates the production of superoxide dismutase. The cancer cells evade apoptosis and survive.

Apoptosis

Apoptosis, or programmed cell death is a critical process as it regulates normal development. Alterations in the pathway have been implicated in a number of diseases including Alzheimers, Parkinsons and acquired immune deficiency syndrome. The ability of cells to evade apoptosis also leads to the development of cancer and furthermore, it is now recognized that mutations along the pathway contribute to drug resistance.^{16,17} Relative to our interests, mitochondria play a central role in apoptosis. Thus, it is not surprising that we have observed changes in abundance of two proteins thought to be involved in apoptosis, adenylate kinase isoenzyme 2 and cofilin.

Cells express four isoforms of the 26 kDa, adenylate kinase enzyme. Adenylate kinase 1, 2 and 3, located in the cytosol, mitochondrial innermembrane space and mitochondrial matrix, respectively, are essential for cell growth and maintenance and thus are ubiquitously expressed at all times. The expression of isozyme 4, on the other hand, is more limited as it appears only in response to the induction of specific pathways related to the energy needs of a given cell type.¹²⁰ In the cell line resistant to adriamycin in the presence of verapamil, there is an increase in abundance of adenylate kinase isoenzyme 2, which functions to regulate the cellular pool of ADP, as it catalyzes the

phosphorylation of AMP to ADP. In addition to this role, it has also been postulated that adenylate kinase 2 may be involved in apoptosis.¹²⁰

In order for apoptosis to occur, soluble proteins located in the innermembrane space of mitochondria, such as cytochrome c and apoptosis inducing factor, must be released into the cytosol where they interact with other proteins to form the apoptosome complex to initiate the caspase cascade. Presently, three models have been suggested to explain the mechanism by which these proteins are released. Briefly, these models propose that; cytochrome c is released through specific channels in the outer mitochondrial membrane that are opened by the Bcl-2 family of proteins, that cytochrome c is released by opening of the permeability transition pore complex that spans the inner and outer membranes, and finally that cytochrome c is released through mitochondrial rupturing. Proteomic analyses have shown that adenylate kinase 2 is released from the innermembrane space in each case, but whether this release is non-specific or could potentially play a role in apoptosis could not be determined. To clarify, an elegant study was done in which Jurkat cells were treated with etoposide, a chemotherapeutic agent, to induce apoptosis.¹²¹ Immunoblot assays that screened for cytochrome c and adenylate kinase 2 in the mitochondrial and cytosolic fractions of these cells revealed that the two proteins are released from mitochondria into the cytosol concomitantly. These results suggest that adenylate kinase 2 is likely to be involved in apoptosis, although its role has yet to be elucidated. Because the isozyme indirectly influences cellular levels of ATP, it has been proposed that it may affect energy metabolism or the activation of the caspase cascade by the apoptosome complex, a process that requires ATP hydrolysis.¹²⁰ On the other hand, the role of adenylate kinase 2

in apoptosis could be different from its normal function. Until its role in apoptosis is elucidated, the altered abundance of adenylate kinase 2 in the resistant cell line cannot be explained.

Unlike adenylate kinase 2, which shows an increase in abundance, we observe a significant decrease in the abundance of cofilin in the cell line resistant to adriamycin. Cofilin is located predominantly in the cytosol of cells where it regulates actin dynamics by increasing the rate of actin depolymerization to promote actin turnover. Also, it is the major component of nuclear and cytosolic actin rods. In addition to this function, it has been demonstrated that cofilin plays a major role in apoptosis; upon early induction of the pathway, it translocates to the mitochondria to induce massive apoptosis.¹²³ These results were demonstrated when mitochondria were isolated from various cancer cells lines and induced to undergo apoptosis by treatment with the anti-cancer drugs staurosporine and etoposide.¹²³ From this work, it was shown that the translocation of cofilin precedes the release of cytochrome c from the innermembrane space of mitochondria, and that following translocation, cofilin accumulates in mitochondria.¹²³ Furthermore, it was also shown that a reduction in cofilin inhibited the release of cytochrome c and prevented the cells from undergoing apoptosis.¹²³ These results suggest that cofilin serves as a pro-apoptotic protein and that a decrease in its abundance can negatively affect apoptosis. Based on this study, and our data, in which we see a decreased abundance of cofilin in the mitochondrial fraction from MCF-7 cells resistant to adriamycin, we suggest that alterations in the apoptotic pathway, upstream of mitochondria, reduce translocation of cofilin from the cytosol to the organelle, which serves to disrupt apoptosis and that this is one mechanism by which resistance is conferred in this cell line.

In the mitoxantrone resistant cell line, we did not observe alterations in proteins that are thought to be associated with apoptosis. Unfortunately, we were not able to identify cytochrome c in either the drug-susceptible or drug resistant cell lines. This can likely be attributed to our isolation procedure, as it has been shown that homogenization can cause premature release of cytochrome c from the innermembrane space of mitochondria into the cytosol.¹²⁴

Mitochondrial homeostasis

In the MCF-7 cell line selected for resistance to adriamycin in the presence of verapamil, we see a decrease in abundance of two proteins essential for mitochondrial homeostasis, GrpE protein homolog 1 and elongation factor Ts. Specifically, both proteins are involved in maintenance of the mitochondrial proteome. GrpE1 is involved with the import of nuclear encoded mitochondrial proteins, while elongation factor Ts plays a role in translation of those proteins that are encoded by the mitochondrial genome.

Of the estimated 1200 mitochondrial proteins, only one percent are encoded by the mitochondrial genome. These proteins are extremely important however, as all thirteen are part of complexes within the electron transport chain, including the ATP synthase complex. Translation of these proteins requires two factors, elongation factor Tu and elongation factor Ts. Elongation factor Tu interacts with amino-acyl tRNA to promote its binding to the active site of mitochondrial ribosomes. This process requires that elongation factor Tu be bound by GTP. Once binding occurs, GTP is hydrolyzed to GDP, making elongation factor Tu inactive. Elongation factor Ts functions to promote recycling of the inactive GDP bound form of elongation factor Tu to the active, GTP

bound state.¹²⁵ It follows then, that a decrease in the abundance of elongation factor Ts could potentially decrease the rate of protein translation, which in turn could ultimately affect the production of ATP as the proteins encoded by mitochondrial DNA are involved in oxidative phosphorylation. In support of this idea, we have identified an additional six proteins, listed in Table 11, that show a decrease in abundance and though their decrease does not meet our criteria of a 2-fold change, they too are involved in translation of proteins encoded by the mitochondrial genome.

In contrast to the mitochondrial genome, nuclear DNA encodes more than ninety-nine percent of mitochondrial proteins, which must be transported to the organelle for it to function properly. Precursor proteins are translated in the cytosol and then brought into the mitochondria, where they are folded and finally shuttled to their proper compartments. Import of the proteins begins when they are bound by one of two cytosolic chaperones, cytosolic heat shock protein 70 and mitochondrial-import stimulation factor. These proteins function to keep the nascent proteins in an unfolded state and to deliver them to the mitochondria, where they enter the matrix after traveling through translocation receptors that span the outer and inner mitochondrial membranes. As the proteins enter the matrix, the mitochondrial form of heat shock protein 70 binds them, so as to prevent aggregation, precipitation of premature folding. Heat shock protein 70 utilizes the energy released from ATP hydrolysis to improve its substrate binding capacity and requires two co-chaperones to function properly, heat shock protein 40 and GrpE protein. Heat shock protein 40 works to accelerate the rate of ATP hydrolysis and strengthen binding of the substrate, while GrpE protein binds to the ATPase domain to accelerate release of the precursor proteins from heat shock

Protein	Relative Abundance Level
28S ribosomal protein S10	0.77±0.08
Ribosomal protein L1	0.77±0.11
39S ribosomal protein L44	0.54±0.01
Elongation factor Tu	0.86±0.09
39S ribosomal protein L39	0.54±0.02
39S ribosomal protein L49	0.67±0.03

Table 11. Relative abundance of proteins involved in translation machinery in the adriamycin resistant MCF-7 cell line.

protein 70.¹²⁶ Once released, the proteins are bound to other chaperones for folding, and then shuttled to their proper location within the organelle.

A role for chaperone proteins in cancer and apoptosis has been demonstrated. Expression of the cytosolic form of heat shock protein 70 is associated with an improved prognosis in some types of cancer, while in others, like breast cancer it is associated with malignancy.¹²⁷ Its role in the inhibition of apoptosis has also been elucidated; it prevents recruitment of procaspase 9 to the apoptosome complex in the cytosol to hinder initiation of the caspase cascade.¹²⁸ Similarly, heat shock protein 40 can interact with Bax to prevent its translocation to mitochondria, a move that is required for the release of cytochrome c and other proteins from mitochondria, thereby also preventing apoptosis.¹²⁹ As of yet, it is not known what, if any role GrpE plays in the progression of cancer or apoptosis. It has been demonstrated that GrpE is essential for import of mitochondrial proteins. Perhaps its decrease represents an impaired rate for the release of mitochondrial proteins from heat shock protein 70. In turn, this could alter translocation of proteins to their proper locations within the mitochondria, which may ultimately compromise proper functioning of the organelle.

Proteins not known to be located in mitochondria

We have observed a decrease in abundance of four proteins that are not known to belong to the mitochondria in both of the drug-resistant MCF-7 cell lines. In the cell line selected for resistance to adriamycin in the presence of verapamil, we see a decrease in pyrroline 5-carboxylate reductase and the hypothetical protein FLJ23469, as shown in Table 4. In the cell line resistant to mitoxantrone, as shown in Table 6, we see a decrease in annexin II and the hypothetical protein FLJ20455. Because these proteins may interact

or associate with mitochondria and we see that they have an altered abundance, their role in cancer progression and/or resistance will be discussed briefly.

Pyrroline-5-carboxylate reductase is located in the cytosol, where it is involved in the final step of proline synthesis; it catalyzes the reduction of pyrroline-5-carboxylate to proline. Proline can then enter the mitochondria where it is oxidized back to pyrroline-5-carboxylate reductase by the mitochondrial enzyme, proline oxidase. Literature indicates that the interconversion of pyrroline-5-carboxylate and proline results in a metabolic shuttle that transfers redox equivalents between the cytosol and mitochondria and reports have proposed that proline oxidation in cells that overexpress proline oxidase results in the generation of reactive oxygen species due to this metabolic shuttling.^{130,131} Although no such link has been suggested for pyrroline-5-carboxylate reductase, it has been reported that the enzyme, along with several others, can be used to distinguish neoplastic from nonneoplastic colon cells.¹³² To date, this protein has not been implicated in cancer drug resistance, but the fact that the abundance of pyrroline-5-carboxylate reductase is increased in colon cancer and decreased in our cells resistant to adriamycin, signals that it could play a role in the switch from drug-susceptible to drug-resistant malignancy.

Annexin II shows a decreased abundance in the cell line resistant to mitoxantrone. The annexin family of proteins contains both calcium and phospholipid binding domains in the amino acid sequence. Annexin II is found in the lamina below the plasma membrane where it cross-links plasma membrane phospholipids with actin and the cytoskeleton and plays a role in apoptosis. Others have noted that the abundance of annexin II is reduced in prostate cancer as compared to non-transformed prostate cells, while its abundance is increased pancreatic cancer cells.^{133,134} In an MCF-7 breast cancer

cell line resistant to 5-fluorouracil, genomic studies showed that there is drug-induced expression of the gene encoding annexin II.¹³⁵ Similar results were provided in a proteomic study that demonstrated an increased abundance of annexin I in several multidrug-resistant cancer cell lines.¹³⁶ Collectively, these data indicate that the annexin protein family, specifically annexin II, is involved in cancer progression and drug resistance. It is puzzling that in our work we see a decrease in abundance of annexin II, while in other resistant cell lines there is an increase of the protein. In order to determine how the altered abundance of this protein contributes to drug resistance, further work must be done.

Unfortunately, little information currently exists on the hypothetical proteins that we observe to have altered abundances. The hypothetical protein, FLJ23469, which exhibits a reduced abundance in the cell line resistant to adriamycin is predicted, with 67% confidence, to be a cytosolic protein. Based on its amino acid sequence, this protein is postulated to have a metabolic activity, but what specific pathway it maybe involved in has not been elucidated. In the mitoxantrone resistant cell line, we report a decrease in abundance of the hypothetical protein FLJ20455. Using Psort, this protein is predicted to belong to the nucleus. The results of the sorting analysis are provided in Table 8. The gene encoding this hypothetical protein was recognized during a study aimed at identifying novel genes that may be involved an immune response in ovarian cancer.¹³⁷ Since that time, no further work has been reported in which a protein has been characterized, so it can only be speculated that this protein may play an immuno-responsive role in cancer.

In the comparative analysis presented in this study, we have identified 15 proteins that show altered abundances in the MCF-7 cell lines selected for resistance to adriamycin in the presence of verapamil and for mitoxantrone. Eleven of the proteins were detected in the adriamycin-resistant cell line. These proteins are involved in a number of mitochondrial pathways including fatty acid oxidation, oxidative phosphorylation and apoptosis. Based on our observations, we suggest that multiple mechanisms can be responsible for the promotion of adriamycin resistance at the mitochondrial level. Conversely, mitochondrial proteins that show altered abundances in the mitoxantrone-resistant cell line only play a role in oxidative phosphorylation. Thus, we offer that at the mitochondria, resistance to mitoxantrone can develop through alterations in electron transport and oxidative phosphorylation.

It is important that additional work be done to further investigate the mechanisms of drug-resistance conferred by the proteins that show an altered abundance. For example, genetic knockout and overexpression studies should be performed to determine if the proteins whose abundances have changed in this study play a role in drug-resistance. If so, these proteins may be exploited as biomarkers and/or drug-targets for novel chemotherapeutic agents.

Summary and prospectus

The objective of this study was to identify mitochondrial proteins whose abundances changed between a drug-susceptible MCF-7 breast cancer cell line and the MCF-7 cell lines selected for resistance to adriamycin in the presence of verapamil and to mitoxantrone. It was also our objective to consider how these proteins contribute to drug resistance. We have identified fifteen proteins that show an altered abundance in the two drug resistant cell lines. For some proteins, such as coproporphyrinogen III oxidase, we were able to suggest a mechanism by which they contribute to drug-resistance. On the other hand, for proteins such as the ATP synthase, α -subunit, we were not able to suggest a mechanism.

In the adriamycin resistant cell line we have detected eleven proteins that show an altered abundance. These proteins are involved in multiple mitochondrial pathways, including fatty acid oxidation, apoptosis and oxidative phosphorylation. In the cell line selected for resistance to mitoxantrone, we see the altered abundance of proteins that involved solely in oxidative phosphorylation. Based on these differences, we offer that resistance to adriamycin can develop through alterations in multiple mitochondrial pathways, while resistance to mitoxantrone, at the mitochondrial level, is the result of alterations in oxidative phosphorylation.

In the cell line selected for resistance to adriamycin in the presence of verapamil, we see an increase in abundance of the protein coproporphyrinogen III oxidase. The increase of this protein suggests that there is an increase in the heme content of the resistant cells. Because heme can transcriptionally activate proteins that protect cells from damage by reactive oxygen species and since one mode of adriamycins toxicity is

the production of free radicals, we propose that the resistant cells have altered the biosynthesis of heme so that they are protected from the toxic effects of adriamycin.

In both drug resistant cell lines, we see an increase in three truncated isoforms of the ATP synthase complex, α -subunit. Accompanying this change we also see a decrease in the full-length protein. Alterations in this and additional subunits of the ATP synthase complex have been linked to malignancy and drug resistance. Unfortunately, we were not able to propose a mechanism for how this resistance can be conferred, but we hypothesize that alterations in this subunit promote drug resistance and that this resistance is likely to be conserved across different classes of chemotherapeutic drugs.

In completion of this project, we have created a proteomic map of MCF-7 mitochondria, which can be used as a reference in future work that utilizes this cell line. In this effort, we have identified about ten percent of the estimated mitochondrial proteins. To increase the coverage of mitochondrial proteins, work is currently being done in our lab that utilizes a shotgun approach. This should allow us to characterize low abundance and basic proteins, often neglected and incompatible with gel based work.

References

1. American Cancer Society. Cancer Facts and Figures 2004. <http://www.cancer.org> (accessed February 2005).
2. Medline Plus. <http://www.nlm.nih.gov/medlineplus/breastcancer.html> (accessed February 2005).
3. Simon, S., Schindler, M. *Proc. Natl. Acad. Sci.* 1994, 91, 3497-504.
4. Gottesman, M.M. *Annu. Rev. Med.* 2002, 53, 615-27.
5. Hanahan D., Weinberg, RA. *Cell.* 2000, 100, 57-70
6. Bates, S.E. *Clinical Cancer Research.* 1999, 5, 3346-48.
7. Longley, D.B., Johnston PG. *J. Pathol.* 2005, 205, 275-92.
8. Thomas, H., Coley, M.H. *Cancer Control.* 2003, 10, 159-65.
9. Gottesman, M.M., Fojo, T., Bates, S.E. *Nat. Rev. Cancer.* 2002, 2, 48-58.
10. Ross, D.D., Yang, W., Abruzzo, LV., Dalton, W.S., Schneider, E., Lage, H., Dietel, M., Greenberger, L., Cole, S.P., Doyle, L.A. *J. Natl. Cancer Inst.* 1999, 91, 429-33.
11. Townsend, D.M., Tew, K.D. *Oncogene.* 2003, 22, 7369-75.
12. Batist, G., Tulpule, A., Sinha, B.K., Katki, A.G., Myers, C.E., Cowan K.H. *J. Biol. Chem.* 1986, 261, 15544-49.
13. Fink, D., Nebel, S., Aebi, S., Zheng, H., Cenni, B., Nehme, A., Christen, R.D., Howell, S.B. *Can. Res.* 1996, 56, 4881-86.

14. Fojo, T. *J. Natl. Cancer Inst.* 1993, 19, 1434-78.
15. Kastan, M.B. *Biochimica et Biophysica Acta.* 1999, 1424, R37-R42.
16. Lowe, S.W., Lin, A.W. *Carcinogenesis.* 2000, 21, 485-95.
17. Johnstone R.W., Ruefli, A.A., Lowe, S.W. *Cell.* 2002, 108, 153-64.
18. Lehnert, M. *European Journal of Cancer.* 1996, 32A, 912-20.
19. Stein, W.D., Bates, S.E., Fojo, T. *Curr. Drug Targets.* 2004, 5, 333-46.
20. Litman, T., Druley, T.E., Stein, W.D. *Cell Mol. Life Sci.* 2001, 58, 931-59.
21. Hayes, J.D., Wolf, C.R. *Biochem. J.* 1990, 272, 281-95.
22. Ohi, Y., Kim, T., Toge, T. *Int. J. Oncol.* 2000, 16, 959-69.
23. Jung, E., Heller, M., Sanchez, J.C., Hochstrasser, D.F. *Electrophoresis.* 2000, 21, 3369-77.
24. Bernardi, P., Petronilli, V., DiLisa, F., Forte, M. *TRENDS in Biochemical Sciences.* 2001, 25, 112-17.
25. Halestrap, A.P., Doran, E., Gillespie, J.P., O'Toole, A. *Biochemical Society Transactions.* 2000, 28, 170-6.
26. Burlacu, A. *J. Cell. Mol. Med.* 2003, 7, 249-57
27. Newmeyer, D., Ferguson-Miller, S. *Cell.* 2003, 112, 481-90.

- 28.Zamzini, N., Kroemer, G. *Nat. Rev. Mol. Cell Bio.* 2001, 2, 67-71
- 29.Martinou, J.C., Green, D.R. *Nat. Rev. Mol. Cell Bio.* 2001, 2, 63-67.
- 30.Zamzini, N., Kroemer, G. *Current Biology.* 2003, 13, R71-R73.
- 31.Grad, J.M., Cepero, E., Boise, L.H. *Drug Resistance Updates.* 2001, 4, 85-91.
- 32.Morisaki, T., Katano, M. *Current Medicinal Chemistry.* 2003, 10, 2517-2521.
- 33.Modica-Napolitano, J.S., Singh, K.K. *Expert Reviews in Molecular Medicine.* 2002, 2, 1-19.
- 34.Singh, K.K., Russell, J., Sigala, B., Zhang, Y., Williams, J., Kesha, v K.F. *Oncogene.* 1999, 18, 6641-6.
- 35.Weissig, V., Boddapati, S.V., D'Souza, G.G.M., Cheng, S.M. *Drug Design Reviews.* 2004, 1, 15-28.
- 36.Duan, Z., Brakora, K.A., Seiden, M.V. *Gene.* 2004, 29, 53-9.
- 37.Soule, K.D., Vazquez, J., Long, A., Albert, S., Brennan, M. *J. Natl. Cancer Inst.* 51, 5, 1973.
- 38.Simstein, R., Burow, M., Parker, A., Weldon, C., Beckman, B. *Experimental Biology and Medicine.* 2003, 228, 995-1003.
- 39.Hathout, Y., Gehrman, M.L., Chertov, A., Fenselau, C. *Cancer Letters.* 2004, 210, 245-53.
- 40.Taylor, C.W., Dalton, W.S., Parrish, P.R., Gleason, M.C., Bellamy, W.T., Thompson, F.H., Roe, D.J., Trent, J.M. *Br. J. Cancer.* 1991, 63, 923-29.

41. Chen, Y.N., Mickley, L.A., Schwartz, A.M., Acton, E.M., Hwang, J.L., Fojo, A.T. *J. Biol. Chem.* 1990, 265, 10073-80.
42. Doyle, L.A., Ross, D.D. *Oncogene.* 2003, 22, 7340-58.
43. Volk, E.L., Schneider, E. *Cancer Research.* 2003, 63, 5538-43.
44. Jung, K., Reszka, R. *Adv. Drug Del. Rev.* 2001, 87-105.
45. Doroshow, J.H., Davies, K.J.A. *J. Biol. Chem.* 1986, 261, 3068-74.
46. Davies, K.J.A., Doroshow, J.H. *J. Biol. Chem.* 1986, 261, 3060-67
47. Kluza, J., Marchetti, P., Gallego, M.A., Lancel, S., Fournier, C., Loyens, A., Beauvillain J.C., Bailly, C. *Oncogene.* 2004, 23, 7018-30.
48. Scudiero, D.A., Monks, A., Sausville, V.A. *J. Natl. Cancer. Inst.* 1998, 90, 862.
49. Mehta, K., Devarajan, E., Chen, J., Multani, A., Pthak, S. *J. Natl. Cancer Inst.* 2002, 94, 1652-53.
50. Childs, A.C., Phaneuf, S.L., Dirks, A.J., Phillips, T., Leeuwenburgh, C. *Cancer Res.* 2002, 62, 4592-8.
51. Nonn, L., Berggren, M., Powis, G. *Molecular Cancer Research.* 2003, 1, 682-89.
52. Grandjean, F., Bremaud, L., Robert, J., Ratinaud, MH. *Biochemical Pharmacology.* 2002, 63, 823-31.
53. Muraoka, S., Miura, T. *Chem. Biol. Interact.* 2003, 145, 67-75.

54. Denis-Gay, M., Petit, JM., Mazat, JP., Ratinaud, MH. *Biochemical Pharmacology*. 1998, 56, 451-57.
55. Nakagawa, M., Schneider, E., Dixon, K.H., Horton, J.K., Kelley, K., Morrow, C., Cowan, K.H. *Cancer Res*. 1992, 52, 6175-81.
56. Volk, E.L., Rohde, K., Rhee, M., McGuire, J.J., Doyle, L.A., Ross, D.D., Schneider, E. *Cancer Res*. 2000, 60, 3514-21.
57. Volk, E.L., Farley, K.M., Wu, Y., Li, F., Robey, R.W., Schneider, E. *Cancer Res*. 2002, 62, 5035-40.
58. Buschini, A., Poli, P., Rossi, C. *Mutagenesis*. 2003, 18, 25-36.
59. Kule, C., Ondrejickova, O., Verner, K. *Mol. Pharmacol*. 1994, 46, 1234-40.
60. Bachmann, E., Weber, E., Zbinden, G. *Cancer Treat. Rep*. 1987, 71, 361-66.
61. Pandey, A., Mann, M. *Nature*. 2000, 405, 837-46.
62. Banks, R.E., Dunn, M.J., Hochstrasser, D.F., Sanchez, J.C., Blackstock, W., Pappin, D.J., Selby, P.J. *Lancet*. 2000, 356, 1749-56.
63. Venter J.C., Adams, M.D., Myers, E.W., Li, P.W., Mural, R.J., Sutton, G.G., Smith, H.O., Yandell, M., Evans, C.A., Holt, R.A., Gocayne, J.D., Amanatides, P., Ballew, R.M., Huson, D.H., Wortman, J.R., Zhang, Q., Kodira, C.D., Zheng, X.H., Chen, L., Skupski, M., Subramanian, G., Thomas, P.D., Zhang, J., Gabor Miklos, G.L., Nelson, C., Broder, S., Clark, A.G., Nadeau, J., McKusick, V.A., Zinder, N., Levine, A.J., Roberts, R.J., Simon, M., Slayman, C., Hunkapiller, M., Bolanos, R., Delcher, A., Dew, I., Fasulo, D., Flanigan, M., Florea, L., Halpern, A., Hannenhalli, S., Kravitz, S., Levy, S., Mobarry, C., Reinert, K., Remington, K., Abu-Threideh, J., Beasley, E., Biddick, K., Bonazzi, V., Brandon, R., Cargill, M., Chandramouliswaran, I., Charlab, R., Chaturvedi, K., Deng, Z., Di Francesco, V., Dunn, P., Eilbeck, K., Evangelista, C., Gabrielian, A.E., Gan, W., Ge, W., Gong, F., Gu, Z., Guan, P., Heiman, T.J., Higgins, M.E., Ji, R.R., Ke, Z., Ketchum, K.A., Lai, Z., Lei, Y., Li, Z., Li, J., Liang, Y., Lin, X., Lu, F., Merkulov, G.V., Milshina, N., Moore, H.M., Naik,

A.K., Narayan, V.A., Neelam, B., Nusskern, D., Rusch, D.B., Salzberg, S., Shao, W., Shue, B., Sun, J., Wang, Z., Wang, A., Wang, X., Wang, J., Wei, M., Wides, R., Xiao, C., Yan, C., Yao, A., Ye, J., Zhan, M., Zhang, W., Zhang, H., Zhao, Q., Zheng, L., Zhong, F., Zhong, W., Zhu, S., Zhao, S., Gilbert, D., Baumhueter, S., Spier, G., Carter, C., Cravchik, A., Woodage, T., Ali, F., An, H., Awe, A., Baldwin, D., Baden, H., Barnstead, M., Barrow, I., Beeson, K., Busam, D., Carver, A., Center, A., Cheng, M.L., Curry, L., Danaher, S., Davenport, L., Desilets, R., Dietz, S., Dodson, K., Doup, L., Ferriera, S., Garg, N., Gluecksmann, A., Hart, B., Haynes, J., Haynes, C., Heiner, C., Hladun, S., Hostin, D., Houck, J., Howland, T., Ibegwam, C., Johnson, J., Kalush, F., Kline, L., Koduru, S., Love, A., Mann, F., May, D., McCawley, S., McIntosh, T., McMullen, I., Moy, M., Moy, L., Murphy, B., Nelson, K., Pfannkoch, C., Pratts, E., Puri, V., Qureshi, H., Reardon, M., Rodriguez, R., Rogers, Y.H., Romblad, D., Ruhfel, B., Scott, R., Sitter, C., Smallwood, M., Stewart, E., Strong, R., Suh, E., Thomas, R., Tint, N.N., Tse, S., Vech, C., Wang, G., Wetter, J., Williams, S., Williams, M., Windsor, S., Winn-Deen, E., Wolfe, K., Zaveri, J., Zaveri, K., Abril, J.F., Guigo, R., Campbell, M.J., Sjolander, K.V., Karlak, B., Kejariwal, A., Mi, H., Lazareva, B., Hatton, T., Narechania, A., Diemer, K., Muruganujan, A., Guo, N., Sato, S., Bafna, V., Istrail, S., Lippert, R., Schwartz, R., Walenz, B., Yooseph, S., Allen, D., Basu, A., Baxendale, J., Blick, L., Caminha, M., Carnes-Stine, J., Caulk, P., Chiang, Y.H., Coyne, M., Dahlke, C., Mays, A., Dombroski, M., Donnelly, M., Ely, D., Esparham, S., Fosler, C., Gire, H., Glanowski, S., Glasser, K., Glodek, A., Gorokhov, M., Graham, K., Gropman, B., Harris, M., Heil, J., Henderson, S., Hoover, J., Jennings, D., Jordan, C., Jordan, J., Kasha, J., Kagan, L., Kraft, C., Levitsky, A., Lewis, M., Liu, X., Lopez, J., Ma, D., Majoros, W., McDaniel, J., Murphy, S., Newman, M., Nguyen, T., Nguyen, N., Nodell, M., Pan, S., Peck, J., Peterson, M., Rowe, W., Sanders, R., Scott, J., Simpson, M., Smith, T., Sprague, A., Stockwell, T., Turner, R., Venter, E., Wang, M., Wen, M., Wu, D., Wu, M., Xia, A., Zandieh, A., Zhu, X. *Science*. 2001, 291, 1304-51.

64. Mann, M., Jensen, O.N. *Nature Biotechnology*. 2003, 21, 255-61.

65. Zhu, H., Bilgin, M., Snyder, M. *Annu. Rev. Biochem.* 2003, 72, 783-812

66. Stevens, E.V., Posadas, E.M., Davidson, B., Kohn, E.C. *Annals of Oncology*. 2004, 15, iv167-iv171

67. Hanash, S. *Nature*. 2003, 13, 226-32.

68. Gorg, A., Weiss, W., Dunn, M.J. *Proteomics*. 2004, 4, 3665-85.

69. O'Farrell, P.H. *J. Biol. Chem.* 1975, 250, 4007-21.
70. Hillenkamp, F., Karas, M. *Int. J. of Mass Spectrometry.* 2000, 200, 71-77.
71. Tanaka, K., Waki, H., Ido, Y., Akita, S., Yoshida, T. *Rapid Communications in Mass Spectrometry.* 1988, 2, 151-53.
72. Fenselau, C. *Anal. Chem.* 1997, 69, 661A-665A.
73. Yates, J.R. *J. Mass Spectrom.* 1998, 22, 1-19.
74. Fenn, J.B., Mann, M., Meng, C.K., Wong, S.F., Whitehouse, C.M. *Science.* 1989, 246, 64-7.
75. Whitehouse, C.M., Dreyer, R.N., Yamashita, M., Fenn, J.B. *Anal. Chem.* 1985, 57, 675-9.
76. Cole, R.B. *J. Mass Spectrom.* 2000, 35, 763-772.
77. Wilm, M., Mann, M. *Anal. Chem.* 1996, 68, 1-8.
78. Perkins, D.N., Pappin, D.J., Creasy, D.M., Cottrell, J.S.. *Electrophoresis.* 1999, 20, 3551-67.
79. Siuzdak, G. *The Expanding Role of Mass Spectrometry in Biotechnology.* 2003. MCC Press, New York.
80. Fenyo, D., Beavis, R.C. *Anal Chem.* 2003, 15, 768-74.
81. Nakagawa, M., Schneider, E., Dixon, K.H., Horton, J.K., Kelley, K., Morrow, C., Cowan, K.H. *Cancer Res.* 1992, 52, 6175-81.
82. Hoppel, C., DiMarco, J.P., Tandler, B. *J Biol Chem.* 1979, 254, 4164-70.

83. Hoppel, C.L., Kerner, J., Turkaly, P., Turkaly, J., Tandler, B. *J Biol Chem.* 1998, 4, 3495-503.
84. Scheffler, N.K., Miller, S.W., Carroll, A.K., Anderson, C., Davis, R.E., Ghosh, S.S., Gibosn, B.W. *Mitochondrion.* 2001, 1, 161-79.
85. Hoving, S., Gerrits, B., Voshol, H., Muller, D., Roberts, R.C., van Oostrum J. *Proteomics.* 2002, 2, 127-34.
86. Shevchenko, A., Wilm, M., Vorm, O. and Mann, M. *Anal. Chem.* 1996, 68, 850-858.
87. Scheffler, I.E. *Mitochondria.* 1999. Wiley-Liss, Inc. Canada.
88. Mann, M. *The Scientist.* 2004, 32-33.
89. Mootha, V.K., Bunkenborg, J., Olsen, J.V. Hjerrild, M., Wisniewski, J.R., Stahl, E., Bolouri, M.S., Ray, H.N, Sihag, S., Kamal, M., Patterson, N., Lander, E.S., Mann, M. *Cell.* 2003, 115, 629-40.
90. Scott, M.S., Thomas, D.Y., Hallet, M.T. *Genome Research.* 2004, 14, 1957-66.
91. Andersen, J.S., Lyon, C.E., Fox, A.H., Leung, A.K.L., Lam, YW., Steen, H., Mann, M., Lamond, A.I. *Current Biology.* 2002, 12, 1-11.
92. Taylor, S.W., Fahy, E., Zhang, B., Glenn, G.M., Warnock, D.E., Wiley, S., Murphy, A.N., Gaucer, S.P., Capaldi, R.A., Gibson, B.W., Ghosh, S.S. *Nature Biotechnology.* 2003, 21, 281-86.
93. Fountoulakis, M., Schlaeger, E.J. *Electrophoresis.* 2003, 24, 260-75.
94. Jaatela, M., Cande, C., Kroemer, G. *Cell Death and Differentiation.* 2003, 28, 1-2.

95. Eisenstein E., Gililand, G.L., Herzberg, O., Moulton, J., Orban, J., Poljak, R.J., Banerjee, L., Richardson, D., Howard, A.J. *Current Opinion in Biotechnology*. 2000, 11, 25-30.
96. Shin, J.H., Yang, J.W., Pecheur, M.L., London, J., Hoeger, H., Lubec, G. *Proteome Science*. 2004, 2.
97. Guda, C., Guda, P., Fahy, E., Subramaniam, S. *Nucleic Acids Research*. 2004, 32, W372-W374.
98. Nakai, K., Kanehisa, M. *Genomics*. 1992, 14, 897-911.
99. Guda, C., Fahy, E., Subramaniam, S. *Bioinformatics*. 2004, 20, 1785-94.
100. John, G.B., Shang, Y., Li, L., Renken, C., Mannella, C.A., Selker, J.M.L., Rangell, L., Bennett, M.J., Zha, J. *Mol. Biol. Cell*. 2005, 16, 1543-54.
101. Janssen, U., Stoffel, W. *J. Biol. Chem*. 2002, 31, 19579-84.
102. Roblick, U.J., Hirschberg, D., Habermann, J.K., Palmberg, C., Becker, S., Kruger, M., Gustafsson, M., Bruch, H.P., Franzen, B., Ried, T., Bergman, T., Auer, G., Jornvall, H. *Cell and Molecular Life Sciences*. 2004, 61, 1246-55.
103. Rinaldo, P., Matern, D., Bennett, M.J. *Annu. Rev. Physiol*. 2002, 64, 477-502.
104. Warburg, O. *Science*. 1956, 124, 269-70.
105. Harper, M.E., Antoniou, A., Villalobos-Menuet, E., Russo, A., Trauger, R., Vendemio, M., George, A., Bartholomew, R., Carlo, D., Shaikh, A., Kupperman, J., Newell, E.W., Bespalov, I.A., Wallace, S.S., Liu, Y., Rogers, J.R., Gibbs, G.L., Leahy, J.L., Camley, R.E., Melamed, R., Newell, M.K. *The FASEB Journal*. 2002, 16, 1550-57.

106. Bini, L., Magi, B., Marzocchi, B., Arcuri, F., Tripodi, S., Cintorino, M., Sanchez, J.C., Frutiger, S., Hughes, G., Pallini, V., Hochstrasser, D.F., Tosi, P. *Electrophoresis*. 1997, 18, 2832-41.
107. Krieg, R.C., Knuechel, R., Schiffmann, E., Liotta, L., Petricoin, E.F., Herrmann, P.C. *Proteomics*. 2004, 4, 2789-95.
108. Tsuru, T., Iada-Saito, H., Kawabata, H., Oh-Hara, T., Hamada, H., Utakoji, T. *Jpn .J. Cancer Res*. 1986, 77, 682-92.
109. Cueva, J.M., Krajewska, M., Heredia, M.L., Krajewski, S., Santamaria, G., Kim, H., Zapata, J.M., Marusawa, H., Chamorro, M., Reed, J.C. *Cancer Research*. 2002, 62, 6674-81.
110. Isidoro, A., Martinez, M., Fernandez, P.L., Ortega, A.D., Santamaria, G., Chamorro, M., Reed, J.C., Cuezva, J.M. *Biochem. J*. 2004, 378, 17-20.
111. Matsuyama, S., Xu, Q., Velours, J., Reed, J.C. *Molecular Cell*. 1998, 1, 327-36.
112. Harris, M.H., Vander Heiden, M.G., Kron, S.J., Thompson, C.B. *Mol. Cell. Biol*. 2000, 20, 3590-96.
113. Shin, YK, Yoo, B., Chang, H., Jeon, E., Hong, SH, Jung, M., Lim, SJ, Park, JG. *Cancer Res*. 65, 2005, 3162-70.
114. Zittomer, R.S, Lowry, C.V. *Microbiological Reviews*. 1992, 56, 1-11.
115. Amillet, J.M., Buisson, N., Labbe-Bois, R. *Curr. Genet*. 1995, 28, 503-11.
116. Taketani, S., Furukawa, T., Furuyama, K. *Eur J Biochem*. 2001, 268, 1705-11.
117. Yen, HC, Oberley, T.D., Vichitbandha, S., Ho, YS., St. Clair, D.K. *J. Clin. Invest*. 1996, 98, 1253-60.

- 118.Navonne, N.M., Polo, C.F., Frisardi, A.L., Andrade, N.E., Battle, A.M. *Int. J. Biochem.* 1990, 22, 1407-11.
- 119.Wissel, P.S., Drummond, G.S., Kappas, A. *Life Sci.* 1990, 47, 1595-9.
- 120.Olson, M., Kornbluth, S. *Curr. Mol. Med.* 2001, 1, 91-122.
- 121.Kohler, C., Gahm, A., Noma, T., Nakazawa, A., Orrenius, S., Zhivotovsky, B. *FEBS Letters.* 1990, 447, 10-12.
- 122.Van Loo, G., Demol, H., Gulp, M., Hoorelbeke, B., Schotte, P., Beyaert, R., Zhivotovsky, B., Gevaert, K., Declercq, W., Vandekerckhove, J., Vandenabeele, P. *Cell Death and Differentiation.* 2002, 9, 301-308.
- 123.Chua, B.T., Volbracht, C., Tan, K.O., Li, R., Yu, V.C., Li, P. *Nature Cell Biology.* 2003, 5, 1083-89.
- 124.Bernardi P., Scorrano, L., Colonna, R., Petronilli, V., Lisa, F. *Eur. J. Biochem.* 1999, 264, 687-701.
- 125.Wieden, HJ., Gromadski, K., Rodnin, D., Rodnina, M.Y. *J. Biol. Chem.* 2002, 277, 6032-36.
- 126.Choglay, A.A., Chapple, J.P., Blatch, G.L., Cheetham, M.E. *Gene.* 2001, 267, 125-34.
- 127.Myung, JK., Afjehi-Sadat, L., Felizardo-Cabatic, M., Slavc, I., Lubec, G. *Protoeme Science.* 2004, 8, 1477-99.
- 128.Beere, H.M., Wolf, B.B., Cain, K., Morimoto, R.L., Cohen, G.M., Green, D.R. *Nature Cell Biology.* 2000, 2, 469-75.

- 129.Gotoh, T., Terada, K., Oyadomari, S., Mori M. *Cell Death Diff.* 2004, 11, 390-402.
- 130.Merrill M.J., Yeh, G., Phang, J.M. *J. Biol. Chem.* 1989, 264, 9352-58.
- 131.Donald, S.P., Sun, X.Y., Hu, C.A., Yu, J., Mei, J.M., Valle, D., Phang, J.M. *Cancer Research.* 2001, 61, 1810-15.
- 132.Herzfeld, A., Greengard, O. *Cancer.* 1980, 46, 2047-54.
- 133.Liu, J., Rothermund, CA., Ayala-Sanmartin, J., Vishwanatha, JK. *BMC Biochem.* 2003, 9, 10.
- 134.Vishwanatha, J.K., Chiang, Y., Kumble, K.D., Hollingsworth, M.A., Pour, P.M. *Carcinogenesis.* 1993, 14, 2575-79.
- 135.Boyer, J., Maxwell, P.J., Longley, D.B., Johnston, P.G. *Anticancer Res.* 2004, 24, 417-23.
- 136.Wang, Y., Serfass, L., Roy, M., Wong, J., Bonneau, A., Georges, E. *Biochem. Biophys. Res. Commun.* 2004, 314, 565-70.
- 137.Luo, L.Y., Soosaipillai, A., Diamandis, E.P. *Biochem. Biophys. Res. Commun.* 2001, 280, 401-6.